NTIA Report 97-338

Interference Simulation for Personal Communications Services Testing, Evaluation, and Modeling

James G. Ferranto

U.S. DEPARTMENT OF COMMERCE
William M. Daley, Secretary

Larry Irving, Assistant Secretary
for Communications and Information

July 1997

PRODUCT DISCLAIMER

Certain commercial equipment, instruments, or materials are identified in this paper to specify adequately the technical aspects of the reported results. In no case does such identification imply recommendation or endorsement by the National Telecommunications and Information Administration, nor does it imply that the material or equipment identified is necessarily the best available for the purpose.

CONTENTS

INTERFERENCE SIMULATION FOR PERSONAL COMMUNICATIONS SERVICES TESTING, EVALUATION, AND MODELING

James G. Ferranto[1]

An interference model applicable to wireless technologies is presented in this report. Specifically, a generic methodology for cellular system self-interference modeling was developed, then applied to two proposed personal communications services (PCS) technologies: the Global System for Mobile-based PCS 1900, and IS-95-based code division multiple access. Resulting system-specific models are discussed in detail, and are used to produce output noise and interference waveforms suitable for implementation in a real-time hardware channel simulator, or as a component of a higher-level software simulation. Example outputs are given for simulations of both technologies, with corresponding statistical analyses of the noise and interference waveform properties. Models described in this report are particularly well-suited for independent PCS system evaluation by other Federal agencies, system manufacturers, and service providers.

Key words: noise; interference; personal communications services; simulation; model

1. INTRODUCTION

Widespread implementation of personal communication services (PCS) is expected to revolutionize telecommunications in the United States within the next few years. The digital nature of PCS, in conjunction with high channel reusability, allows a variety of user services in dense coverage areas. Commercial and residential PCS services include near-wireline quality voice and low-speed data in a mobile environment. Extensive control channel designs allow extended mobility management, roaming, security, and priority access services not previously available in analog cellular systems.

A combination of low-cost, wide availability, and extended services makes PCS a highly desirable collection of services for Federal wireless requirements.[2] Consequently, the Federal government plans on making extensive use of commercial PCS where practical. However, certain Federal users

1 The author was with the Institute for Telecommunication Sciences, National Telecommunications and Information Administration, U.S. Department of Commerce, Boulder, CO 80303 when this work was done.

2 The Federal Wireless Policy Committee has summarized Federal wireless requirements in a document entitled “Current and Future Requirements for Federal Wireless Services in the United States,” which has been presented to relevant wireless standards organizations. In addition, the United States Government is currently developing a Government-wide procurement program for wireless services and devices.

mandate specific additional services that must operate acceptably in the PCS environment. For example, special Federal requirements include priority access and channel assignment (PACA) in both nonemergency and emergency wireless applications, and enhanced security services provided by STU-III telephony. These special applications may impose additional performance and interoperability requirements that are specific to the particular PCS technology, and to the corresponding deployment.

Even without considering special Federal user requirements, a strong need for PCS evaluation methods is apparent. PCS systems are largely untested in actual deployment scenarios. Because predeployment field testing of all aspects of an actual PCS system is prohibitively time consuming and expensive, alternative methods for evaluation are required. To aid assessment of proposed PCS technologies, the Institute for Telecommunication Sciences (ITS) has developed synergistic programs for PCS network testing, modeling, and evaluation. Beneficiaries of these programs include other Federal agencies, wireless service providers (especially resource-limited service providers), and wireless equipment manufacturers. Outputs include quantitative and qualitative performance metrics, interoperability studies, and scenario plans for present and future PCS system operation.

Essential elements for accurate PCS network testing, modeling, and evaluation are system-specific interference models and their corresponding hardware implementations. Interference model development is detailed in this report. First, a brief overview of the ITS simulation methodology is provided for perspective.

1.1 PCS Testing, Modeling, and Evaluation Program Simulation Methodology

ITS' expertise in both physical-layer and network-layer modeling provides a unique in-house interlayer analysis methodology. Work structure for PCS system modeling is divided by layer in a hierarchical manner: the results of each layer analysis provide the parameters for adjacent layers. Abstraction is used to simplify higher-layer models, and to reduce computational complexity which often makes a model impractical. First, the physical-layer analysis data is supplied to the link-level analysis; this drives the network-layer analysis, and so on. Conversely, certain parameters in the lower layers are set based on higher-layer conditions. For example, channel self-interference (a physical-layer issue) in a code-division multiple access (CDMA) system is proportional to the number of current active links (a network-layer issue, Figure 1.1).

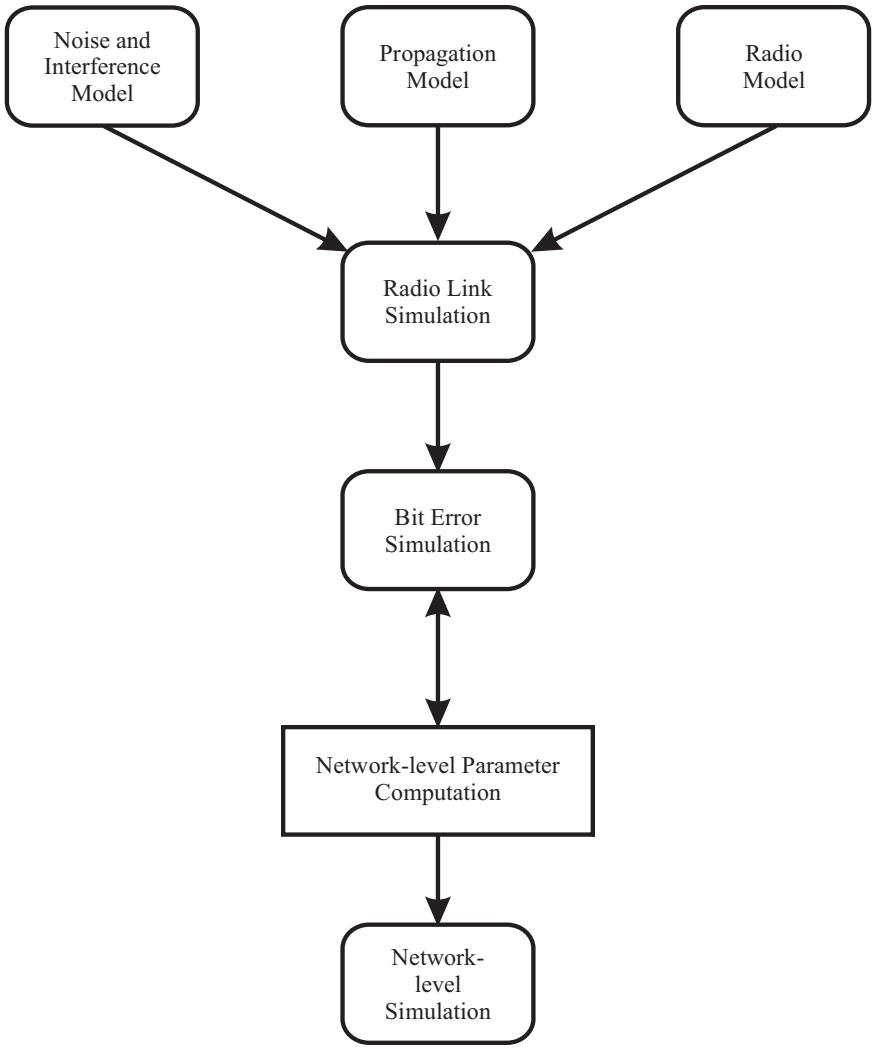

Figure 1.1. Layered approach to wireless simulation.

1.1.1 Radio Link Simulation (Physical Layer)

The radio link analysis encompasses all physical effects on a PCS mobile station/base station pair. Three major components, shown as the top three boxes in Figure 1.1, provide the description of the radio link environment:

1. **Propagation Model:** The propagation model is developed from both theoretical derivation and observed data. The propagation model describes effects of the physical channel on the communication waveform. Attenuation, multipath, and Doppler shift profiles are all components of the propagation model.
2. **Noise and Interference Model:** This model includes all extra-waveform impediments to the proposed PCS system. The noise and interference waveform

model is comprised of three components: 1) complex, modulated, zero-mean Gaussian noise; 2) interference from other users of the PCS frequency band; and 3) impulsive artificial and natural noise.

3. **Radio Simulation:** Radio simulation includes all effects of the radio receiver/transmitter design on communication. Modulators, demodulators, encoders, and antennas are all part of the receiver/transmitter design.

1.1.2 Bit Error Simulation (Physical Layer)

A statistical model that allows mapping of the major link variables into parameters of a statistical distribution is derived from detailed bit error information obtained from the radio link simulation. This statistical distribution is a function of all the link variables, including the channel, modem, coding, equalization, signal-to-noise ratio (SNR), and all interference. Interference is generated using the techniques described within this report. The output of the bit error simulation is a bit error mask that provides statistics for the network-layer analysis.

1.1.3 Network-level Parameter Computation and Network Simulation (Data Link Layer and Above)

The bit error mask created by the bit error simulation is used as input data for a systemwide PCS network simulation. Using discrete event simulation tools and abstraction techniques, ITS is capable of simulating a complete PCS system. First, the statistical bit error model is used to profile packet or frame error statistics (this decreases simulation time significantly, which is an optional but highly desirable step). The discrete event simulator is then used to model the PCS system, or a particular component of the PCS system. Any level of system detail is possible; the only limitations are simulation and development time for the model. The following issues may be addressed in the network simulation:

- interoperability,
- security,
- protocol analysis,
- mobility,
- priority access,
- channel sharing, and
- deployment planning.

1.2 Noise/Interference Modeling and Channel Simulation

An important consideration in the assessment of proposed PCS systems is acceptable performance in an RF noise and interference (N/I) environment. Service quality on all layers of communication are affected by the nature of the N/I, with some applications more susceptible to certain types of N/I than others. For example, if a brief impulsive noise causes a bit error in a voice application resulting in packet loss, a user may hear only a "click" or "pop." However, that same packet loss, under the same N/I conditions, can completely disrupt a STU-III secure telephone conversation (bit count integrity is required for the synchronous data stream carrying STU-III voice information). Alternatively, the Gaussian-type interference caused by a heavily loaded CDMA RF channel may induce errors that are more uniformly distributed in time, which may be more readily corrected by higher communication layers. Clearly, the distribution of errors caused by impediments in the PCS air interface depends on the type of N/I encountered. A comprehensive N/I model is needed.

Complete characterization of the PCS environment includes system-specific models for N/I. As previously mentioned, the N/I waveform model is comprised of three components: 1) complex, modulated, zero-mean Gaussian noise; 2) interference from other users of the PCS frequency band; and 3) impulsive artificial and natural noise. Derivations for the second component, interference from other users of the PCS frequency band, are presented in this report. Components 1) and 3) are detailed in [1-6], and are beyond the scope of this report; an informative survey of all three N/I components in the 2-GHz licensed PCS band is provided in Section 2. A generic method for wireless cellular interference generation is described in Section 3, and system-specific interference waveforms for the global system for mobile (GSM)-based PCS 1900, and IS-95-based CDMA are presented in detail in Sections 4 and 5.

ITS N/I models are tailored for use in real-time channel simulation. To aid evaluation of system performance, PCS testing includes extensive use of real-time hardware channel simulators. Channel simulation provides a cost-effective means of testing PCS radio technologies and proposed common air-interface standards. ITS incorporates hardware channel simulation of the PCS air-interface propagation environment as part of the PCS testing, modeling, and evaluation program. Future work will address an efficient hardware implementation of the ITS N/I waveform models.

2. NEED FOR NOISE AND INTERFERENCE MODELING IN THE 2-GHZ PCS ENVIRONMENT

Complete specification of the PCS RF channel must include a credible model of the system-specific N/I environment. Incidental channel impediments are termed "noise," and originate from both natural and artificial sources. "Interferers," by contrast, are waveforms intentionally radiated in the RF channel that disrupt or degrade a desired waveform. Interferers are generated by sources both external and internal to the affected PCS system, and may include other wireless systems sharing a common geographical area and frequency band.

Preliminary studies of the noise environment at 2 GHz show that the natural noise contribution is relatively small. Sources of artificial noise are ranked in order of severity as follows [1]:

1. Automotive ignitions.
2. Transportation and generation facilities.
3. Industrial equipment.
4. Consumer products.
5. Lighting systems.
6. Medical equipment.

Background noise from these sources appears to be very low, even including the automotive ignition sources. However, point or individual sources may be quite significant noise generators, with noise levels well above that of background noise. Some indoor environments may also foster noise levels above background noise. Further investigation is needed in this area [1]. Blackard et al., [2] state that photocopiers, elevators, and microwave ovens (all elements of the indoor office/retail environment) are significant sources of impulsive noise in certain PCS frequency bands.

2.1 Interference Environment

Interferers, in contrast to most noise sources, are a major hindrance to wireless communication at 2 GHz. In a multiple access environment using microcellular deployment, the most significant unwanted waveform sources will be interferers rather than noise sources. For this reason, PCS systems are interference-limited. PCS system interference is categorized as either external or internal. External sources of interference are generated by systems outside a given PCS system. These include microwave links in the PCS frequency band, and other PCS systems sharing the geographical area. Microwave link interference to PCS systems has been discounted by several sources [7,8]. However, PCS systems may interfere with microwave links.

Intrasystem interferers are (by definition) self-generated by the PCS system, and can be categorized as either intracellular or intercellular. The nature of both types of internal interference is specific to a particular technology. For example, time-division multiple access (TDMA) systems do not experience intracell interference if all users in the cell are properly synchronized. CDMA systems inherently create intracell interference by overlaying user waveforms within a cell's frequency allocation. Furthermore, variations of the different technologies have made the interference highly system-specific. For example, CDMA systems with joint detection do not experience intracell interference, at the cost of an SNR degradation [9]. Hybrid CDMA/TDMA systems create their own unique interference characteristics. Proper modeling of the interferers requires a system-specific analysis of the waveforms involved.

Development of an N/I model for a hardware implementation requires a quantitative description of the N/I waveform that must be added to the received waveform. In [6], a general framework for such a description of the N/I waveform is proposed. The described waveform is represented as the sum of three components: 1) a complex, zero-mean, modulated Gaussian noise; 2) a summation of impulsive artificial and natural noise processes; and 3) a summation of interference processes generated by other users in the PCS frequency band.

2.1.1 Statistical Interference Models

Most descriptions of the interference environment in the literature, e.g., [3, 4, 10, 11, 12], present statistical models of the interference waveform behavior, rather than a model of the waveform itself. These models tend to be general to the PCS environment, giving interference statistics in form generic to any of the many relevant stochastic distributions, in conjunction with desired waveform distributions, suited to cochannel interference statistics, e.g., Rayleigh, Rician, lognormal, and Nakagami. Some models [13] describe the total statistical N/I environment, e.g. the Middleton Class A, B, and C statistical-physical model. Outputs of these models are BER studies, system outage probabilities, intercell and intracell noise amplitude and phase probability density functions (PDFs), and others. Models that are technology-specific indicate system performance based on properties inherent to a particular technology.

Conflicts sometimes exist between these models. One model claims the well-accepted Nakagami model for the Rician fading of the desired waveform is not appropriate, and the ramifications may extend into the interference model results [12]. Another model claims that Rayleigh fading may not be a good assumption for the desired waveform in a microcellular architecture, and thus the fading statistics of the desired and interferer waveforms must be adapted accordingly [3].

A derived statistical model may not be sufficient for complete characterization of the interference environment. In particular, complex multiple access waveforms from multiple mobile stations may create an interference environment that cannot be expressed with a simple distribution function. For example, a Gaussian approximation for cochannel interference from adjacent cells is appropriate for narrowband TDMA (in certain cases), but may not be valid for a CDMA system with a single dominant interferer. Accurate modeling of CDMA may therefore involve a complete simulation of the interference sources [13]. While this may be computationally intensive, models can be developed that capture the essence of the waveform interference. The simplified waveform then can be precomputed for use in a real-time hardware simulation.

Power control algorithms also add a layer of complexity to the waveform statistics. For example, a CDMA system with perfect power control and several concurrent channels in use has an interference waveform which is approximately Gaussian. However, imperfections in the power control algorithm may cause a non-Gaussian interference waveform, particularly in shadowing or "near/far" conditions.

2.1.2 Standards Requirements for Interference Levels in PCS Systems

Many wireless developers use carrier-to-interference power ratios (C/I), or carrier-to-noise plus interference ratios C/(N+I), to predict the performance of proposed PCS systems. Standards organizations, such as the Joint Technical Committee (JTC) on Wireless Access, require that the PCS system developer provide the interference density as a first order statistic, namely the self-interference power level created by the PCS system. In the JTC, the interference density is defined as the interference power at a receiver input located at the border of an interior cell. Interference levels for each proposed PCS system are provided by the system proposer(s), along with a justification statement [5]. Separate and optional contributions to the JTC suggest developing C/I as a function of the PCS system load. Adjacent cell interference and external interference levels are not specified.

Because each system provider specifies the interference level independently, there may be problems in interpreting the additive effects of intersystem interference. More importantly, because the interference characteristics of the proposed systems are quantified as a single average power level, higher-order statistics that may greatly impact system performance are not considered. Although C/I measures give an indication of PCS system performance in an interference environment, they may not provide the complete picture.

2.1.3 System-specific Models and Interference Simulation

Many systems developers and researchers, faced with limitations imposed by the above interference measures and models, have turned to simulation techniques for PCS system performance modeling. Because waveform simulations are computationally intensive, the simulations are usually software-based and not in real time (references [14-16] give theoretical and computational analyses of PCS system performance based on Monte Carlo techniques, or system descriptions that may be adapted to simulation techniques). These analyses tend to be more system-specific than the statistical models described earlier. Haas, et al. make the assertion that intercell interference measures have been pessimistic, and that interferers from an adjacent cell may not cause problems, even with a three-cell reuse pattern [15]. Such claims must be substantiated through measurement or simulation.

Other studies use system-specific software simulation of the interference sources. In [17], the TDMA simulation tool BERSIM is used to import channel response data into another simulation tool that simulates a 1.25-MHz bandwidth CDMA system. Channel processing is accomplished by downconverting the system waveforms to baseband complex envelope form, convolving the waveform with the channel impulse response, then adding interference and Gaussian noise. The discrete nature of the simulation requires sampling of the waveforms involved; in this case, at one fourth the chip transmission rate. Intracell interferers are assigned a uniformly distributed random delay and phase, then added to the desired waveform before convolution with the channel impulse response. All interferers are assumed to have equal amplitudes (a power equalization assumption), which may be overly simplistic. Intercell interference does not seem to be included in the simulation. Clearly, a method is needed to develop a sufficiently-detailed interference model that is computationally viable in simulation.

2.2 Hardware Simulation of PCS Channels in the Noise/Interference Environment

Several manufacturers offer real-time RF channel simulators appropriate to the PCS environment. These simulators typically have baseband input bandwidths between 5- and 8-MHz, and feature multipath, propagation loss, and Doppler shift effects. Multipath capabilities usually include at least six tapped delay line paths. Propagation loss can be chosen independently for each path in most cases. Some models are developed for particular technologies, such as GSM. In summary, these simulators have features that characterize the PCS RF channel, with one significant exception: the N/I environment.

Most commercial simulators possess two independent channels that allow cochannel interference tests via transmission of the interference waveform through a separate multipath channel, and use a power combiner to add the interferer to the desired waveform. However, these simulators do not produce the interference waveform itself. (At least one manufacturer provides Gaussian noise sources for the RF channel, but no interferers are included). Consequently, the interference waveform must be generated by the PCS system evaluator. This waveform obviously is highly dependent on the PCS system, but generic models for each technology class can be adapted to emulate specific PCS systems. For example, models for generic CDMA, TDMA, and hybrid CDMA/TDMA can be adapted to the many specific PCS systems under consideration in the JTC. Most likely, PCS system developers model interference waveforms as part of the design process, but these models tend to be proprietary and nonstandardized between competing technologies.

PCS evaluators need a viable, independent source for the interference waveform model specific to each system under test. The waveform must be detailed enough to include higher-order statistical properties that may affect proposed PCS system performance. This may require full software simulation of the N/I environment, with results that can be adapted to a hardware implementation. However, the hardware implementation of the interference waveform must also be efficient to accommodate a real-time interface with a RF channel simulator. Software simulation of the interference can identify both important waveform aspects, and relatively insignificant elements of the waveform that add unnecessary complexity to the simulation.

2.3 Summary

System-specific models of N/I waveforms must be developed for PCS tests that use RF channel hardware simulators. Implementation of the models may include software simulation of the interference waveform, and adaptation of the results to hardware capable of processing the required waveforms in real time. Disclosure of PCS system specifications will be required for proper development of the N/I models. Ideally, the model development and validation will be conducted by an independent PCS system evaluator with involvement in assessment of each of the PCS technologies under test.

ITS has developed system-specific interference models for two licensed PCS technologies to date: the GSM-based PCS 1900, and CDMA-based on IS-95. The method for developing the intrasystem interference waveforms for these systems, which includes cochannel interference and adjacent channel interference, is described in the next section.

3. PCS CELLULAR GEOMETRY FOR INTRASYSTEM COCHANNEL INTERFERENCE

Development of an intrasystem interference waveform based on spatial considerations includes specification of a PCS cellular system geometry. In most analyses of this type, a hexagonal cellular geometry is used, with each cell having six adjacent cells. Although this geometry is relatively awkward to manage in simulation, most PCS deployment descriptions use it. For ITS models, the single base station is located at the center of the cell, but a circular geometric pattern is assumed. As shown in Figures 3.1-3.7, cells have been augmented to be circular. This results in some minor overlap, but makes the geometry easier to manipulate. This representation actually reflects reality since base stations in "real" cells will not radiate hexagonal patterns, and some overlap is expected for complete area coverage. Overlap also allows future addition of noncircular cell patterns, such as those created by directional antennas.

3.1 Assumptions

The following assumptions are made for the PCS cellular geometry: 1) all cells within the PCS system are the same size, 2) each cell contains N_u mobile stations, 3) one RF carrier is simulated per cell, and 4) a **primary cell** contains the base station or mobile stations experiencing the interference.

The primary cell is the focus of the interference waveform simulation. Because the licensed PCS technologies use frequency division duplexing (FDD), interference waveforms must be developed for both the uplink and downlink. On the uplink, it contains the base station experiencing interference from mobile stations outside the primary cell transmitting on the same RF. In CDMA systems, mobile stations within the primary cell also contribute to the interference waveform. The primary cell also contains mobile stations that receive interference from nearby base stations transmitting on the same downlink RF carrier as the primary cell base station. Uplink and downlink cases for the intrasystem cochannel interference waveform are summarized as follows:

1. Uplink interference (two components)

   Component 1: Mobile stations in interfering cells create an interference waveform at the primary cell's base station. This is the intercell interference component.

   Component 2: Mobile stations within the primary cell interfere with each other via intracell interference. This is an inherent property of CDMA systems; TDMA systems with timing problems may also demonstrate intracell interference.

2. Downlink interference (conditionally two components):

Component 1: Base stations in interfering cells create interference at each of the mobile stations in the primary cell, forming the intercell interference component of the interference waveform.

Component 2 (conditional): The base station in the primary cell generates a multiplexed waveform that interferes with other mobile stations in the primary cell. This should only be a problem in CDMA systems; TDMA waveforms will be internally combined within the base station, so synchronization of time slots should not be a problem.

Component 2 in both cases above may have to be generated by patching real-time outputs of the actual PCS transmitters into a channel simulator, with proper multipath, delay, Doppler shift, and propagation loss factors. This is readily apparent for TDMA systems, since (for uplink transmissions) a mobile station under test must synchronize itself into a time slot assigned by the base station. This requires the base station to have control of time slot assignments for the entire uplink (i.e. all control channels which are dynamically allocating channels to the mobile stations). This cannot be simulated by blindly filling the other time slots with modulated energy. Prerecording actual mobile station waveforms for insertion into the channel simulator may prove difficult, if not impossible because of the state-dependent nature of the PCS medium access protocols.

Figure 3.1 shows the geometry for a confederation of cells in the PCS system. It is independent of any specific PCS system technology. Each cell is modeled as a circle with the base station at the geometric center, with the familiar cellular hexagon subscribing the circle. R_C is defined as the radius of the base station circle, and R_H is the "short radius" of the hexagon subscribing the base station circle. Relationships between R_C and R_H are shown in Figure 3.2.

3.2 Interference Waveform Notation

Ferranto and Lemmon describe a method for representing an interference waveform from a nearby cell based on Cartesian coordinate translation of the desired waveform expression [18]. This description is used in the following discussion, with some minor notational changes.

The primary cell, as defined in Section 3.1, is surrounded by 6 adjacent interfering cells, and 12 additional interfering cells surround the primary cell and 6 adjacent interferers. The distance from and angle to the n^{th} mobile station relative to the primary cell's base station are defined as $r_{p,n}$ and $\theta_{p,n}$, respectively. N_U mobile stations are present in the primary cell. $x_{p,n}$ and $y_{p,n}$ are the Cartesian x and y distances, respectively, of the n^{th} mobile station from the base station. These relationships are shown graphically in Figure 3.3.

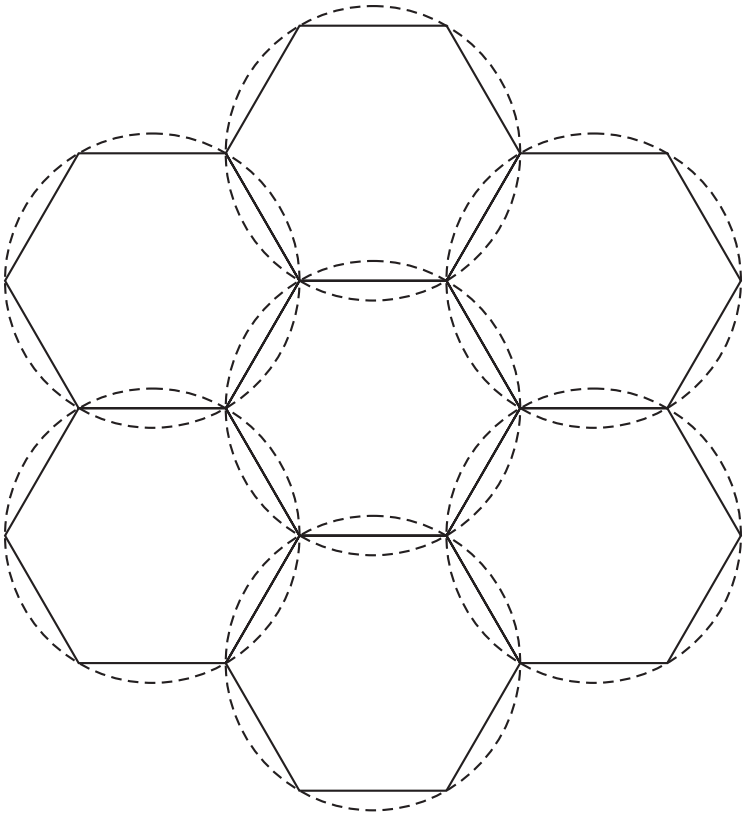

Figure 3.1. Hexagonal cells in a PCS deployment with circular geometry overlay.

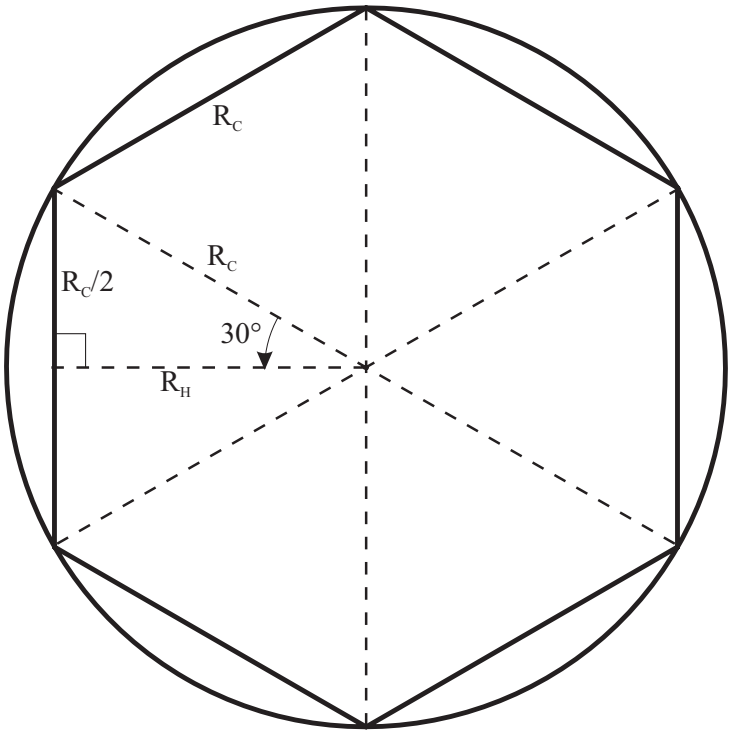

R_C = radius of circle

R_H = "short radius" of hexagon = R_C cos 30°

Figure 3.2. Geometry and notation for a single PCS cell.

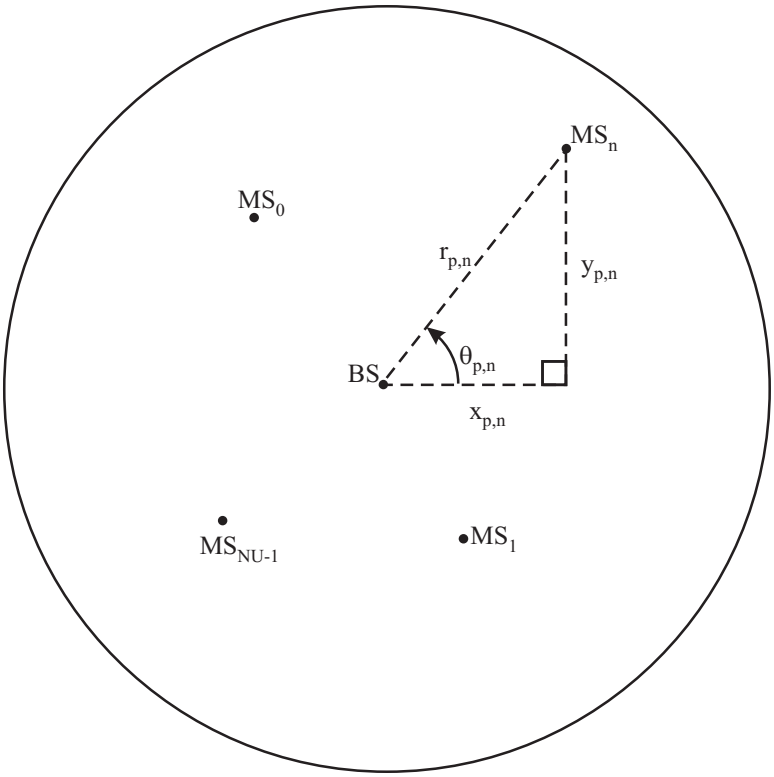

Figure 3.3. Geometric relationships between base stations and mobile stations within a single PCS cell.

As a framework for the system-specific interference waveform expressions, generic waveform terminology is derived in terms of complex baseband representations of the interference. Complex baseband notation used in the remainder of this report is described in detail in Appendix B. Waveforms in complex baseband form are denoted by an overline. Expressions are defined as follows:

$\overline{x_{FI\,(k,n)}}(t)$ is the complex baseband expression for the interference waveform from the n^{th} interferer in interfering cell k ("F" indicates that the expression is defined over one "frame" for the downlink case, and the "I" represents the "interferer"). Depending on the context, the interferer may be either a mobile station, or a base station. Two cases exist:

1. For uplink, n represents the n^{th} interfering mobile station in the k^{th} cell. For TDMA systems, $\overline{x_{FI\,(k,n)}}(t)$ is defined over one time slot. For CDMA systems, $\overline{x_{FI\,(k,n)}}(t)$ is not time-limited.

2. For downlink, n indicates the n^{th} mobile station in the primary cell experiencing interference from the base station in interfering cell k. $\overline{x_{FI\,(k,n)}}(t)$ is defined over one frame for TDMA systems, and is not time-limited for CDMA systems.

$\overline{x_{FI\,(k,n)}}(t)$ is the basic building block for the interference waveform expressions. In the N/I model, it is the only expression referenced to the transmitter (i.e., all other expressions represent the interference waveform incident at the receiver). All other interference functions are expressed as summations of $\overline{x_{FI\,(k,n)}}(t)$. For example:

$\overline{x_{FI\,(k,-)}}(t)$ is defined as the sum of all uplink interferer mobile station waveforms created in interfering cell k, incident at the primary cell's base station.

$\overline{x_{FI}}(t)$ is the aggregate uplink interference waveform incident at the primary cell's base station.

$\overline{x_{FI\,(-,n)}}(t)$ is the downlink interference waveform caused by all interfering base stations, as seen by the n^{th} mobile station in the primary cell.

Expressions for the uplink and downlink interference functions depend on the technology. However, generic expressions can be formed with parameter specification of a CDMA- or TDMA-based technology. These generic expressions are shown below, with the parameter b specifying CDMA or TDMA:

For uplink,

$$\overline{x_{FI\,(k,-)}}(t) = \sum_{n=0}^{N_U-1} \overline{x_{FI\,(k,n)}}\left(t - nbT_U - \frac{r_{k,n}}{c}\right) a_{k,n}\left(r_{k,n}, \theta_{k,n}\right)$$
$$\overline{x_{FI}}(t) = \sum_{k=0}^{N_I-1} \overline{x_{FI\,(k,-)}}(t), \tag{3.1}$$

and for downlink,

$$\overline{x_{FI\,(-,n)}}(t) = \sum_{k=0}^{N_I-1} \overline{x_{FI\,(k,n)}}\left(t - \frac{r_{k,n}}{c}\right) a_{k,n}\left(r_{k,n}, \theta_{k,n}\right), \tag{3.2}$$

where, for both Equation (3.1) and (3.2):

c is the speed of radio wave propagation,

T_U is the duration of a TDMA time slot,

N_U is the number of mobile stations (users) per cell,

N_I is the number of interfering cells,

$r_{k,n}$ is the distance between the point interferer and the interference reception point (this is defined in detail in the next section),

$\theta_{k,n}$ is the angle of the point interferer with respect to the interference reception point (this is defined in detail in the next section),

$a_{k,n}(r_{k,n}, \theta_{k,n})$ is a propagation loss and Doppler shift function,

$\frac{r_{k,n}}{c}$ is the propagation delay, and

b indicates TDMA (b = 1) or CDMA (b = 0).

The parameter *b* allows flexibility in the notation to accommodate both TDMA and CDMA. For TDMA systems, each communication link between mobile station and base station makes full use of the RF channel during its assigned time slot; *b* then "activates" the time delay in $\overline{x_{FI\,(k,-)}}(t)$. For CDMA systems, each communication link shares the same time and frequency domains, and therefore communication links overlay one another.

Note that $\overline{x_{FI\,(k,n)}}(t)$ must be defined within the specifications of a particular PCS technology. For example, the single interferer represented by $\overline{x_{FI\,(k,n)}}(t)$ is defined over one time slot in Equation (3.1) for TDMA, but is defined over one frame in Equation (3.2) for TDMA. For CDMA, frames and time slots (in the context of interference generation) become meaningless, and $\overline{x_{FI\,(k,n)}}(t)$ is defined over an arbitrary period of time. For example, an IS-95-based CDMA system may define $\overline{x_{FI\,(k,n)}}(t)$ in terms of chip duration or spreading code length.

3.3 Intercell Uplink Interference

By performing translations with respect to reference Cartesian coordinate systems, expressions for interference to the primary cell from nearby cells can be derived. Interference waveforms all have the same form as the desired waveforms derived for the primary cell, with the exception of the coordinate translation, because the interferers are assumed to belong to a common PCS system. This of course assumes the nearby cells are using the same modulation scheme and system configuration as the primary cell. However, the aggregate interference expression may be imposed upon any system under test. For example, an interference waveform created by a PCS 1900 system may be applied to an IS-95-based PCS system (or any system) under test.

3.3.1 Uplink Cell Geometry

Uplink interference is caused by mobile stations in nearby cells (and in the primary cell for CDMA) transmitting unwanted waveforms to the base station in the primary cell. The k^{th} interfering cell is defined graphically in Figure 3.4.

In Figure 3.4,

$d_k = \sqrt{d_{x_k}^2 + d_{y_k}^2}$ is the distance between the primary cell's base station and the k^{th} interfering cell's base station,

$x_{k,n}, y_{k,n}$ are the *x* and *y* distances of the n^{th} mobile station in the k^{th} interfering cell from the k^{th} cell's base station, respectively,

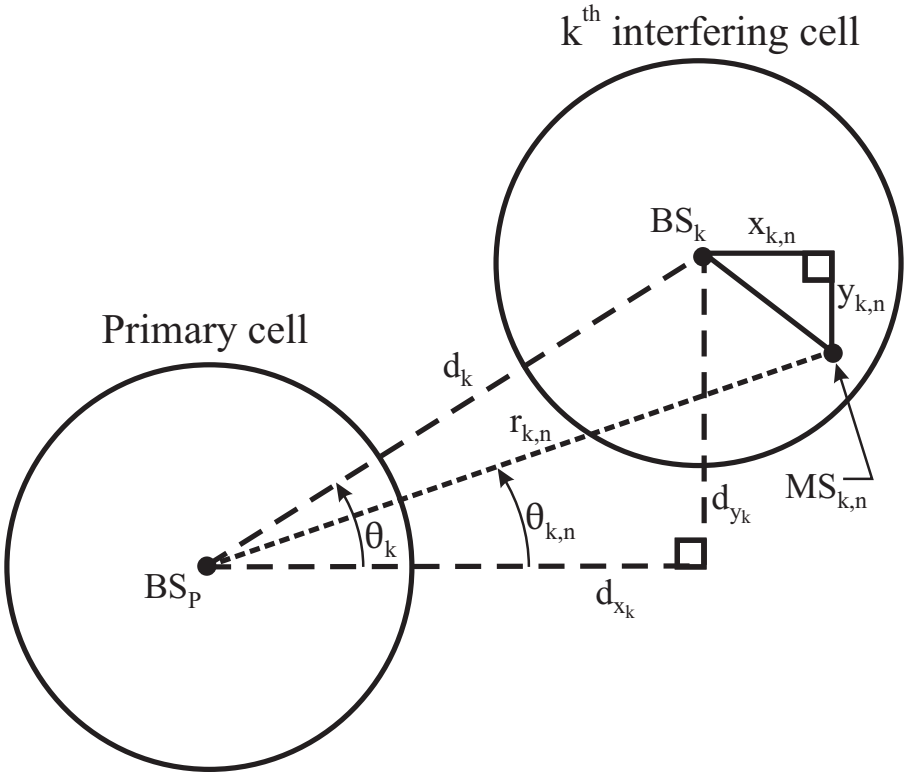

Figure 3.4. Cartesian coordinate translation for an interfering cell.

θ_k is the angle of interfering cell *k*'s base station with respect to the primary cell's base station,

$\theta_{k,n}$ is the angle of the n^{th} mobile station in interfering cell *k* with respect to the primary cell's base station, and

$r_{k,n}$ is the distance of the n^{th} mobile station in interfering cell *k* with respect to the primary cell's base station.

From simple geometry:

$$r_{k,n} = \sqrt{(x_{k,n} + d_{x_k})^2 + (y_{k,n} + d_{y_k})^2}, \tag{3.3}$$

and

$$\theta_{k,n} = \arctan\left[\frac{(y_{k,n} + d_{y_k})}{(x_{k,n} + d_{x_k})}\right]. \tag{3.4}$$

3.3.2 Adjacent Cell Distances

In the hexagonal pattern shown in Figure 3.1, cells adjacent to the primary cell are all equidistant, and the primary cell's base station is separated from each adjacent cell's base station by distance d_k, where

$$d_k = 2R_H = 2R_C \cos\left(\frac{\pi}{6}\right), \quad 0 \le k \le 5. \tag{3.5}$$

Plotting the adjacent cell base station locations on the Cartesian coordinate system with the primary cell's base station at the origin yields the geometry shown in Figure 3.5.

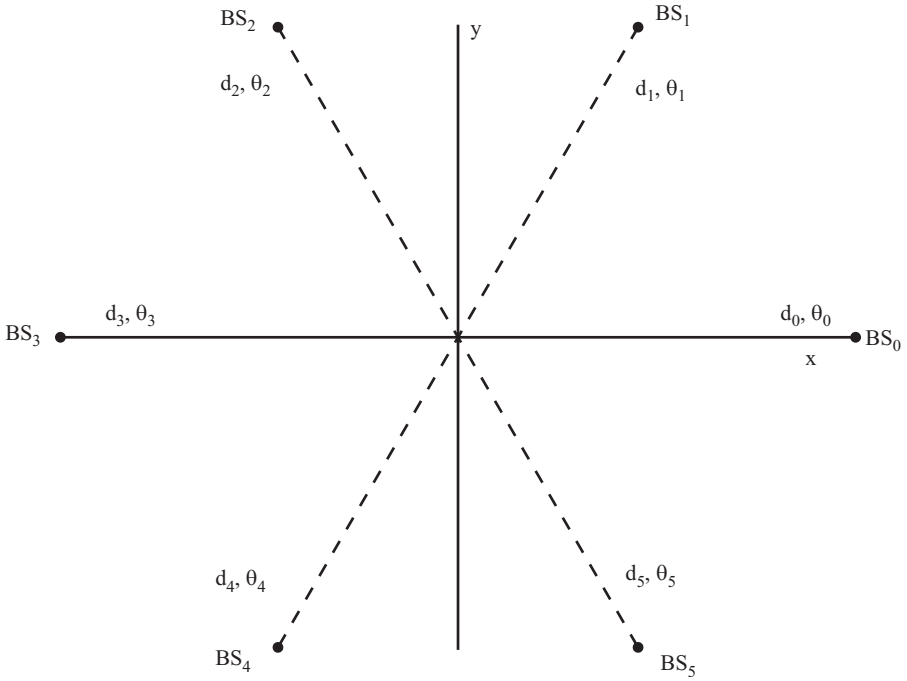

Figure 3.5. Geometric relations of adjacent cells.

Clearly, in Figure 3.5,

$$\theta_k = k\frac{\pi}{3}, \quad 0 \le k \le 5. \tag{3.6}$$

So for adjacent cells only,

$$\begin{aligned} d_{x_k} &= d_k \cos\theta_k = 2R_C \cos\left(\frac{\pi}{6}\right)\cos\left(\frac{k\pi}{3}\right), \quad 0 \le k \le 5 \\ d_{y_k} &= d_k \sin\theta_k = 2R_C \cos\left(\frac{\pi}{6}\right)\sin\left(\frac{k\pi}{3}\right), \quad 0 \le k \le 5. \end{aligned} \tag{3.7}$$

Equation (3.7) can then be substituted into Equations (3.1), (3.3), and (3.4) to find the uplink interference waveform from adjacent cells. In Equation (3.1), the number of interfering cells NI is set equal to six.

3.3.3 Second-level Cell Distances

The second layer of interfering cells from the primary cell are not equidistant, as was the case for cells adjacent to the primary cell. Of the twelve cells that comprise the second layer, half are at distance $3R_C$ (as measured from the primary cell base station to an interfering cell base station), and half are at distance $4R_H = 4R_C \cos\frac{\pi}{6}$, where R_C and R_H are as defined in Section 3.1. Numbering for the second-layer cells is arbitrary. Numbers 6 through 17 are used to distinguish second-layer cells from adjacent cells. Figure 3.6 demonstrates the relationships graphically. In Figure 3.6, for even k:

$$\begin{aligned} d_k^E &= 4R_C \cos\tfrac{\pi}{6} \\ \theta_k &= \frac{(k-6)\pi}{6}, \quad \text{where} \\ d_{x_k}^E &= 4R_C \cos\tfrac{\pi}{6}\cos\theta_k \\ d_{y_k}^E &= 4R_C \cos\tfrac{\pi}{6}\sin\theta_k, \end{aligned} \tag{3.8}$$

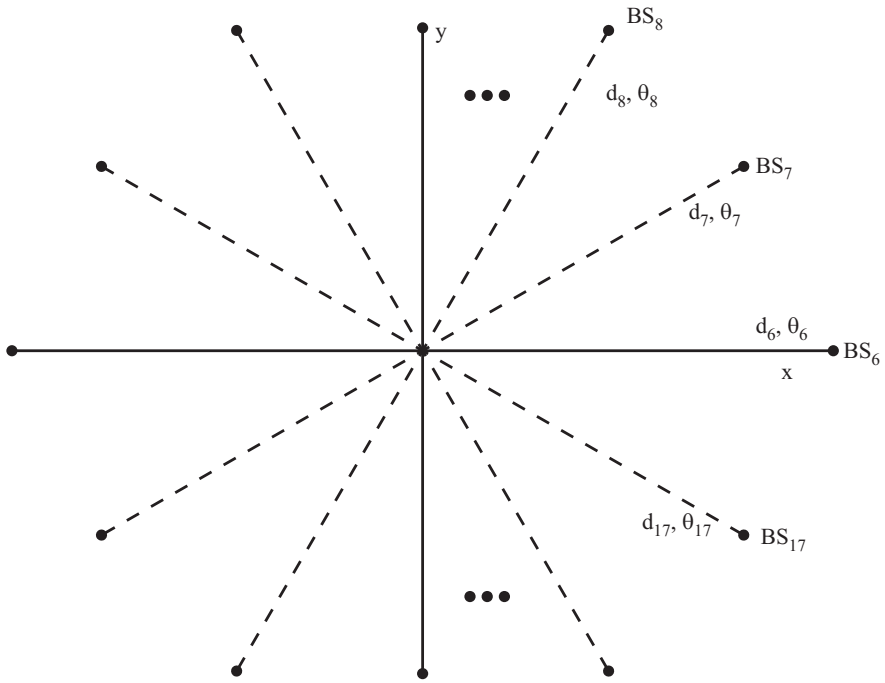

Figure 3.6. Second-layer interfering cell distances.

and for odd k,

$$
\begin{aligned}
d_k^O &= 3R_C \\
\theta_k &= \frac{(k-6)\pi}{6}, \quad \text{where} \\
d_{x_k}^O &= 3R_C \cos\theta_k \\
d_{y_k}^O &= 3R_C \sin\theta_k .
\end{aligned} \tag{3.9}
$$

As in Section 3.3.2, Equations (3.8) and (3.9) can be substituted into Equations (3.1), (3.3), and (3.4) to find the interference waveform from the second layer of cells surrounding the primary cell. In this case, N_I will equal 12 in Equation (3.1). The total uplink interference waveform is the sum of the adjacent and secondary interference waveforms. This analysis can be extended to the third, fourth, and greater layers of surrounding interfering cells, but doing so makes the interference waveform computation much more intensive. Layers beyond the second layer are typically far enough away to be discounted in the interference computation. For this reason, ITS analysis employs adjacent interfering cells and second-layer interfering cells only.

3.4 Intercell Downlink Interference

Analysis for intercell downlink interference is similar to the analysis for intercell uplink interference as described in Section 3.3. Intercell downlink interference is caused by base stations in nearby cells interfering with mobile stations in the primary cell. For CDMA systems, the base station in the primary cell may cause additional interference. In this section, the intercell downlink interference expressions are described.

3.4.1 Downlink Cell Geometry

Intercell downlink interference geometry is quite similar to the geometry specified for intercell uplink interference; in fact, the geometries are complementary. The k^{th} interfering cell geometry is shown in Figure 3.7.

In Figure 3.7,

$d_k = \sqrt{d_{x_k}^2 + d_{y_k}^2}$ is the distance between the primary cell's base station and the k^{th} interfering cell's base station,

$x_{p,n}, y_{p,n}$ are the x and y distances of the n^{th} mobile station in the primary cell with respect to the primary cell's base station,

θ_k is the angle of interfering cell k's base station with respect to the primary cell's base station,

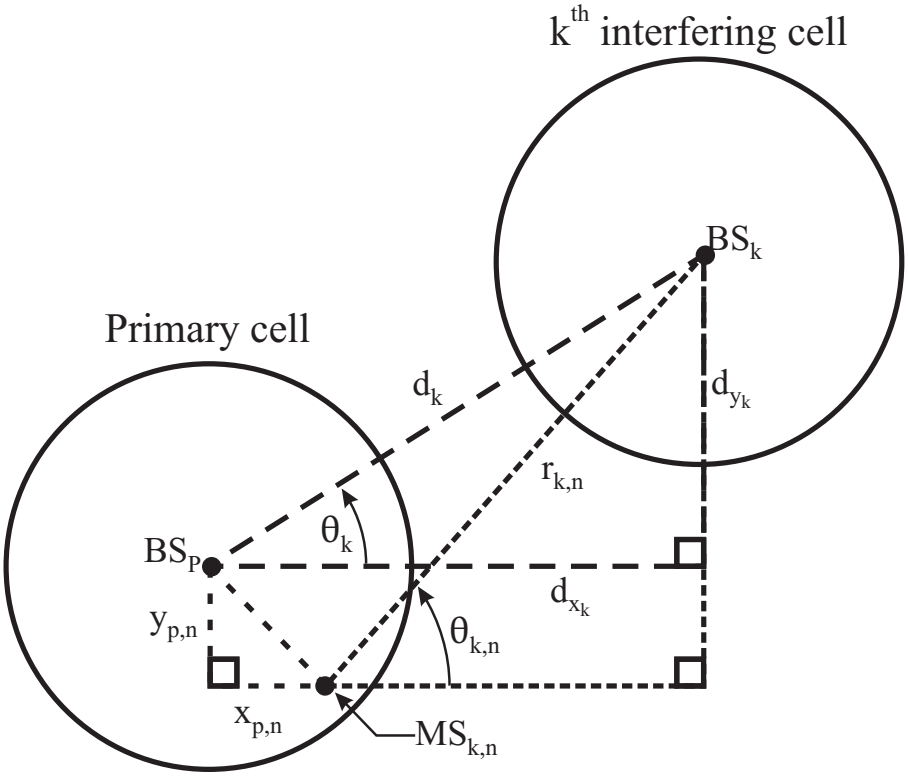

Figure 3.7. Cartesian coordinate translation for an interfering cell.

$\theta_{k,n}$ is the angle of the base station in interfering cell k with respect to the n^{th} mobile station in the primary cell, and

$r_{k,n}$ is the distance of the base station in interfering cell k with respect to the n^{th} mobile station in the primary cell.

From simple geometry,

$$r_{k,n} = \sqrt{(d_{x_k} - x_{p,n})^2 + (d_{y_k} - y_{p,n})^2}, \tag{3.10}$$

and

$$\theta_{k,n} = \arctan\left[\frac{(d_{y_k} - y_{p,n})}{(d_{x_k} - x_{p,n})}\right]. \tag{3.11}$$

3.4.2 Adjacent Cell Distances

Adjacent cell distance calculations for the downlink interference waveform are identical to those detailed in Section 3.3.2. The downlink interference waveform component from adjacent cells can be found by substituting Equations (3.5), (3.6), and (3.7) into Equations (3.2), (3.10), and (3.11).

3.4.3 Second-level Cell Distances

Second-level cell distance calculations for the downlink interference waveform are identical to those detailed in Section 3.3.3. The downlink interference waveform component from second-level cells can be found by substituting Equations (3.8) and (3.9) into Equations (3.2), (3.10), and (3.11).

3.5 Summary

In this section, generic expressions for intrasystem interference were developed using a cellular geometry. In Sections 4 and 5, system-specific interference waveforms based on these generic expressions are presented for GSM-based PCS 1900, and IS-95-based CDMA PCS.

4. GLOBAL SYSTEM FOR MOBILE-BASED PCS 1900 INTERFERENCE WAVEFORM

4.1 PCS 1900 Physical-layer Overview

PCS 1900 is a narrowband TDMA system based on GSM, and designed for use in the 2-GHz licensed PCS frequency band. It offers a range of digital services for public applications, including both voice and data. JTC contribution [19] specifies the air-interface standard for PCS 1900, and was used for all PCS 1900 interference model derivations in this report.

PCS 1900 is a complete mobile system. As such, its standard includes all layers of communication, including networking, interworking with fixed networks, and other higher-layer signaling protocols that have indirect impacts on the interference model. Although the ITS interference model for PCS 1900 uses the physical-layer specification exclusively, these indirect impacts also have an effect on the interference environment. A certain deployment scenario, as managed by higher-layer entities, may result in increased channel use and therefore increased system interference. These issues are handled by the link- and network-level simulation as part of ITS methodologies described in Section 1. The physical-layer interference model is developed with these higher-layer issues in mind.

To obtain a PCS 1900 interference waveform, a model of the physical layer, as specified in [19], is developed. PCS 1900 employs 200-kHz RF channels in a frequency division duplexing scheme. The licensed uplink band (1850-1910 MHz) and downlink band (1930-1990 MHz) may each theoretically support up to 298 PCS 1900 RF channels (not including two 200-kHz guard bands), although frequency reuse, frequency hopping algorithms, and specific equipment designs restrict the number of concurrent active RF channels in a given cell. PCS 1900 TDMA is based on eight time slots per frame, with 156.25 bit durations allocated per time slot, including guard times. Each time slot lasts 0.5769 ms, therefore the total modulation rate is approximately 270.8 kb/s. Each transmission within an assigned time slot is called a burst. The data rate per user depends on the type of burst used within each time slot, and the number of time slots used per frame per user.

Figure 4.1 shows the reference configuration for the PCS 1900 physical layer. This includes channel coding, interleaving, and encryption, which do not directly contribute to the interference waveform. For noise and interference modeling purposes, the data content of the interferer is not important, as long as sufficient randomness exists in the data stream. Important factors are the modulation scheme, transmitted power levels, propagation environment, and geometric distributions of the interferers. Interference modeling techniques allow abstraction of all

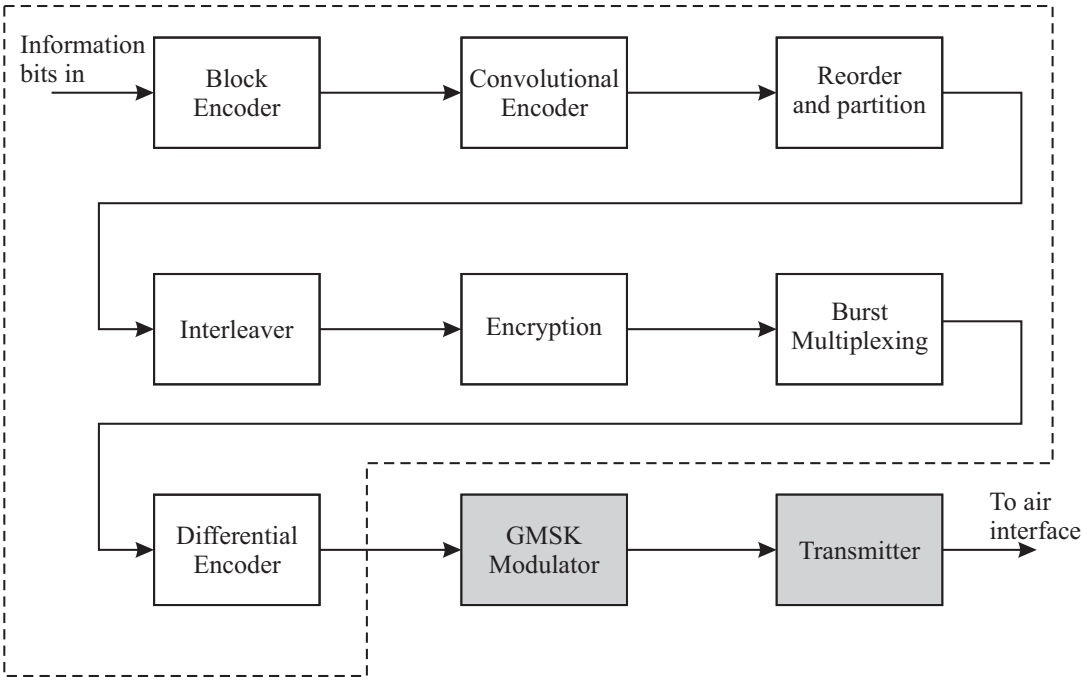

Figure 4.1. Physical-layer configuration for PCS 1900 (mobile station or base station).

communication devices that manipulate the data stream before modulation. Abstracted communication devices are contained within the dotted line in Figure 4.1. These form the "transmission data" block shown in Figure 4.2.

Figure 4.2. Abstracted physical-layer configuration for PCS 1900.

4.2 Theoretical Definition for PCS 1900-based Gaussian Minimum-Shift Keying

Gaussian minimum-shift keying (GMSK) is used for PCS 1900 base station and mobile station transmitters. Theoretical definitions for PCS 1900-based GMSK are presented in [19], and are defined in terms of the N/I waveform notation presented in Section 3. These definitions do not allow practical waveform generation as specified, but their development is necessary before computer simulation and hardware implementation for a channel simulator is possible. The practical implementation is described in Sections 4.6 and 4.7.

Transmission data output sequences are differentially encoded via modulo two addition given by

$$\xi_i = d_i \oplus d_{i-1}, \tag{4.1}$$

where $d_i \in [0,1]$ represents the i^{th} data bit value. The modulated bipolar value then becomes $\alpha_i = 1 - 2\xi_i$, where $\alpha_i \in [-1,1]$, which is passed to the GMSK modulator.

Notation used for a generalized phase-modulated waveform is developed in Appendix A. The GMSK phase term is given by:

$$\varphi(t, \boldsymbol{\alpha}) = \frac{\pi}{2} \sum_{i=-\infty}^{\infty} \alpha_i q(t - iT), \tag{4.2}$$

where the modulation index h is equal to 0.25 in Equation (A.4).[3] The pulse $q(t)$ is expressed as follows:

$$\begin{aligned} q(t) &= \int_{u=-\infty}^{t} g(u)du, \quad \text{where} \\ \mathrm{g(t)} &= \mathrm{h(t)} \otimes \mathrm{rect}\left(\frac{\mathrm{t}}{\mathrm{T}}\right) \\ \mathrm{h(t)} &= \frac{1}{\sqrt{2\pi}\sigma T} \exp\left[\frac{-t^2}{2\sigma^2 T^2}\right], \quad \text{and} \\ \sigma &= \frac{\sqrt{\ln(2)}}{2\pi \mathrm{BT}}. \end{aligned} \tag{4.3}$$

In Equation (4.3), modulating bit rate $1/T$ is 270.833 kb/s, and the time-bandwidth product TB is 0.3. In addition, a normalization constraint requires that $q(t)$ converge to unity as t approaches infinity.

The theoretical modulated RF carrier waveform for PCS 1900-based GMSK is converted to complex baseband form (see Appendix B) for implementation in the noise and interference model. The GMSK waveform output from the transmitter is expressed in bandpass form as:

$$x(t, \boldsymbol{\alpha}) = \sqrt{\frac{2E_s}{T}} \cos\left[2\pi f_c t + \varphi(t, \boldsymbol{\alpha}) + \varphi_0\right], \tag{4.4}$$

where $\varphi(t, \boldsymbol{\alpha})$ is defined in Equation (4.2), f_c is the carrier frequency, E_s is the energy/modulating bit, and φ_0 is a random phase term that is constant over the entire mobile station's assigned time slot. Using notation developed in Appendix B,

---

3 In [19], the modulation index h is specified as 0.5. The scale factor is different because the phase expression in Equation (4.2) is defined with a multiplier of 2π, instead of the π scale factor defined in [19].

$$
\begin{aligned}
x(t) &= \mathrm{Re}\left[x_{+}(t)\right] \\
&= \mathrm{Re}\left[\bar{x}(t)e^{j2\pi f_c t}\right] \\
&= \mathrm{Re}\left[R(t)e^{j\left[\varphi(t,\alpha)+\varphi_0\right]}e^{j2\pi f_c t}\right].
\end{aligned} \tag{4.5}
$$

Therefore $R(t) = \sqrt{\dfrac{2E_s}{T}}$, and

$$
\bar{x}(t,\boldsymbol{\alpha}) = \sqrt{\frac{2E_s}{T}}\exp\left[j\varphi(t,\boldsymbol{\alpha}) + j\varphi_0\right], \tag{4.6}
$$

which represents the PCS 1900-based GMSK complex envelope from a single transmitter. This expression applies to both base station and mobile station transmitters.

4.3 PCS 1900 Modulated Waveform Generation

One approach to PCS 1900-based GMSK waveform simulation is to develop the pulse $\alpha_i g(t)$ for each possible input symbol. These pregenerated pulses then can be transmitted in a random order, as specified by the output data stream from the abstracted transmission data block shown in Figure 4.2.

For GMSK, the two possible pulses, corresponding to $\alpha_i \in [-1,1]$, are generated by exciting a pulse-shaping filter with impulse response $g(t)$. Excitations corresponding to the two possible symbol values are represented by $u_{-1}(t) = -\delta(t)$ and $u_{+1}(t) = \delta(t)$, where $\delta(t)$ is the Dirac delta function. For $u(t) = u_{+1}(t) = \delta(t)$, $\alpha_{+1} g(t) = g(t)$. Similarly, for $u(t) = u_{-1}(t) = -\delta(t)$, $\alpha_{-1} g(t) = -g(t)$. The pulse-shaping filter is shown graphically in Figure 4.3.

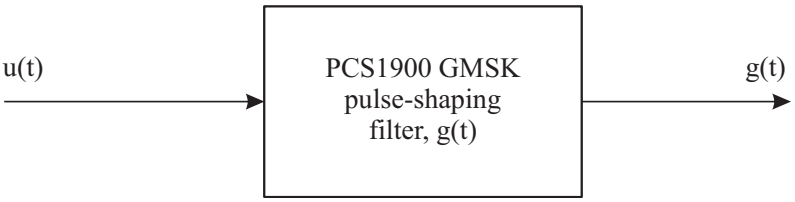

Figure 4.3. PCS 1900 GMSK pulse generation.

Pulses equal to $\pm g(t)$ are precomputed using Equation (4.3), and transmitted every T seconds, where $g(t)$ represents input symbol $\alpha_i = 1$, and $-g(t)$ represents input symbol $\alpha_i = -1$. The pulses $g(t)$ are used to modulate the instantaneous frequency $f_I(t)$ given by Equation (A.5). In an actual hardware implementation, this may be accomplished with an FM modulator, or by using lookup table techniques. For simulation, $\varphi(t,\boldsymbol{\alpha})$ is represented mathematically by Equations (4.2) and (4.3).

Everything prior to the generation of $\varphi(t,\boldsymbol{\alpha})$ in Equation (4.2) can be precomputed. The following section presents time-domain expressions for $\varphi(t,\boldsymbol{\alpha})|_{i=0}$ corresponding to each of the two possible symbol values. These then may be implemented as a component of the complex baseband expression for the GMSK waveform by appropriate delaying and summing of individual phase terms. This is demonstrated in Section 4.7, which details the simulation methodology.

4.3.1 Time-domain Representation of the Phase Expression

The PCS 1900-GMSK phase is most easily expressed in the time domain. Again, the PCS 1900-GMSK pulse $g(t)$ defined in Section 4.3 is the convolution of the Gaussian filter $h(t)$ described by Equation (4.3) with the rectangular function, $g(t) = h(t) \otimes \text{rect}\left(\frac{t}{T}\right)$. The convolution can be accomplished by remaining in the time domain, then solving the resulting integral. The convolution may also be solved as a multiplication in the frequency domain, but a nontrivial inverse Fourier transform of the phase term makes this impractical. Expressing $g(t) = h(t) \otimes \text{rect}\left(\frac{t}{T}\right)$ in Equation (4.3) as a convolution integral,

$$g(t) = \int_{\tau=-\infty}^{\infty} h(\tau)\text{rect}\left(\frac{t-\tau}{T}\right)d\tau. \tag{4.7}$$

To eliminate the rect[·] function, note that $\text{rect}\left(\frac{t-\tau}{\text{T}}\right)$ equals $\frac{1}{T}$ over the range $-\frac{1}{2} < \frac{t-\tau}{\text{T}} < \frac{1}{2}$, or $t - \frac{T}{2} < \tau < t + \frac{T}{2}$. Then $g(t)$ becomes:

$$g(t) = \frac{1}{T}\int_{\tau=t-\frac{T}{2}}^{t+\frac{T}{2}} h(\tau)d\tau. \tag{4.8}$$

Substituting Equation (4.3) into Equation (4.8), and defining constants a and b for Equation (4.3) as follows,

$$\begin{aligned} h(t) &= b \cdot \exp\left(-\frac{t^2}{a^2}\right), \quad \text{where} \\ a^2 &= 2\sigma^2 T^2, \quad \text{and} \\ b &= \frac{1}{\sqrt{2\pi}\sigma T}, \end{aligned} \tag{4.9}$$

$g(t)$ is then expressed as

$$g(t) = \frac{b}{T}\int_{\tau=t-\frac{T}{2}}^{t+\frac{T}{2}} \exp\left(-\frac{\tau^2}{a^2}\right)d\tau. \tag{4.10}$$

Changing the integration variables to $s = \frac{\tau}{a}$ and $ds = \frac{d\tau}{a}$, Equation (4.10) becomes,

$$g(t) = \frac{ab}{T}\int_{s=\frac{t}{a}-\frac{T}{2a}}^{\frac{t}{a}+\frac{T}{2a}} \exp\left(-s^2\right)ds. \tag{4.11}$$

Next, g(t) is expressed as two integrals by splitting the region of integration,

$$g(t) = \frac{ab}{T} \int_{s=\frac{t}{a}-\frac{T}{2a}}^{\infty} \exp\left(-s^2\right) ds - \frac{ab}{T} \int_{s=\frac{t}{a}+\frac{T}{2a}}^{\infty} \exp\left(-s^2\right) ds. \tag{4.12}$$

The integrals in Equation (4.12) can be expressed in terms of the complementary error function, which is defined as:

$$\operatorname{erfc}(w) = \frac{2}{\sqrt{\pi}} \int_{s=w}^{\infty} \exp\left(-s^2\right) ds. \tag{4.13}$$

Substituting Equation (4.13) into Equation (4.12), and replacing the constants *a* and *b* defined in Equation (4.9), the expression for $g(t)$ becomes:

$$g(t) = \frac{1}{2T}\left[\operatorname{erfc}\left(\frac{2\pi B\left(t-\frac{T}{2}\right)}{\sqrt{2\ln 2}}\right) - \operatorname{erfc}\left(\frac{2\pi B\left(t+\frac{T}{2}\right)}{\sqrt{2\ln 2}}\right)\right], \tag{4.14}$$

where TB is defined in Equation (4.3). For $i = 0$, the PCS 1900-GMSK phase term is expressed as:

$$\varphi(t,\alpha)|_{i=0} = \frac{\pi}{2} \int_{\tau=-\infty}^{t} g(\tau) d\tau. \tag{4.15}$$

Values other than $i = 0$ may be simulated by shifting the phase expression by T seconds for each symbol. The aggregate phase expression is computed by summing Equation (4.15) over all values of *i*.

Note that the integration in Equation (4.15) cannot be solved analytically. It must be computed numerically, or solved by expansion in a power series. The ITS N/I model uses numerical integration to precompute the phase for each of the two possible symbols. The phase component created by each symbol must be time-limited for computer simulation. In a real PCS implementation, the Gaussian pulse $g(t)$ will be truncated symmetrically to an even integer multiple of length T. For the ITS N/I model, the Gaussian pulse is truncated such that it is nonzero only on the interval $[-2T < t < 2T]$. Consecutive symbols are simulated by shifting the pulse by T seconds for each symbol after precomputation, then summing over all phase components.

As an option, the phase expression may be approximated by a power series. Although the ITS model does not employ the power series approximation, the derivation is presented as an alternative time-domain implementation. This method is presented for those who wish to avoid a numerical integration. However, the final expression (given in Equation (4.23)) proves to be much more difficult to implement than the numerical integration method described in Section 4.3.2.

First, the complementary error function expression for $g(t)$ in Equation (4.14) is converted to the error function. Since $\text{erfc}(w) = 1 - \text{erf}(w)$, Equation (4.14) can be written as:

$$g(t) = \frac{1}{2T}\left[\text{erf}\left(\frac{2\pi B\left(t+\frac{T}{2}\right)}{\sqrt{2\ln 2}}\right) - \text{erf}\left(\frac{2\pi B\left(t-\frac{T}{2}\right)}{\sqrt{2\ln 2}}\right)\right], \tag{4.16}$$

and letting

$$\mathrm{u}_1 = \text{erf}\left(\frac{2\pi B\left(t+\frac{T}{2}\right)}{\sqrt{2\ln 2}}\right) \quad \text{and} \quad \mathrm{u}_2 = \text{erf}\left(\frac{2\pi B\left(t-\frac{T}{2}\right)}{\sqrt{2\ln 2}}\right), \tag{4.17}$$

where it is understood that u_1 and u_2 are both time functions, Equation (4.16) becomes:

$$g(t) = \frac{1}{2T}\cdot\left[\text{erf}(u_1) - \text{erf}(u_2)\right]. \tag{4.18}$$

Erf(x) can be expanded into a power series, given by [20],

$$\text{erf}(x) = \frac{2}{\sqrt{\pi}}\sum_{k=1}^{\infty}\frac{(-1)^{k+1}x^{2k-1}}{(k-1)!(2k-1)}, \tag{4.19}$$

which is integrable. Then, substituting Equation (4.18) into Equation (4.15) yields:

$$\varphi(t,\boldsymbol{\alpha})|_{i=0} = \frac{\pi}{4T}\int_{\tau=-\infty}^{t}\left[\text{erf}(u_1) - \text{erf}(u_2)\right]d\tau. \tag{4.20}$$

Combining Equations (4.19) and (4.20) results in:

$$\varphi(t,\boldsymbol{\alpha})|_{i=0} = \frac{\pi}{4T}\int_{\tau=-\infty}^{t}\left[\sum_{k_1=1}^{\infty}\frac{(-1)^{k_1+1}u_1^{2k_1-1}}{(k_1-1)!(2k_1-1)} - \sum_{k_2=1}^{\infty}\frac{(-1)^{k_2+1}u_2^{2k_2-1}}{(k_2-1)!(2k_2-1)}\right]d\tau. \tag{4.21}$$

By letting $-nT$ be the lower limit of the integration, where n is the integral number of modulated symbol durations T on each side of the origin for the 0^{th} symbol only, Equation (4.21) becomes (substituting for u_1 and u_2):

$$\varphi(t,\boldsymbol{\alpha})|_{i=0} = \frac{\sqrt{\pi}}{2T}\int_{\tau=-nT}^{t}\sum_{k_1=1}^{\infty}\frac{(-1)^{k_1+1}\left(\frac{2\pi B\left(\tau+\frac{T}{2}\right)}{\sqrt{2\ln 2}}\right)^{2k_1-1}}{(k_1-1)!(2k_1-1)}d\tau - \frac{\sqrt{\pi}}{2T}\int_{\tau=-nT}^{t}\sum_{k_2=1}^{\infty}\frac{(-1)^{k_2+1}\left(\frac{2\pi B\left(\tau-\frac{T}{2}\right)}{\sqrt{2\ln 2}}\right)^{2k_2-1}}{(k_2-1)!(2k_2-1)}d\tau. \tag{4.22}$$

which may then be integrated as follows:

$$\varphi(t,\boldsymbol{\alpha})|_{i=0} = \frac{\sqrt{2\ln 2}}{4\sqrt{\pi}BT}\left[\sum_{k_1=1}^{\infty}\frac{(-1)^{k_1+1}\left(\frac{2\pi B\left(\tau+\frac{T}{2}\right)}{\sqrt{2\ln 2}}\right)^{2k_1}}{2k_1(k_1-1)!(2k_1-1)} - \sum_{k_2=1}^{\infty}\frac{(-1)^{k_2+1}\left(\frac{2\pi B\left(\tau-\frac{T}{2}\right)}{\sqrt{2\ln 2}}\right)^{2k_2}}{2k_2(k_2-1)!(2k_2-1)}\right]_{\tau=-nT}^{t} \tag{4.23}$$

4.3.2 Calculation of the PCS 1900-GMSK Phase Pulse Using Numerical Integration

In the previous sections, expressions for the phase of the PCS 1900 GMSK waveform were derived in terms of the phase pulse $g(t)$ in the time domain. Theoretically, $g(t)$ is defined over the interval $[-\infty < t < \infty]$, and $g(t)$ must also be integrated from negative infinity to t to obtain the phase component from each transmitted symbol in every PCS 1900 time slot. Of course, this is impossible to implement in a channel simulation directly; therefore, approximations that reflect actual PCS 1900 modulator and transmitter operation must be made.

The noise and interference model is precomputed $g(t)$ and the integration is performed numerically in Unix-based software using the time-domain expressions described in Section 4.3.1. This is not as time-consuming as it sounds, because only two possible symbol values exist for the PCS 1900 GMSK system, corresponding to $+g(t)$ and $-g(t)$. This results in a one-time single integration accomplished separately from simulations that use the phase expression. Other higher-level simulations use time-shifted versions of this precomputed phase expression.

Note that the precomputed integration of $g(t)$ corresponds to the phase component resulting from a single PCS 1900-GMSK symbol. Because GMSK modulation possesses memory properties, the actual phase value for each transmitted symbol duration will be the accumulated sum of phase values from previously transmitted symbols within the PCS 1900 time slot. The resultant phase

value is computed by higher-level simulation as the sum of all precomputed and time-shifted phase components, and is not part of the precomputation routine.

To precompute the phase expression component from a single PCS 1900-GMSK transmitted symbol, several pieces of information are needed. These include the modulated symbol duration, the 3-dB bandwidth of the Gaussian filter $G(f)$ corresponding to impulse response $g(t)$, the integer number n of modulated bit durations needed to integrate $g(t)$, and the number of samples N needed to accurately represent $g(t)$. Equation (4.18) is the starting point, which is repeated here for convenience:

$$g(t) = \frac{1}{2T}\left[\text{erf}(u_1(t)) - \text{erf}(u_2(t))\right]. \tag{4.24}$$

Functions u_1 and u_2 are given in Equation (4.17). To obtain $\varphi(t,\alpha)|_{i=0} = \varphi(t,\alpha_0) \stackrel{\Delta}{=} \varphi(t)$, which represents the phase value due to the $i = 0^{th}$ symbol value only, $g(t)$ must be integrated numerically over a finite interval.

Practical GMSK modulators integrate the Gaussian pulse over an integral number of modulated symbol lengths. This is accomplished in the simulation by phase precomputation. Phase precomputation is realized by iteratively integrating $g(t)$ from $-nT$ to t, increasing t for each iteration to approximate a continuous time function. If T is the symbol duration, the phase expression due to the $i = 0^{th}$ symbol becomes (using Equation (4.20)):

$$\varphi(t) = \frac{\pi}{4T}\int_{\tau=-nT}^{t}\left[\text{erf}(u_1(\tau)) - \text{erf}(u_2(\tau))\right]d\tau. \tag{4.25}$$

Substituting $u_1(t)$ and $u_2(t)$ in Equation (4.25),

$$\begin{aligned} u_1(\tau) &= u_1 = \frac{2\pi B}{\sqrt{2\ln 2}}\left(\tau + \frac{T}{2}\right) \\ u_2(\tau) &= u_2 = \frac{2\pi B}{\sqrt{2\ln 2}}\left(\tau - \frac{T}{2}\right) \end{aligned} \tag{4.26}$$

and

$$du_1 = \frac{2\pi B}{\sqrt{2\ln 2}}d\tau = du_2 \tag{4.27}$$

yields

$$\varphi(t) = \frac{\pi}{4T}\left(\frac{\sqrt{2\ln 2}}{2\pi B}\right)\int_{u_1=\frac{2\pi B}{\sqrt{2\ln 2}}\left(-nT+\frac{T}{2}\right)}^{\frac{2\pi B}{\sqrt{2\ln 2}}\left(t+\frac{T}{2}\right)} erf(u_1)du_1 - \frac{\pi}{4T}\left(\frac{\sqrt{2\ln 2}}{2\pi B}\right)\int_{u_2=\frac{2\pi B}{\sqrt{2\ln 2}}\left(-nT-\frac{T}{2}\right)}^{\frac{2\pi B}{\sqrt{2\ln 2}}\left(t-\frac{T}{2}\right)} erf(u_2)du_2. \quad (4.28)$$

A computer program was written to iteratively perform the integration in Equation (4.28) from $-nT$ to $t = mT_p$, where m is an iteration counter defined from $m = 1$ to $m = N$, and T_p is the phase expression's sampling interval. An adaptive-recursive Newton-Cotes algorithm was used for the integration. Figure 4.4 shows the phase pulse *g(t)*; Figure 4.5 displays the resulting phase after performing the integration in Equation (4.28).

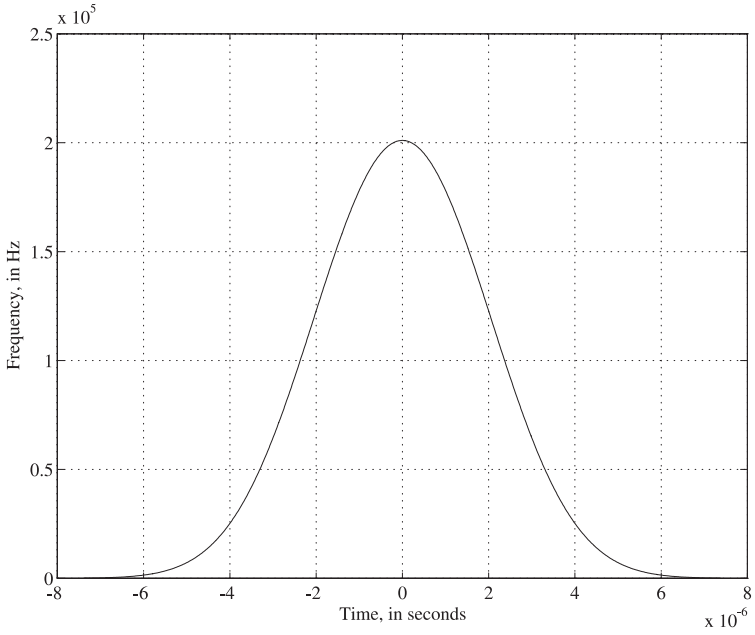

Figure 4.4 GMSK phase pulse, $g(t)$.

4.4 Power Considerations

In addition to geographic distribution and modulation type, the output power level of PCS 1900 transmitters must be quantified in the N/I model. The output power of a PCS 1900 mobile station or base station transmitter is defined as the time average over the useful part of a burst (time slot), as measured at the output to the passive radiation apparatus. This does not include dummy bits transmitted during ramp-up and ramp-down transitions at the beginning and at the end of a burst,

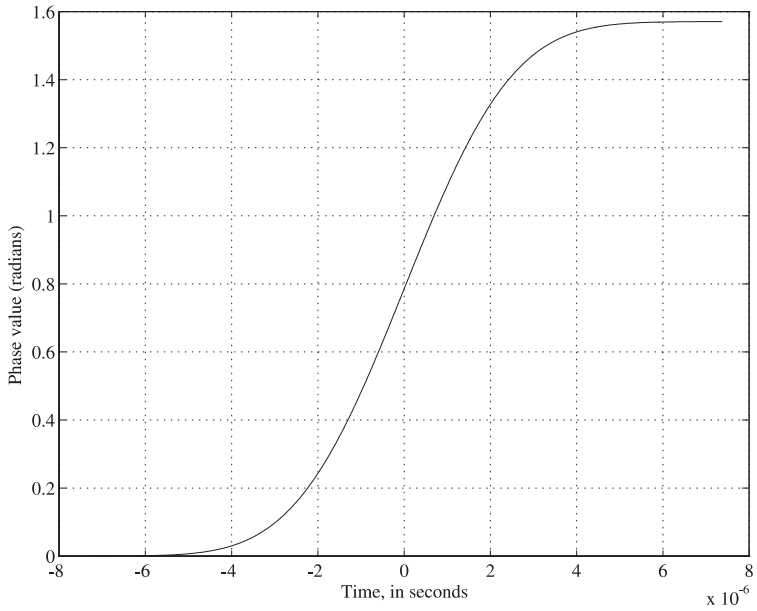

Figure 4.5 Resulting phase $p(t)$ after integration of Equation (4.28).

respectively. Calculations and expressions below reflect the power levels at a transmitter reference point. This reference point is used for all output waveform amplitude calculations in the ITS N/I model. Figure 4.6 shows the power measurement point X at the transmitter.

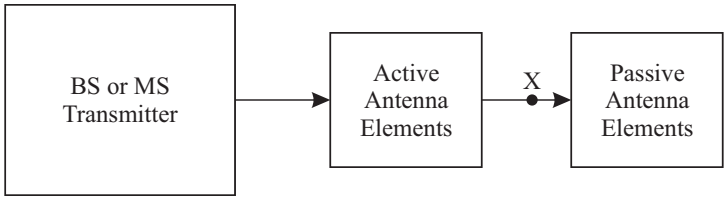

Figure 4.6. PCS 1900 reference diagram showing the power measurement point, X.

The average power per PCS 1900 burst is defined by:

$$P_{av,B} = \frac{1}{T_B}\int_{t=0}^{T_B} \frac{2E_S}{T}\cos^2\left[2\pi f_c t + \varphi(t,\alpha)\right]dt = \frac{E_s}{T}, \tag{4.29}$$

where T_B is the time duration of the burst, E_S is the energy per symbol, and T is the symbol duration. As expected, the constant envelope expression yields a constant average power value.

For the mobile station, the maximum transmitted power, $\left(\frac{E_S}{T}\right)_{\max}$, is 2W, as specified in [19]. The PCS 1900-based GMSK complex envelope defined in Equation (4.6) then becomes, for a maximum power transmission from a single mobile station:

$$\bar{x}(t,\boldsymbol{\alpha})\big|_{\max,\mathrm{MS}} = 2\exp\left[j\varphi(t,\boldsymbol{\alpha}) + j\varphi_0\right] \quad \text{V.} \tag{4.30}$$

Likewise, the maximum transmitted power from a PCS 1900 base station per RF carrier $\left(\frac{E_S}{T}\right)_{\max}$, is equal to 40 W, with the total power output from all RF carriers transmitted from the base station not exceeding 1000 W. The PCS 1900-based GMSK complex envelope defined in Equation (4.6) for a maximum power transmission on one RF carrier from a single base station is then given by:

$$\bar{x}(t,\boldsymbol{\alpha})\big|_{\max,\mathrm{BS}} = \sqrt{80}\exp\left[j\varphi(t,\boldsymbol{\alpha}) + j\varphi_0\right] \quad \text{V.} \tag{4.31}$$

Maximum power requirements provide an upper bound for the N/I waveform. The actual interference power incident at the receiver under study will typically be the sum of multiple interferers, with each interferer subject to channel impairments via a separate propagation path. Channel impairments and losses, which are functions of distance, location, and velocity, are included in the N/I model after determining output waveform levels at the power reference point.

4.5 Timing and Synchronization

For a receiver operating in a multiple access wireless environment, waveform acquisition involves some method of gaining timing and synchronization before information is transmitted on the link. TDMA systems, such as PCS 1900, will maintain symbol, slot, and frame synchronization on all logical channels on the forward link because the waveform is combined within the base station before transmission. Symbol synchronization is not assumed between different base station transmissions on the forward link.

However, the reverse link multiple access waveform symbols are generally not synchronized from time slot to time slot. Each mobile station will transmit its modulated symbol stream with a random phase term that is constant over the entire time slot. In addition, geographic distribution of mobile stations within the cell will result in a time offset of the symbol stream that is proportional to the distance from the base station. For these reasons, a random $U(0,2\pi]$ phase term and $U(0,T]$ offset is added to each symbol stream on the reverse link.

4.6 Interference Expressions

In Section 3, the PCS cellular geometry for intrasystem interference was described, and technology-independent interference waveform expressions were developed. In Section 4 up to this point, a physical-layer description of a single PCS 1900 modulator was given. For characterization of the total intrasystem N/I environment for PCS 1900, the description of the single PCS 1900 modulator

must be extended to represent the numerous interferers typically encountered at any given time during a call session. This is accomplished by duplicating the single PCS 1900 modulator expression once for each of the interferers, and distributing them via the geometric expressions described in Section 3. In addition to geometric distribution, the expressions of Section 3 also incorporate delay, propagation loss, and Doppler shift functions that may be chosen arbitrarily. Multipath may be included by duplicating each single interferer N_p times, where N_p is the integer number of paths. Each path must be delayed and weighted as specified by an appropriate multipath model.

Two cases are considered for the PCS 1900-specific interference waveform: 1) uplink intercell interference, and 2) downlink intercell interference. Because PCS 1900-GMSK modulation is used for both base station and mobile station transmissions, the modulation expressions described earlier in Section 4 apply to both uplink and downlink; only the transmitted power level differs.

4.6.1 Uplink Interference Expressions

Uplink intrasystem interference from PCS 1900 is caused by mobile stations in nearby cells radiating unwanted energy into the receiver frequency band of the primary cell's base station. PCS 1900 generates a waveform with eight time slots per simplex RF carrier, hence the maximum number of interfering mobile stations is eight/cell/RF carrier. Adjacent RF channels may be considered by frequency-shifting the entire interference waveform by the adjacent channel distance, which is 200 kHz for PCS 1900. Mobile stations in the primary cell all should be synchronized to the proper assigned time slot.

Equation (3.1) provides generic expressions for uplink intrasystem interference. Because PCS 1900 is a TDMA technology, the parameter *b* is given the value 1 to simulate the time slot offsets from each mobile station in an interfering cell. Equation (3.1) then becomes:

$$\begin{aligned} \overline{x_{FI\,(k,-)}}(t) &= \sum_{n=0}^{N_U-1} \overline{x_{FI\,(k,n)}}\left(t - nT_U - \frac{r_{k,n}}{c}\right) a_{k,n}\left(r_{k,n}, \theta_{k,n}\right) \\ \overline{x_{FI}}(t) &= \sum_{k=0}^{N_I-1} \overline{x_{FI\,(k,-)}}(t), \end{aligned} \tag{4.32}$$

where $\overline{x_{FI\,(k,n)}}(t)$ represents the interference waveform created by the nth mobile station in interfering cell k, defined over one time slot only. $\overline{x_{FI\,(k,n)}}(t)$ is given by Equation (4.6), which as a function of α, *n*, and *k* is written as:

$$\overline{x_{FI\,(k,n)}}(t,\alpha) = \sqrt{\frac{2E_S}{T}} \exp\left[j\varphi_{FI\,(k,n)}(t,\alpha) + j\varphi_{0,FI\,(k,n)} \right], \tag{4.33}$$

and $\boldsymbol{\alpha} = \boldsymbol{\alpha}(k,n)$ represents the symbol stream from the n^{th} mobile station in cell k. $\varphi_{FI\,(k,n)}(t,\boldsymbol{\alpha})$ is defined over one time slot as a continuously modulated phase based upon the transmitted symbol stream $\boldsymbol{\alpha} = \boldsymbol{\alpha}(k,n)$, and $\varphi_{FI\,(k,n)}$ is a random phase term that is constant over the entire time slot.

$\varphi_{FI\,(k,n)}(t,\boldsymbol{\alpha})$ may be computed using any of the techniques described in Section 4. The phase corresponding to an entire time slot is:

$$\varphi_{FI\,(k,n)}(t,\boldsymbol{\alpha}) = \sum_{m=1}^{N_{bits}} \alpha_1 \varphi(t - mT) \;\; 0 \le t \le T_u \,, \tag{4.34}$$

where T is the modulated symbol duration, N_{bits} is the number of bits (symbol durations) per time slot, and T_u is the duration of a time slot. $\varphi(t)$ is given by Equation (4.34), and represents the phase component due to a single positive $(\alpha_1 = +1)$ modulated GMSK symbol. Because only two symbol states exist for GMSK, $\varphi(t)$ and $-\varphi(t)$ (corresponding to $\alpha_1 = +1$ and $\alpha_1 = -1$, respectively), the phase term for the entire time slot may be expressed as time-delayed versions of $\varphi(t) = \varphi_{FI\,(k,n)}(t,\alpha)|_{i=0}$, scaled by either +1 or -1. Note that each symbol spans more than T seconds, therefore symbols will overlap.

In Equation (4.32), $\overline{x_{FI\,(k,-)}}(t)$ represents the sum of all interfering mobile stations from the k^{th} interfering cell, as seen at the primary cell's base station, and $\overline{x_{FI}}(t)$ is the aggregate interference waveform from all NI interfering cells. Note that $\overline{x_{FI\,(k,-)}}(t)$ and $\overline{x_{FI}}(t)$ are defined over one PCS 1900 frame (eight time slots), corresponding to 4.6 ms. A summary of all values in Equations (4.32)-(4.34) is given in Table 4.1.

Table 4.1. Summary of Reverse Link Parameter Values

Parameter/Function	Description	Value
N_{bits}	Number of bits (symbol durations) per time slot	156.25
N_U	Number of time slots per RF carrier	8
N_I	Number of interfering cells	Integer variable
T	Modulated symbol duration	6/1.625 x 10^6 s
T_u	Time slot duration	$N_{bits}T$ s
$\boldsymbol{\alpha} = \boldsymbol{\alpha}(k,n)$	Symbol stream from the nth mobile station in cell k	Random or user-defined
$\varphi_{0,FI(k,n)}$	Random phase term that is constant over each interfering mobile station's time slot	Random or user-defined; suggest uniform $[0,2\pi)$ probability density function (pdf)
$\sqrt{\frac{2E_s}{T}}$	Maximum transmission level from each mobile station interferer	2 V; see Section 4.4
c	Waveform propagation speed in medium	Typically 3 x 10^8 m/s
$a_{k,n}(r_{k,n}, \theta_{k,n})$	Propagation loss/Doppler shift function	Many models possible; see Section 3.3
TB	Time-bandwidth product	0.3

4.6.2 Downlink Interference Expressions

GSM downlink interference is caused by base stations outside the primary cell transmitting unwanted energy to mobile stations within the primary cell. Because the phase modulation for the downlink interferers is identical to the uplink phase modulation, they will have a form similar to Equations (4.33) and (4.34) of the previous section, with a slightly different interpretation.

Equation (3.2) gives the generic expression for downlink intrasystem interference, repeated for convenience:

$$\overline{x_{FI\,(-,n)}}(t) = \sum_{k=0}^{N_I-1} \overline{x_{FI\,(k,n)}}\left(t - \frac{r_{k,n}}{c}\right) a_{k,n}\left(r_{k,n}, \theta_{k,n}\right). \tag{4.35}$$

In Equation (4.35), $\overline{x_{FI\,(k,n)}}(t)$ represents the interference waveform to the n^{th} mobile station from the base station in interfering cell k, which is defined over one frame consisting of eight time slots. $\overline{x_{FI\,(k,n)}}(t)$ is given by Equation (4.6), which, just as for the uplink interference waveform, becomes a function of $\boldsymbol{\alpha}$, n, and k as follows:

$$\overline{x_{FI\,(k,n)}}\left(t, \boldsymbol{\alpha}\right) = \sqrt{\frac{2E_s}{T}} \exp\left[j\varphi_{FI\,(k,n)}\left(t, \boldsymbol{\alpha}\right) + j\varphi_{0,FI\,(k,n)} \right], \tag{4.36}$$

where $\boldsymbol{\alpha} = \boldsymbol{\alpha}(k)$ represents the symbol stream from the k^{th} interfering cell's base station to the n^{th} mobile station in the primary cell. Note that the symbol stream is not a function of n, since all mobile stations in the primary cell will encounter the same common symbol stream from the k^{th} interfering cell's base station. $\varphi_{FI\,(k)}(t, \boldsymbol{\alpha})$ is now defined over one time frame as a continuously modulated phase term based upon the transmitted symbol stream $\boldsymbol{\alpha} = \boldsymbol{\alpha}(k)$, and $\varphi_{0,FI\,(k)}$ is a random phase term that is constant over the entire frame.

$\varphi_{FI\,(k)}(t, \boldsymbol{\alpha})$ may be computed using any of the techniques described in Section 4. The phase corresponding to an entire frame is:

$$\varphi_{FI\,(k)}(t, \boldsymbol{\alpha}) = \sum_{m=1}^{N_{bits} \cdot N_U} \alpha_1 \varphi(t - mT) \qquad 0 \le t \le T_F \tag{4.37}$$

where T is the modulated symbol duration, N_{bits} is the number of bits (symbol durations) per time slot, and T_F is the duration of a frame. $\varphi(t)$ is given by Equation (4.34), and represents the phase component due to a single positive $(\alpha_1 = +1)$ modulated GMSK symbol. Because only two symbol states exist for GMSK, $\varphi(t)$ and $-\varphi(t)$ (corresponding to $\alpha_1 = +1$ and $\alpha_1 = -1$, respectively), the phase expression for the entire frame may be expressed as time-delayed versions of $\varphi(t) = \varphi_{FI\,(k)}(t, \alpha_i)|_{i=0}$, scaled by either +1 or -1. As in the reverse link, the GMSK phase terms will

overlap. From Equation (4.35), $\overline{x_{FI(-,n)}}(t)$ represents the sum of all N_I interfering base station waveforms as seen by the n^{th} mobile station in the primary cell. A summary of all values in Equations (4.35)-(4.37) is given in Table 4.2. Many are identical to those described in Section 4.6.1.

Table 4.2. Summary of Forward Link Parameter Values

Parameter/Function	Description	Value
N_{bits}	Number of bits (symbol durations) per time slot	156.25
N_U	Number of time slots per RF carrier	8
N_I	Number of interfering cells	Integer variable
T	Modulated symbol duration	$6/1.625 \times 10^6$ s
T_F	Frame duration	$N_U N_{bits} T$ s
$\alpha = \alpha(k)$	Symbol stream from the base station in the k^{th} interfering cell	Random or user-defined
$\varphi_{0,FI(k)}$	Random phase term that is constant over each interfering base station's frame	Random or user-defined; suggest uniform $[0,2\pi)$ pdf
$\sqrt{\frac{2E_s}{T}}$	Maximum transmission level from each base station interferer	$\sqrt{80}$ V; see Section 4.4
c	Interference waveform propagation speed	Typically 3×10^8 m/s
$a_{k,n}(r_{k,n}, \theta_{k,n})$	Propagation loss /Doppler shift function	Many models possible; see Section 3.4
TB	Time-bandwidth product	0.3

4.7 Computer Simulation of the PCS 1900 Noise and Interference Environment

As part of the model validation and verification process, a computer simulation of the PCS 1900 N/I analytical model was developed. Computer simulation provides valuable insight into the nuances of model implementation in a real-time hardware channel simulator. As an added benefit, the computer simulation may be used as a tool to study N/I scenarios based on parametric inputs. For example, a study of cell size vs. interference level may be conducted by iteratively running the simulation, while increasing the cell size parameter. Power-level impacts may be profiled by explicitly setting the transmitted power level of each individual interferer.

The simulation code is designed to be flexible and readily adaptable to many types of TDMA-based PCS systems. Because PCS 1900 uplink and downlink interference waveforms are very similar, running simulations for each requires only minor changes in the TDMA-based code. The PCS 1900 uplink N/I simulation is described below. Section 4.7.1 describes the methodology used for computer simulation of interference to the PCS 1900 uplink, and Section 4.7.2 presents corresponding sample simulation outputs.

4.7.1 Uplink Simulation Methodology for Noise and Interference Generation

Simulation of the PCS 1900 uplink interference provided the aggregate interference waveform caused by nearby interfering cells, as seen at the primary cell's base station receiver. A few assumptions were made to simplify the computations, and to randomize certain parameters as follows:

1. All interfering cells within a given iteration of the program are equidistant from the primary cell's base station.
2. Each simulation iteration calculates the aggregate waveform due to a single radius within each layer of interfering cells. For example, the interference waveform from cells adjacent to the primary cell will be computed in one iteration, since all cells are equidistant. Since two different distances are needed for the second layer of interfering cells, two iterations are required. The total waveform is computed by adding several simulation iterations together. Obtaining the interference waveform due to interferers in both adjacent- and second-layer cells therefore requires three simulation iterations.
3. All interfering cells transmit on the same RF carrier frequency. Cells not contributing to the overall interference waveform (e.g., resulting from a cell reuse pattern) may be "zeroed out" during the computation.
4. PCS 1900 frames from interfering cells are aligned (this may be changed as a simulation parameter).
5. Symbols are not aligned from interferer to interferer. A random $U(0,T]$ delay is incorporated in each symbol stream.

The methodology for computing the aggregate uplink interference waveform is not complicated, although the details are rather involved. The major steps, in order of execution, are as follows:

1. Load all parameters for the simulation. These parameters are given in Table 4.3 with corresponding descriptions and values.

Table 4.3. Uplink Interference Waveform Simulation Parameters

Parameter/Function	Description	Value
f_c	Channel carrier frequency; included as a parameter for frequency-dependent channel models	Ranges from 1850 to 1910 MHz
P_{av}	Average (maximum) transmit power of each mobile station	2 W
symbol	Number of possible symbol values; for GMSK, two symbol values are possible	2

Parameter/Function	Description	Value
T	Modulated symbol duration	6/1.625 x 10^6 s
N_s	Total number of modulated symbol intervals, including guard times, per time slot	156.25
N_g	Total number of guard symbol intervals per time slot (assumes NORMAL GSM burst type)	8.25
N_u	Number of users per frame in primary cell uplink waveform	8
$N_u I$	Number of users per frame in each nearby cell's interference waveform	8
c	Waveform propagation speed in medium	3 x 10^8 m/s
R	Cell radius	500 m
d_{x_k}	Linear X distance of each interfering cell's base station with respect to the primary cell's base station	1000 m (depends on R and the geographical location of the interfering cell)
d_{y_k}	Linear Y distance of each interfering cell's base station with respect to the primary cell's base station	1000 m (depends on R and the geographical location of the interfering cell)
N_{ic}	Number of interfering cells	Varies according to the iteration. Equals 6 for adjacent cells, but may be set to any number
$a_{k,n}(r_{k,n}, \theta_{k,n})$	Propagation loss/Doppler shift function; may also be set explicitly to demonstrate a particular power distribution	Default is the simple $1/r^4$ propagation loss law

2. Load the precomputed phase expression for a single PCS 1900-GMSK symbol. A separate program was written to precompute the the phase expression from a single PCS 1900-GMSK symbol, as described in detail in Section 4.3.2. This expression is defined symmetrically over 4T sec., and contains 1000 samples. Since the phase expression is highly oversampled, it is first decimated by the parameter decfactor. This reduces the computational load considerably. The decimation factor also defines the simulation bandwidth for the N/I waveform.

3. Filter the phase expression (optional). The phase expression may be filtered to meet specified transmission emissions limits. Several different types of filtering are provided in the program.

Steps 4-6 are used to form a reference desired uplink waveform for the primary cell. This waveform is not part of the aggregate interference waveform.

4. Calculate positions of users in the primary cell. Mobile stations are randomly placed in the primary cell. The base station is assumed to be at the origin. Default distribution of mobile stations is random uniform. In polar coordinates, this means that the angular

distribution is $U[0,2\pi)$, and the distance from the base station has pdf $\frac{2r}{R^2}$. The coordinates for each mobile station are stored in polar form.

5. Calculate propagation loss/Doppler shift function for each mobile station. Any propagation loss/Doppler shift function may be implemented in this step. The default is a simple $\frac{1}{r^4}$ propagation loss law.

6. Calculate the burst from each user. This is accomplished by looping over each time slot of the PCS 1900 frame. In the process, a random symbol sequence is created for each time slot. The sequences are modulated in complex baseband form, then shifted and superimposed to form a single PCS 1900 frame. In the process, the propagation loss function is incorporated, and guard times included. Modulated symbol streams from each mobile station include a random $U[0,2\pi)$ phase term, and random $U[0,T)$ delay.

In steps 7-10, the aggregate interference waveform is computed. The interference component from each interfering cell is computed iteratively, then all the components are combined.

7. Calculate positions of mobile stations in each interfering cell. Interfering mobile stations are randomly placed in the k^{th} interfering cell. Default distribution of mobile stations is random uniform, with angular distribution $U[0,2\pi)$, and base station distance r with pdf $\frac{2r}{R^2}$. Translation of coordinates is accomplished in accordance with the expressions derived in Section 3.3. The coordinates for each mobile station are stored in polar form.

8. Calculate propagation loss/Doppler shift function for each mobile station in the kth interfering cell. Again, any propagation loss/Doppler shift function may be implemented in this step. The default is a simple $\frac{1}{r^4}$ propagation loss law.

9. Calculate the burst from each user in the k^{th} interfering cell. This is accomplished by looping over each time slot of the PCS 1900 frame. Similarly, a random symbol sequence is created for each time slot. The sequences are modulated in complex baseband form, then shifted and superimposed to form a single PCS 1900 frame. Equations used were derived in Section 4.6.1. In the process, the propagation loss function is incorporated, and guard times are included. Modulated symbol streams from each mobile station include a random $U[0,2\pi)$ phase term and random $U[0,T)$ delay.

10. Compute the aggregate waveform. Steps 7 - 9 are executed for each interfering cell. After each iteration k, the k^{th} interference component is added to the aggregate interference waveform, which is defined over one PCS 1900 frame. This is expressed analytically by the second part of Equation (4.32).

11. Compute the interference waveform statistics. These include spectral plots, voltage envelope histograms, power envelope histograms, and phase distributions.

4.7.2 Example Results

Many different N/I scenarios may be created by setting the simulation parameters accordingly, and consequently a large number of different simulation studies may be conducted. As an example, simulations were run for the default values listed in Table 4.3. Three simple cases were chosen to demonstrate the capabilities of the simulation tool:

Case 1: Six interfering cells, all adjacent to the primary cell.
Case 2: Twelve interfering cells, all equidistant from the primary cell.
Case 3: Fifty interfering cells, all equidistant from the primary cell.

For cases 2 and 3, significant overlap in coverage area occured, while case 1 reflects a more realistic scenario. Three plots were created for each case, showing statistics of the aggregate interference waveform in the following order: 1) the voltage envelope histogram, 2) the power envelope histogram, and 3) the phase distribution histogram.

Results for Case 1. Figures 4.7, 4.8, and 4.9 show the voltage envelope, power envelope, and phase histograms, respectively, of the interference waveform caused by six adjacent interfering cells. The amplitude envelope distribution appears Rayleigh-distributed, although it is quite distorted in form. The large value at zero is caused by the guard times, and the simulation assumption that frames in adjacent cells are aligned (when frames are aligned, so are the guard times—resulting in a large number of zero values). Randomization of frame alignment in the simulation simply involves circularly rotating each interfering cell waveform component before aggregation.

Similarly, the power envelope distribution appears as a distorted exponential in Figure 4.8. The phase distribution of Figure 4.9 is roughly uniformly distributed on the interval $[-\pi, \pi)$. Again, the large count value at zero is caused by the guard times.

Results for Case 2. In Figures 4.10, 4.11, and 4.12, the number of simulated interfering cells was increased to twelve, with all other parameters the same as for the other cases. Notice that the amplitude envelope profile given in Figure 4.10 appears more Rayleigh-distributed, the power envelope in Figure 4.11 appears more exponential, and the phase distribution in Figure 4.12 appears more uniform than those for case 1.

Results for Case 3. The results for the fifty interfering cells of case 3 demonstrate further smoothing of the distributions, as shown by Figures 4.13, 4.14, and 4.15.

Figure 4.16 shows a sample unfiltered aggregate interference waveform spectrum. Longer samples of the interference waveform were derived by concatenating numerous instances of the single frame generated by the simulation.

In summary, this simple case has demonstrated the trend towards a Gaussian interference waveform as the number of approximately equidistant (equipower) interferers increases. If the equipower assumption holds, the interference environment for the PCS 1900 uplink may be modeled as Gaussian noise. However, if the equipower assumption—indirectly specified by the transmit power of each interfering mobile station—does not hold, what are the consequences?

By setting the power levels explicitly for each interfering mobile station, it is readily demonstrated that the interference waveform is not purely Gaussian. Figure 4.17 shows the resulting distorted amplitude envelope when a single interfering mobile station has its transmitted waveform multiplied by a factor of ten. The distribution and power level of interferers may be explicitly set to any value.

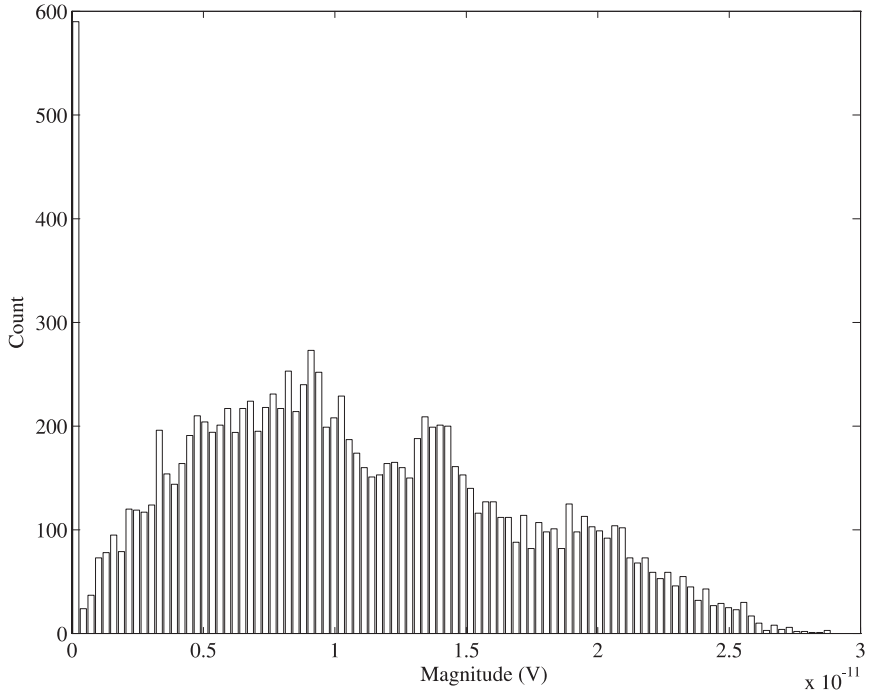

Figure 4.7. Voltage envelope histogram for case 1.

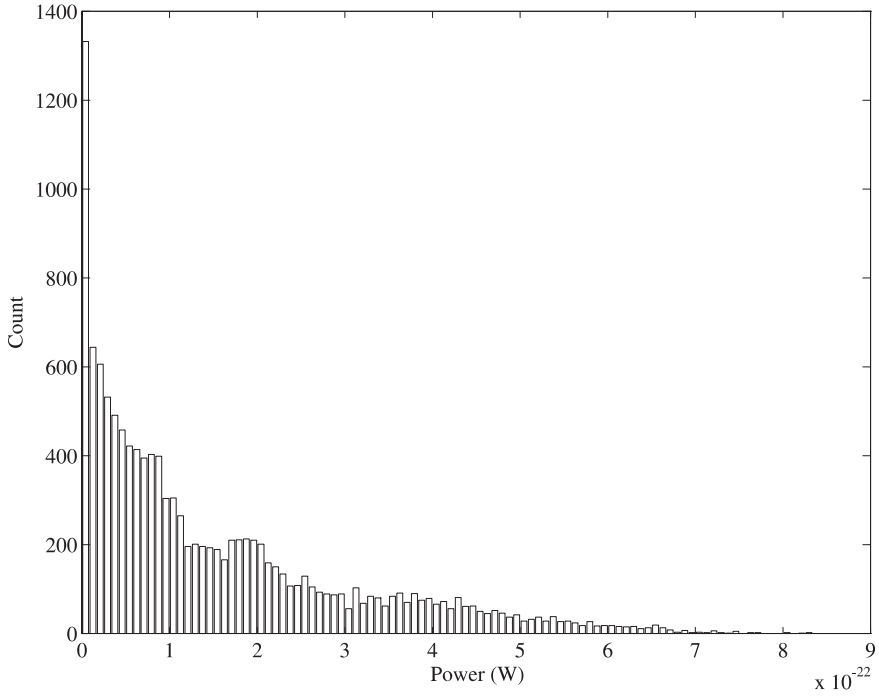

Figure 4.8. Power envelope histogram for case 1.

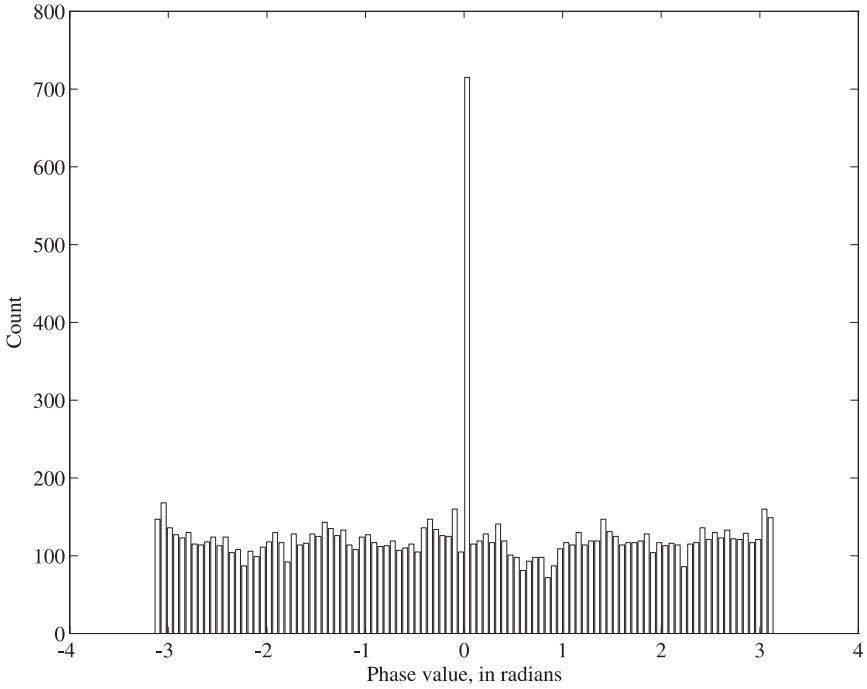

Figure 4.9. Phase envelope histogram for case 1.

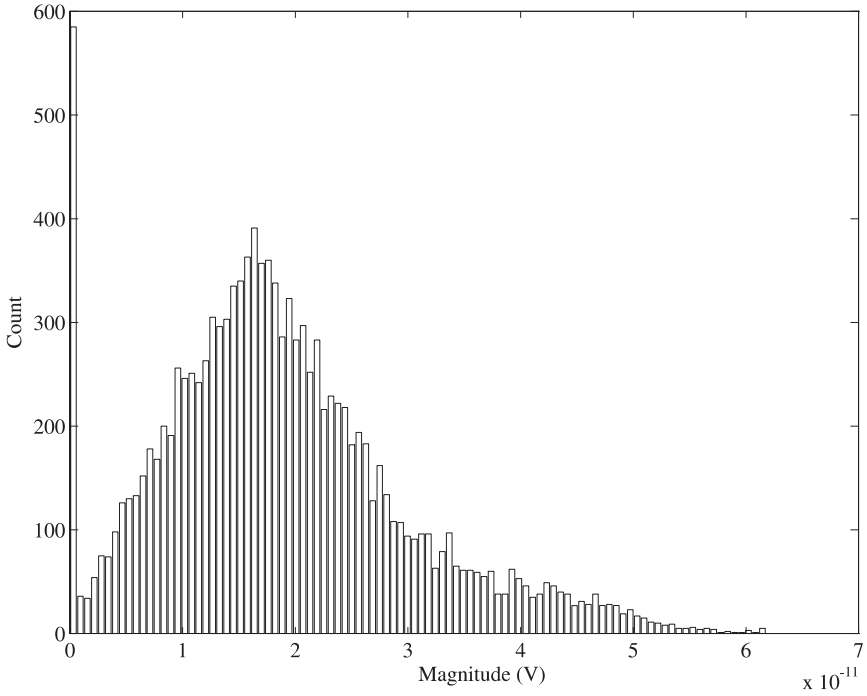

Figure 4.10. Voltage envelope histogram for case 2.

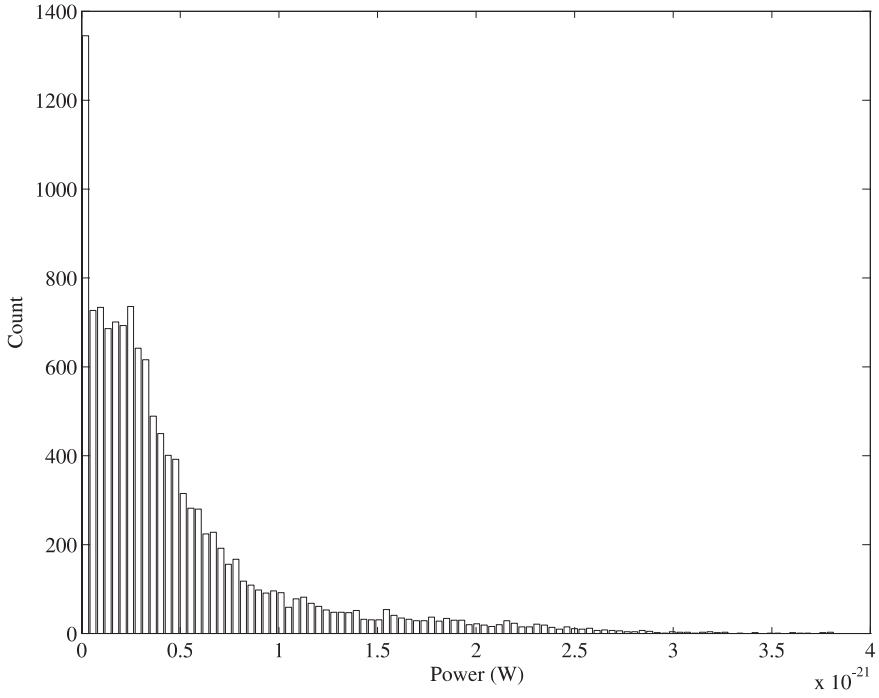

Figure 4.11. Power envelope histogram for case 2.

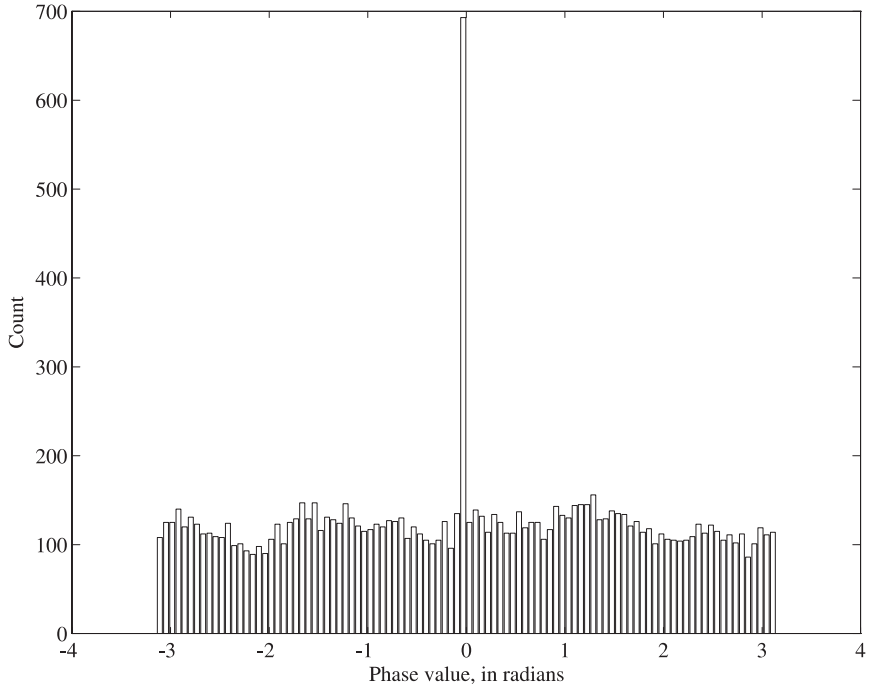

Figure 4.12. Phase envelope histogram for case 2.

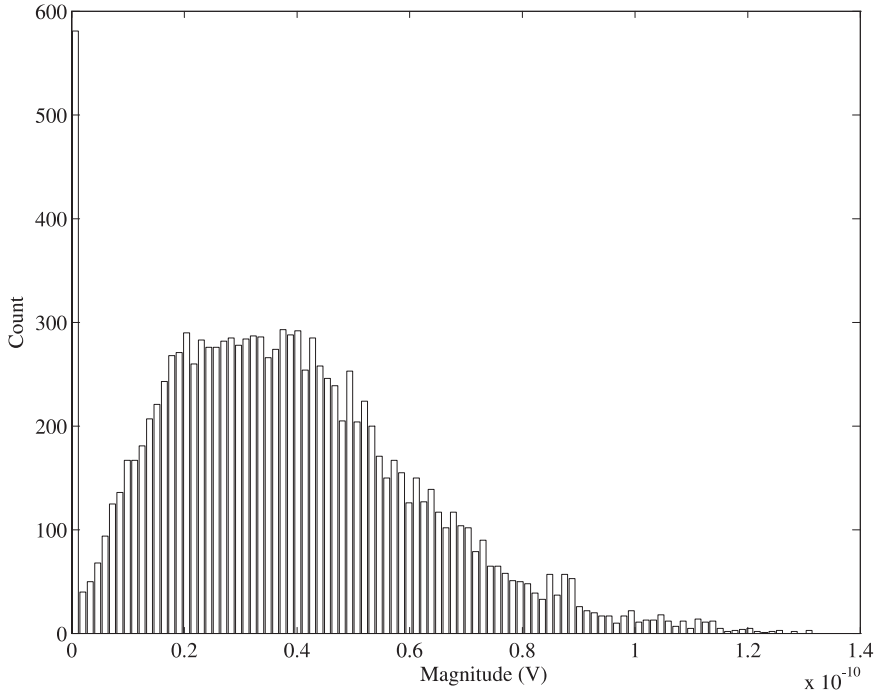

Figure 4.13. Voltage envelope histogram for case 3.

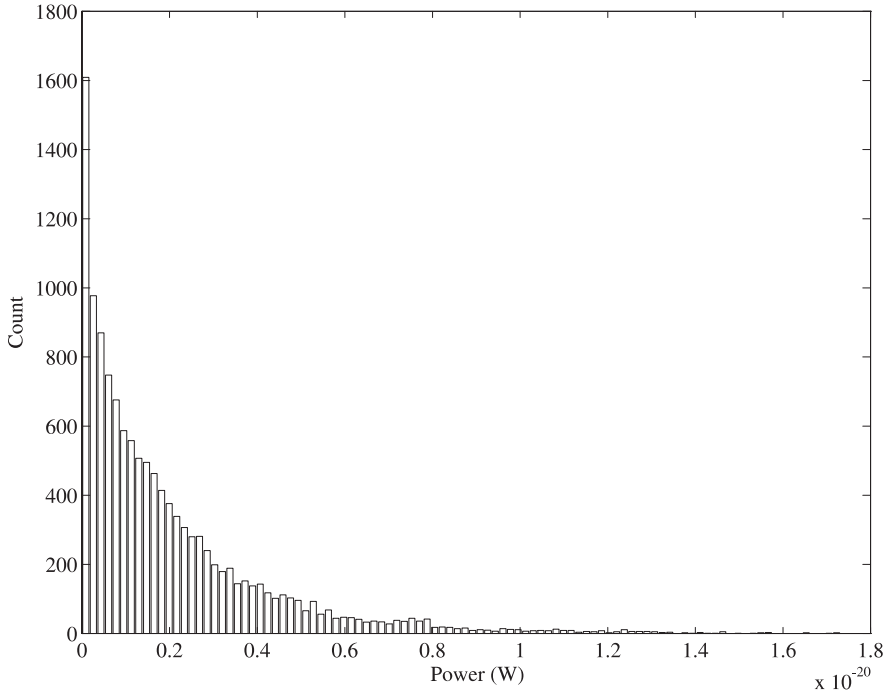

Figure 4.14. Power envelope histogram for case 3.

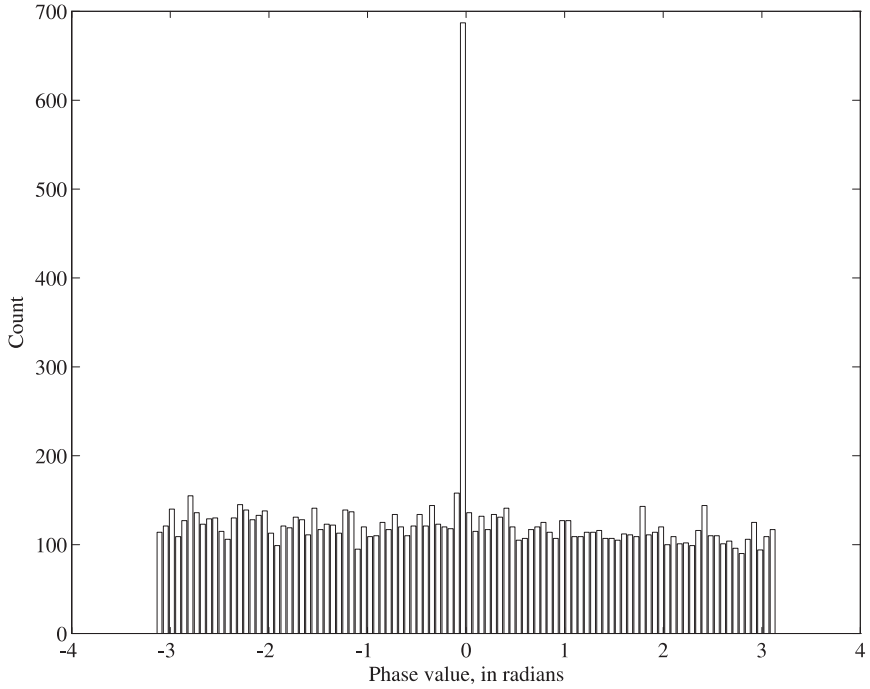

Figure 4.15. Phase envelope histogram for case 3.

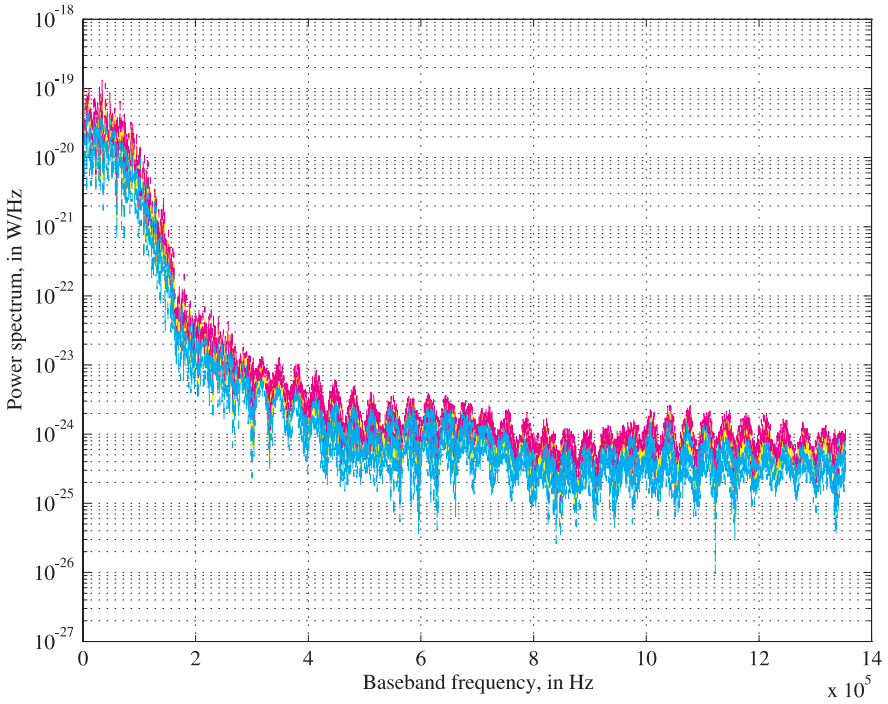

Figure 4.16. Unfiltered aggregate interference waveform spectrum for case 3.

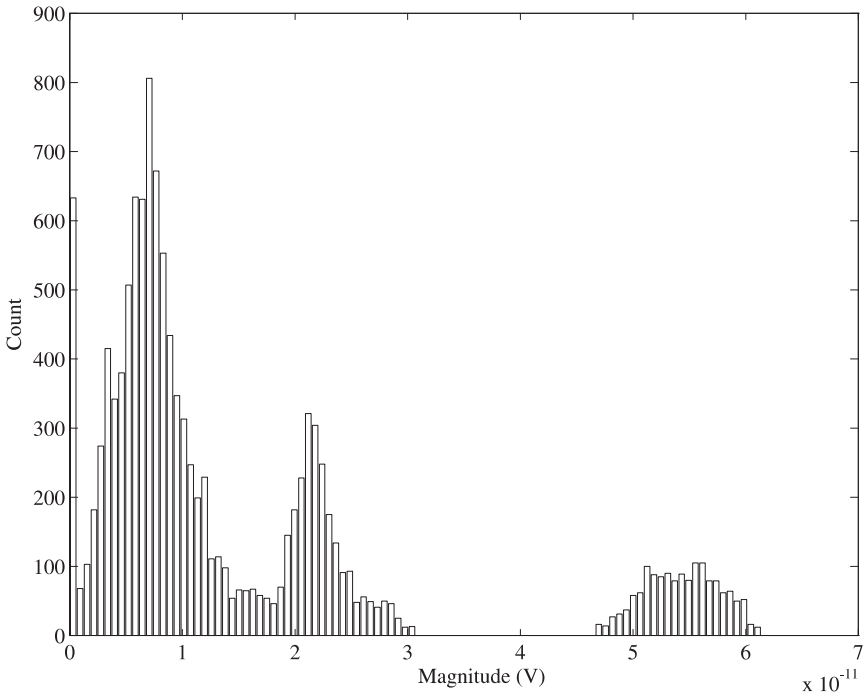

Figure 4.17. Voltage envelope histogram for case 1, with a single dominant interferer.

5. IS-95-BASED CDMA-PCS INTERFERENCE WAVEFORM

5.1 CDMA-PCS Physical-layer Overview

Another PCS system targeted for use in the licensed 2-GHz PCS frequency band is the proposed IS-95-based CDMA, also called CDMA-PCS. Like PCS 1900, CDMA-PCS promises a wide range of digital services for public large cell applications, including both voice and data. Both systems offer similar digital user services, but have different implementations on the physical layer, which result in different performance in the N/I environment. All interference model derivations for CDMA-PCS described in this report are based on the letter ballot version of the CDMA-PCS standard [21].[4]

Physical-layer specifications for CDMA-PCS are based on CDMA, which allows many communication links to simultaneously occupy an RF channel in both time and frequency dimensions. Unlike TDMA systems, the number of concurrent links occupying a given CDMA RF channel is not strictly limited. However, practical limits do exist for CDMA capacity. Self-interference created by several CDMA-PCS transmitters occupying the same RF resource causes reduced capacity. Links are distinguished by pseudorandom codes that possess strong autocorrelative properties, and weak cross-correlative characteristics. Ideally, a receiver in a CDMA system will have perfect correlation with its assigned link, and all other links sharing the RF channel will appear as noise. This depends on the design of the CDMA codes, and the system deployment.

Unlike its PCS 1900 counterpart, CDMA-PCS employs distinctly different designs on the forward and reverse links. Commonality exists, however, in the chipping sequence rate of 1.23 Mchips/sec. This chipping sequence, after modulation, occupies a 1.23-MHz bandwidth. Logical channels are distinguished by two parameters: 1) the RF carrier frequency and 2) the logical channel-specific spreading code. Data rates up to 14.4 kbps are provided per logical channel.

5.1.1 Reverse Link Design

On the reverse link (uplink), two types of logical channels are specified: 1) access channels and 2) traffic channels. Access channels are used by the mobile station to establish traffic channel links with the base station, and to respond to base station signaling. Traffic channels communicate voice, data, and signaling information to the base station from the mobile station. For N/I modeling purposes, the traffic and access channels are assumed identical, except for the private spreading codes.

---

4 Document number T1P1/94-088 (J-STD-008), released 12/12/94. The ballot version specifies technical requirements for CDMA-PCS compatibility.

Figure 5.1 shows the reference configuration for the CDMA-PCS reverse link, which assumes a 9.6-kbps logical traffic channel. Other logical channel rates and the access channels will have a slightly different configuration. This includes error-coding, block-interleaving, and symbol repetition, which do not directly contribute to the N/I waveform in the model.

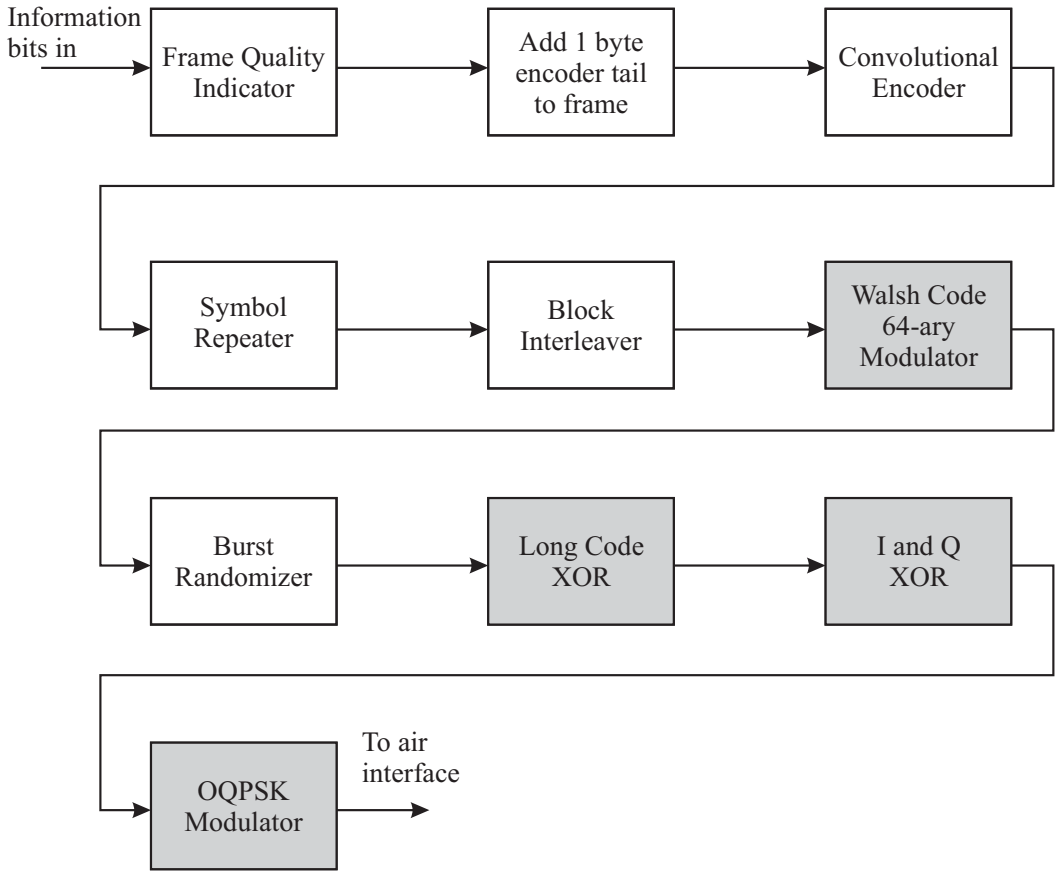

Figure 5.1. CDMA-PCS reverse link block diagram.

Shaded blocks in Figure 5.1 represent functions which may be explicitly represented in the N/I model. The 64-ary Walsh code modulator takes groups of 6 symbols from the interleaver, and maps each group into one of 64 Walsh codes. Each Walsh code is 64 "chips" long. These are passed to a burst randomizer at 307 kchips/sec. The burst randomizer masks out redundant data generated by the symbol repeater. For N/I modeling purposes, this function is ignored. The Walsh codes are then xor'ed with a private pseudorandom code which is 2^{42} -1 chips long. In the process, each Walsh chip is modulo-2 added to four long code chips, resulting in a chip stream at 1.23 Mchips/sec. The long code distinguishes individual users within the RF channel resource. Although ultimately the long code is the same for every user, a sufficient "offset" in the code, resulting in near-othogonal properties, is emulated by proper application of a user-specific privacy mask. The long code has sufficient length to support many concurrent offsets.

After long code-spreading, the symbol stream is split into I and Q components, which are modulo-2 added synchronously to corresponding I and Q spreading codes of length 2^{15} each. The I and Q codes are the same for every mobile station sharing the same RF resource for a given cell. Nearby cells also make use of the same I and Q codes, but use a time offset sufficient for decorrelation with other nearby cells. Offset quadrature phase-shift keying (OQPSK) is then used to modulate the I and Q symbol streams, which are then transmitted over the air interface.

Functions that do not affect the N/I waveform directly are omitted in the model. However, more detail is needed in modeling CDMA-PCS because the correlation properties of the N/I waveform directly impact the performance of the correlator-based receiver. For this reason, the model allows direct implementation of the spreading codes used by the interferers in the aggregate waveform. As an alternative, random chip generators may be substituted for the actual chip sequence generators. This reduces the computational complexity of the N/I waveform considerably. Figure 5.2 shows the resulting abstraction that applies to the reverse link waveform.

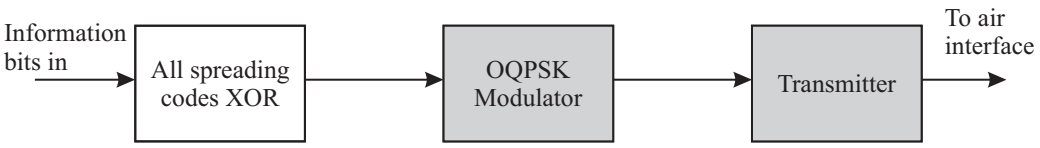

Figure 5.2. Abstracted reverse link block diagram.

5.1.2 Forward Link Design

For the forward link (downlink), four types of logical channels are defined: 1) the pilot channel, 2) the sync channel, 3) paging channels, and 4) traffic channels. The pilot channel is simply a spread spectrum waveform modulated by Walsh function 0 that serves as a synchronization beacon for mobile stations within range of the RF carrier. The sync channel provides timing information for each mobile station, once pilot channel synchronization is established. Paging channels are used to communicate system overhead information and signaling messages from the base station to the mobile station.

Forward link design for CDMA-PCS differs significantly from the reverse link in modulation scheme, synchronization, and spreading code methodology. Because all forward link logical channels are combined within the base station, all are synchronized. For this reason, a mobile station may extract all timing information from the base station pilot and sync channels, and demodulation is therefore accomplished coherently. Forward link Walsh functions are used to distinguish logical channels, in contrast to orthogonal modulation implementation on the reverse

link. Figure 5.3 shows the reference configuration for the CDMA-PCS forward link, which again assumes a 9.6-kbps logical channel.

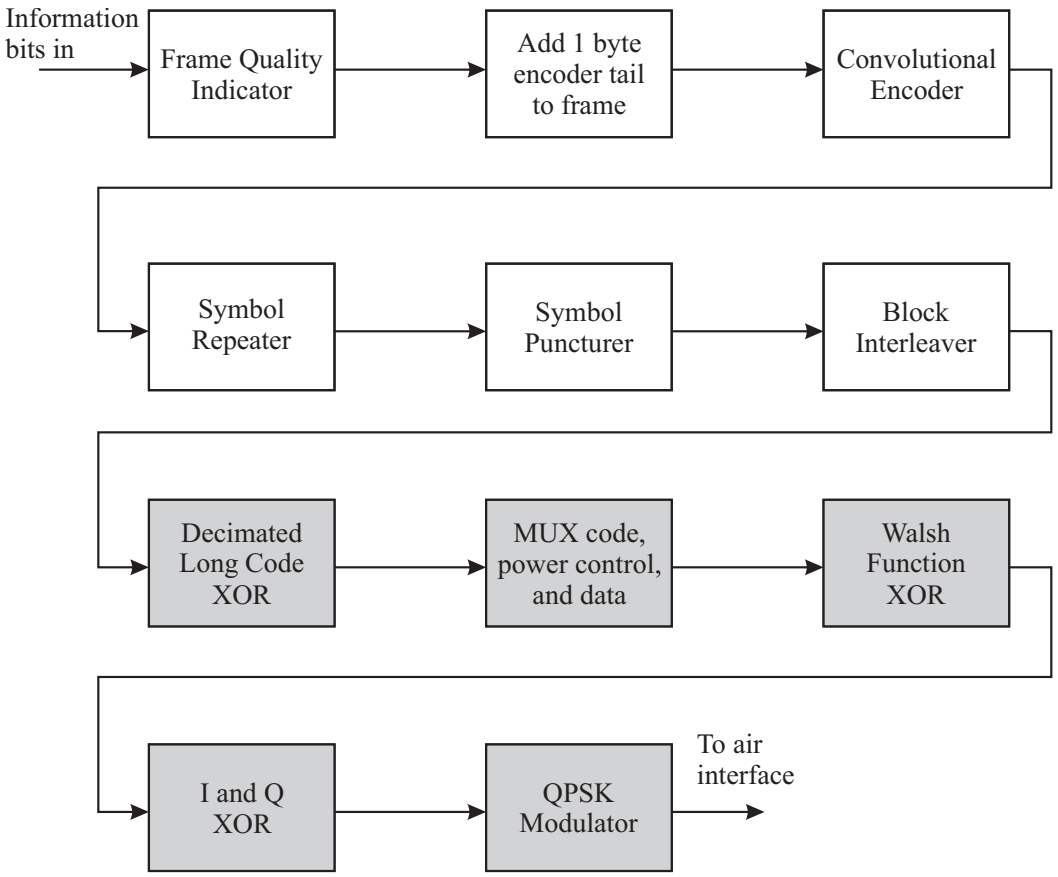

Figure 5.3. CDMA-PCS forward channel block diagram.

Shaded blocks in Figure 5.3 represent functions that may be explicitly represented in the N/I model. These blocks directly affect the correlative properties of the mobile station receiver. The symbol stream output from the block interleaver is modeled as a random bit stream, which is then modulo-2 added to a logical-channel-specific long code decimated by a factor of 64. The symbol stream is then multiplexed with power control information and a version of the long code decimated by a factor of 1536. The multiplexed symbol stream is then modulo-2 added to the logical-channel-specific Walsh function, then I and Q spread at 1.23 Mchips/sec before modulation. The forward channel uses QPSK without an offset.

Although the amount of processing in the forward (and reverse) CDMA-PCS links seems prohibitive for an explicit N/I waveform simulation with many interferers, many of the blocks may be simplified by aggregating them together. For example, if sufficient randomness is built into the symbol stream output from the block interleaver, the remaining shaded blocks—with the exception of the

modulator—may be replaced by an equivalent code spreading function. This code-spreading function is based on the actual codes used in the CDMA-PCS system. Figure 5.4 shows this abstraction.

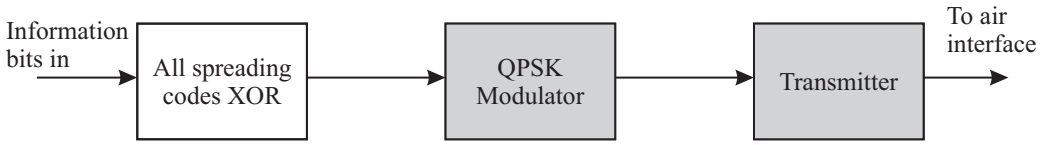

Figure 5.4. Abstracted forward link block diagram.

To further simplify the N/I simulation, random number generators can replace the actual chipping sequence generators. This substitution will not capture the correlative properties of the actual pseudorandom codes, but works well if the codes are near-orthogonal.

5.2 Offset QPSK Waveform Expression (Reverse Link)

Mobile station modems implement OQPSK on the reverse link. The mobile station output symbol stream, after the xor function with the mobile station-specific long code, is separated into in phase and quadrature symbol streams for modulation. The I and Q separation provides diversity in the transmitted symbol stream. Unlike traditional uses of quadrature modulation that alternate successive bits before transmission, CDMA-PCS I and Q symbol streams each carry the same information.

In CDMA-PCS OQPSK, the modulator power divides the long-coded symbol stream into two identical components, then spreads each component with corresponding I and Q pseudorandom sequences. The Q symbol stream is delayed by one-half a chip duration to form the offset. Next, I and Q symbol streams are baseband filtered, then quadrature modulated. The complete reverse link process is shown in Figure 5.5.

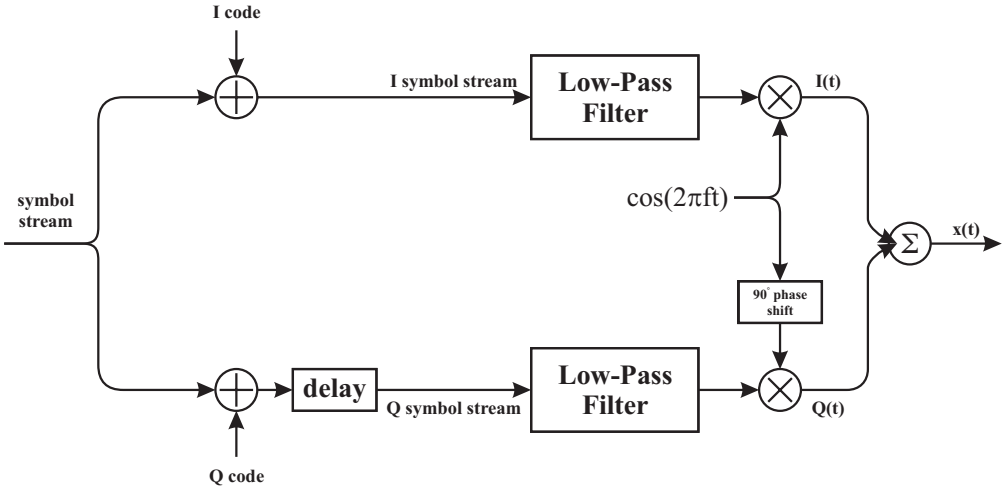

Figure 5.5. Offset quadrature phase-shift keying for the CDMA-PCS reverse link.

In terms of the generalized phase-modulated waveform given by Equation (A.3), the complex baseband representation of a single transmitted OQPSK waveform is given by Equation (5.1):

$$\bar{x}(t,\boldsymbol{\alpha}) = \sqrt{\frac{2E_s}{T}} \exp\left[j\varphi(t,\boldsymbol{\alpha}) \right]. \tag{5.1}$$

In Equation (5.1), $\varphi(t,\boldsymbol{\alpha})$ is the continuous information-carrying phase expression. For OQPSK, the phase expression $\varphi(t,\boldsymbol{\alpha})$ will transition between four states as shown in Figure 5.6. Note that transitions between state pairs 1,3 and 0,2 never occur. This is a consequence of offsetting the Q symbol stream. As a result, instantaneous phase changes are limited to $\pi / 2$ radians.

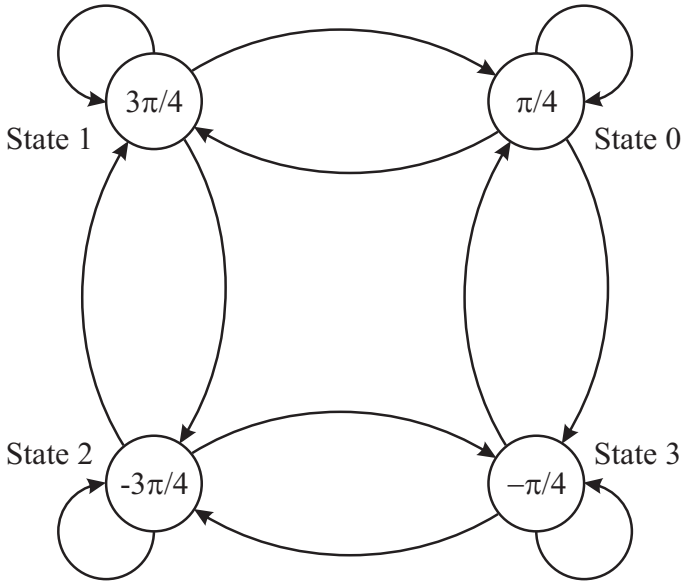

Figure 5.6. Offset quadrature phase-shift keying state transition diagram.

The simple four-state model shown in Figure 5.6 represents an idealized OQPSK modulator, with instantaneous transitions between phase states every *T/2* sec., where *T* is the chip duration. More realistically, baseband-shaping of the I and Q components of the phase determines the spectral limits of the output waveform. In effect, baseband-shaping creates a continuum of intermediate "states" between the four states shown in Figure 5.6, eliminating the instantaneous transitions entirely.

For N/I modeling purposes, many methods may be used to emulate the phase term $\varphi(t,\boldsymbol{\alpha})$; two are discussed in this report. One approach is to use a Markov chain model to emulate the phase state changes, and filter the entire phase expression after modulation. Another approach is the explicit modeling of the I and Q symbol streams, which are then baseband filtered and mapped into the phase expression. This essentially involves the same processing as the real reverse link, shown in

Figure 5.5. The approach used depends on the amount of detail desired in the N/I simulation, and the computational simplicity desired. Both approaches are described in the following two sections.

5.2.1 Markov Chain Model

Markov chain models offer many computational advantages over "brute force" methods of generating an unfiltered random OQPSK waveform from a single modulator. This is because each phase transition is represented by a single data point. This corresponds to two phase transitions per chip duration, or approximately 2.46 Msamples/sec/modulator. While this appears large, for filtered versions using I and Q symbol streams, each stream must be sampled at the simulation bandwidth, which is typically 4-16 times the RF bandwidth. This results in a sampling rate of approximately 5-20 Msamples/sec for each of the two output symbol streams per modulator. Each symbol stream must then be filtered separately before transmission.

Unfortunately, there are also many disadvantages to using the Markov chain model. For each additional modulator, the number of samples necessary increases linearly until the simulation bandwidth is reached. This is due to the noncoherent nature of each mobile station transmission, and because each transmitted symbol stream will have a random time offset with respect to other transmitting mobile stations. In addition, filtering the Markov chain output according to CDMA-PCS specification is difficult, and requires a sampling rate at the simulation bandwidth. Also, because the Markov chain model is stochastic, the correlative properties of the spreading codes are not taken into account. For these reasons, the Markov chain model is not used in the ITS N/I model.

Despite the disadvantages associated with the Markov chain model, the methodology is presented here for those who wish to use it. Although not practical for modeling large numbers of interferers, the Markov chain model may prove useful for single-interferer analyses, and for modem-emulation studies.

The Markov chain model is based on the state diagram shown in Figure 5.6. Defining $\pi_{n,m}$ as the probability of transitioning from state *n* to state *m*, the transition matrix for the state diagram is defined as:

$$\boldsymbol{\Pi} = \begin{bmatrix} \pi_{0,0} & \pi_{0,1} & \pi_{0,2} & \pi_{0,3} \\ \pi_{1,0} & \pi_{1,1} & \pi_{1,2} & \pi_{1,3} \\ \pi_{2,0} & \pi_{2,1} & \pi_{2,2} & \pi_{2,3} \\ \pi_{3,0} & \pi_{3,1} & \pi_{3,2} & \pi_{3,3} \end{bmatrix} = \begin{bmatrix} \pi_{0,0} & \pi_{0,1} & 0 & \pi_{0,3} \\ \pi_{1,0} & \pi_{1,1} & \pi_{1,2} & 0 \\ 0 & \pi_{2,1} & \pi_{2,2} & \pi_{2,3} \\ \pi_{3,0} & 0 & \pi_{3,2} & \pi_{3,3} \end{bmatrix}, \tag{5.2}$$

where the zero probability transitions are caused by the half-chip offset in the Q symbol stream. The phase states are related to the I and Q symbol values as summarized in Table 5.1.

Table 5.1 OQPSK Phase State Mapping

State	Phase Value	I Symbol Value	Q Symbol Value
0	$\pi/4$	0	0
1	$3\pi/4$	1	0
2	$-3\pi/4$	1	1
3	$-\pi/4$	0	1

Transitions from state i to state i+1 occur at times $\frac{nT}{2}$, where n is the set of non-negative integers. If all symbols are assumed equiprobable, the transition matrix becomes:

$$\boldsymbol{\Pi} = \begin{bmatrix} \frac{1}{3} & \frac{1}{3} & 0 & \frac{1}{3} \\ \frac{1}{3} & \frac{1}{3} & \frac{1}{3} & 0 \\ 0 & \frac{1}{3} & \frac{1}{3} & \frac{1}{3} \\ \frac{1}{3} & 0 & \frac{1}{3} & \frac{1}{3} \end{bmatrix}, \tag{5.3}$$

Equation (5.3) can be confirmed by solving the steady-state probability vector equation $\boldsymbol{p} = \boldsymbol{p\Pi}$, where the sum of elements in the vector $\boldsymbol{p} = \begin{bmatrix} p_0 & p_1 & p_2 & p_3 \end{bmatrix}$ equals unity, and p_j is the probability that the Markov chain is in state j. The resultant p_j are all equal to 0.25, indicating that all states are equiprobable.

From the perspective of the primary cell's base station, the interference waveform component from each mobile station is received with a random phase that is constant over the transmission, and a random time offset that is proportional to the distance of the mobile station from the base station. Because the reverse link phase is inherently noncoherent at the base station receiver, the phase component from each mobile station will be determined by separate, independent, and identical Markov chains. For computational purposes, the states of the individual Markov chains may be represented compactly and updated via the following steps:

1. Define a Markov "flag" matrix $\boldsymbol{M}$ of dimension $\{N_u, S\}$, where N_u is the number of interfering mobile stations, and S is the integer number of phase states. Matrix $\boldsymbol{M}$ stores the phase transitions of each interfering mobile station. Rows of $\boldsymbol{M}$ identify individual mobile stations, and columns indicate the current phase state. A "1" in a column indicates the current phase state. For OQPSK, S=4.

2. Choose initial states for ***M***. This can be accomplished by randomly choosing a state for each mobile station. This means one column for each row of ***M*** is randomly set to "1."

3. Choose a random phase constant for each row of ***M***. The n^{th} mobile station waveform will arrive at the base station with a constant random phase φ_{0n}. A uniform $[0,2\pi)$ distribution is appropriate.

4. Form a phase state equation that stores the phase of each mobile station. Define $\boldsymbol{s} = [s_0 \ s_1 \ s_2 \ \cdots \ s_s]$, where s_i is the value of the i^{th} state, and $\boldsymbol{\varphi}_0 = [\varphi_{00} \ \varphi_{01} \ \varphi_{02} \ \cdots \ \varphi_{0N_u}]$; and where φ_i is the current phase value, including the random offset, of the i^{th} mobile station. Also, let $\varphi_0 = [\varphi_{00} \ \varphi_{01} \ \varphi_{02} \ \cdots \ \varphi_{0N_u}]$ represent the random phase constant matrix, where φ_{0i} is the random phase offset of the i^{th} mobile station. A phase state equation can then be formulated as: $\boldsymbol{\varphi} = \boldsymbol{sM}^{\boldsymbol{T}} + \varphi_0$.

5. Update the ***M*** matrix. States of the ***M*** matrix will be updated for every mobile-station-initiated change of phase. For OQPSK, the state of each row will be updated every $T/2$ sec. Because time delays are associated with propagation for each mobile station, a random time offset uniformly covering a single chip duration is included. Thus, each row of the ***M*** matrix is updated twice every T sec., resulting in $2N_u$ updates per chip duration for the entire interference waveform. ***M*** can be updated by:

   a. Defining a *{1, Nu}* time vector ***T*** with elements distributed $U[0, T/2)$.

   b. Ordering the elements of ***T*** from smallest to largest.

   c. Updating consecutive rows of ***M*** at times specified by the elements of ***T***. For example, row M_0 is updated at time T_0, M_1 is updated at time T_1, and so forth. The state of ***M*** can be updated for OQPSK by only observing columns *(j-1, j, j+1)* modulo *S*, where *j* is the current state, and choosing state *(j-1, j, j+1)* modulo *S* with probability 1/3.

   d. Add $T/2$ to all elements of ***T*** when all rows of ***M*** have been updated, then proceed as in step 5c.

6. Update the phase state equation in step 4.

Obviously, the Markov chain method becomes cumbersome for large numbers of interfering mobile stations.

5.2.2 I and Q Explicit Model

An alternative method of OQPSK waveform generation uses an explicit model of the modulator, as shown in Figure 5.5. While this method is more computationally intense than the Markov chain model for small numbers of interferers, the many advantages make this the preferred method for the ITS N/I model. Explicit modeling allows inclusion of the actual spreading codes, in addition to direct application of baseband filtering used in the real system design. If desired, abstractions are easily incorporated that simplify the model further (e.g., use of a random number generator in place of a spreading code generator). In addition, for large numbers of interferers, the computational complexity is actually less than a comparable Markov chain model.

Computational complexity for the I and Q explicit model is based on the simulation sampling rate, which is typically 4-16 times the baseband bandwidth of the RF waveform. For an explicit model, the simulation sampling rate is independent of the number of interferers, because all waveforms are sampled at identical times, i.e., synchronously. For CDMA-PCS, the simulation sampling rate typically ranges from 5-20 Msamples/sec. For the N/I model, the lower sampling rate is used.

Modeling the N/I waveform explicitly is straightforward. The 1.23-Mchip/sec input symbol stream, after modulo-2 addition to the long code, is power divided into I and Q components, which are then modulo-2 added to corresponding I and Q codes. The Q symbol stream is delayed by one-half a chip duration, and then both I and Q streams are placed through the lowpass filter. The streams are next modulated in quadrature. This process, in complex baseband form, is shown in Figure 5.7.

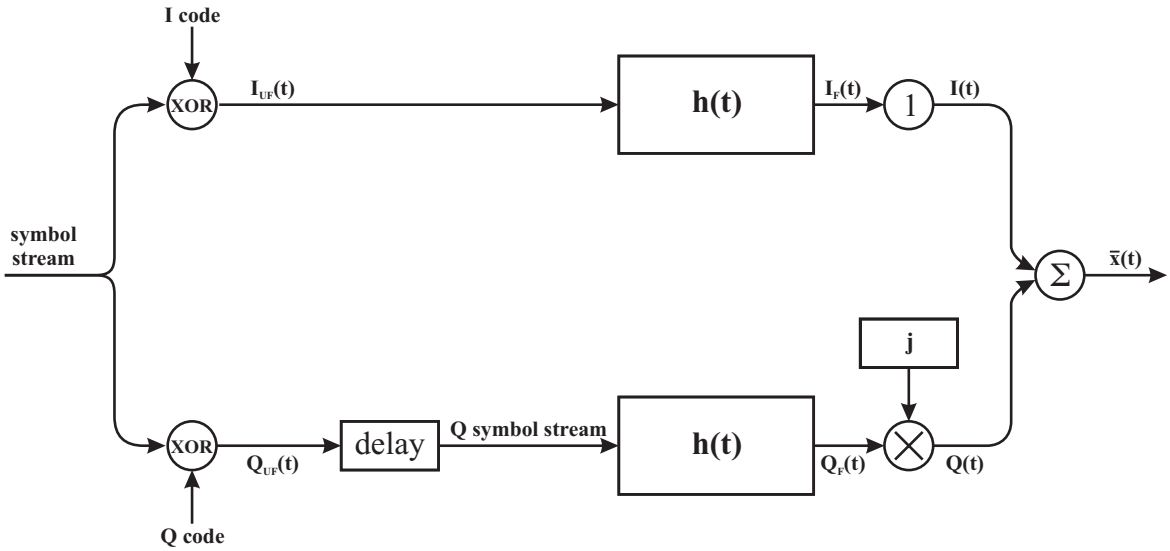

Figure 5.7. CDMA-PCS OQPSK modulator, in complex baseband form.

The modulator output in Figure 5.7 is the sum of in phase and quadrature components:

$$x(t) = I_F(t)\cos(2\pi f_c t) + Q_F(t)\sin(2\pi f_c t), \tag{5.4}$$

which is in canonical form. The complex baseband representation is simply:

$$\bar{x}(t) = I_F(t) - jQ_F(t). \tag{5.5}$$

In terms of the unfiltered I and Q symbol streams, the complex baseband output is given by the convolution:

$$\bar{x}(t) = h(t) \otimes \left[I_{UF}(t) - jQ_{UF}\left(t - \frac{T_c}{2} \right) \right]. \tag{5.6}$$

The complex baseband output $\bar{x}(t)$ is simply the sum of I and Q symbol streams, with appropriate linear filtering. Filter limits are given in [21]. Details of the technique used for simulation of the reverse link modulation is given in Section 5.7, including sampling method, code implementation, and filter design.

Abstraction may be included during many steps of the process. For example, the input symbol stream may be replaced by a random number generator, at the cost of losing the correlative properties of the Walsh and long codes. I and Q spreading codes may be replaced similarly.

5.3 QPSK Waveform Expression (Forward Link)

Base station modems implement baseband-filtered QPSK on the forward link. The modulation scheme is identical to that for the reverse link, except the Q symbol stream is not offset.

As in the reverse link, the CDMA-PCS QPSK modulator accepts the long-coded symbol stream, divides it into two identical components, then modulo-2 adds each component with corresponding I and Q pseudorandom sequences. For the forward link, the Q symbol stream is not delayed. I and Q symbol streams are next baseband filtered, then quadrature modulated. The complete forward link process is shown in Figure 5.8. The complex baseband representation of a single transmitted QPSK waveform is given by Equation (5.7):

$$\bar{x}(t,\alpha) = \sqrt{\frac{2E_s}{T}} \exp\left[j\varphi(t,\alpha) \right], \tag{5.7}$$

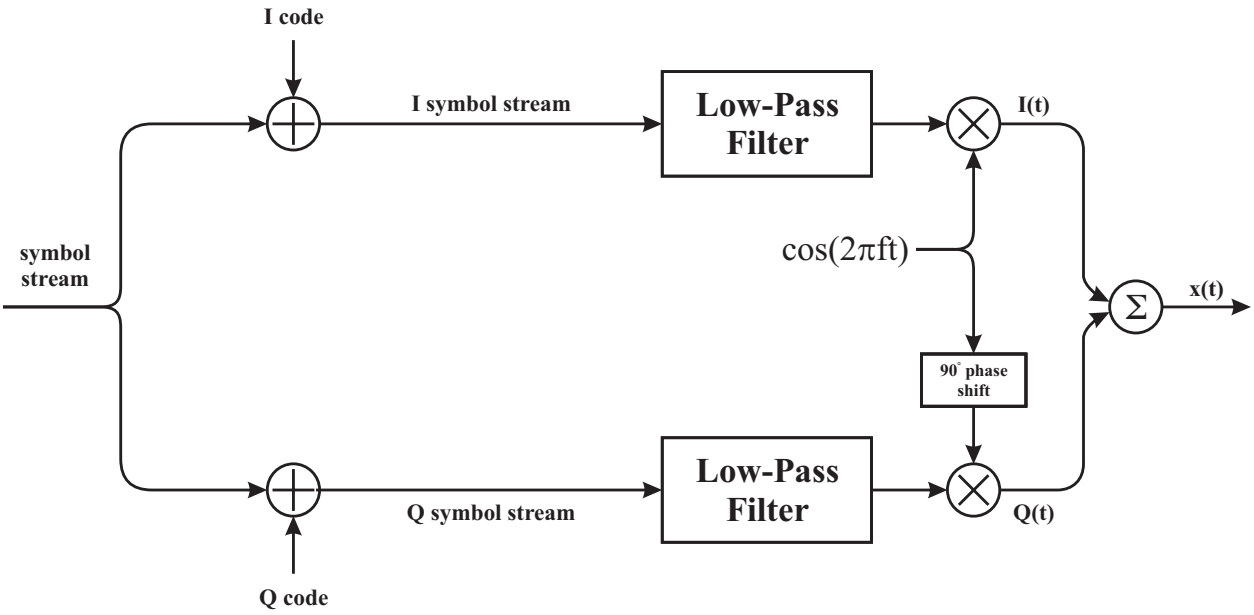

Figure 5.8. QPSK for the CDMA-PCS forward link.

where $\varphi(t,\alpha)$ is the continuous information-carrying phase expression. This expression is identical to the phase expression given for the reverse link in Equation 5.1. For QPSK, the phase expression $\varphi(t,\alpha)$ will transition between four states as shown in Figure 5.9.

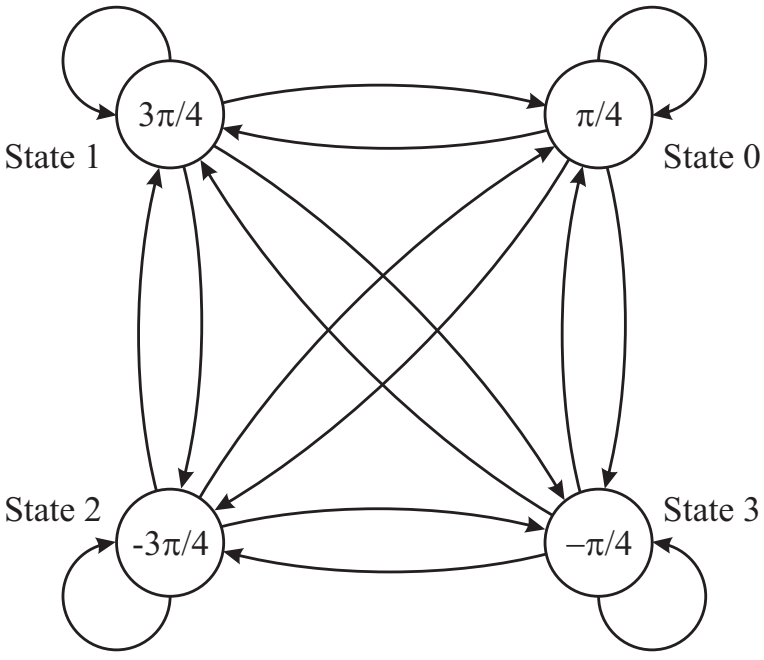

Figure 5.9. QPSK phase state transition diagram.

Unlike OQPSK, transitions between state pairs 1,3 and 0,2 do occur. Phase changes happen only once per chip, since the I and Q symbol streams are aligned. However, instantaneous phase changes of radians result, which are more difficult to manage in an actual transmitter/receiver pair.

The phase term $\varphi(t,\alpha)$ may be emulated via any of several methods, as was the case for the reverse link. Both the Markov chain model and the I and Q explicit model described in Section 5.2 apply, with some minor changes. The methodologies are the same for each case. Rather than repeat each methodology, only the changes are identified below.

For the Markov chain model, the transition matrix becomes:

$$\boldsymbol{\Pi} = \begin{bmatrix} \pi_{0,0} & \pi_{0,1} & \pi_{0,2} & \pi_{0,3} \\ \pi_{1,0} & \pi_{1,1} & \pi_{1,2} & \pi_{1,3} \\ \pi_{2,0} & \pi_{2,1} & \pi_{2,2} & \pi_{2,3} \\ \pi_{3,0} & \pi_{3,1} & \pi_{3,2} & \pi_{3,3} \end{bmatrix}. \tag{5.8}$$

Note that the zero transition probabilities disappear, although the phase values in Table 5.1 still apply. If all symbols are assumed equiprobable, all the transition probabilities are equal to 0.25. Computation of the phase state equation is the same, except the phase state of each individual interferer is updated every *T* sec., instead of every *T/2* sec.

For the I and Q explicit model, Equation (5.6) becomes:

$$\bar{x}(t) = h(t) \otimes \left[I_{UF}(t) - jQ_{UF}(t) \right]. \tag{5.9}$$

5.4 CDMA-PCS Power Control

An important element of any CDMA system design is power control on the reverse link. An improperly balanced CDMA system will suffer significant losses in capacity. A well-known case of CDMA system imbalance is referred to as the "near/far" problem, where a mobile station "near" the base station receiver transmits well above the levels of other "far" away mobile stations on the same RF channel. Of course, the power levels received at the base station from each mobile station may depend on factors other than geographic distribution. More generally, the mobile station transmit powers will be distributed in envelope in a time-variant manner. The ITS N/I model allows specification of the transmit power of each mobile station in the overall N/I waveform.

The CDMA-PCS system uses both open and closed loop power control. For open loop power control, the product of the power received at the mobile station and the power transmitted from the mobile station is a defined constant. The farther away the mobile station is with respect to the base station, the greater the allowed mobile station transmit power. Specifically, the output power characteristics of the mobile station (traffic channel) are governed by formulae for initial power transmission level, and open loop estimation during a call session. A change in the mean input power level to the mobile station will trigger a proportional change to the output power level in the opposite direction. Open loop power control is governed solely by the mobile station.

In addition, a closed loop correction controlled by the base station allows mobile station power adjustments to ±24 dB from the open loop estimate. Closed loop power control bits are transmitted from the base station periodically, and instruct the mobile station to increase or decrease transmitted power levels by a nominal increment (typically 1 dB).

Rather than implement the CDMA-PCS power control algorithm directly in the uplink N/I model, functionality is included to choose a distribution of power levels from interferers. Weighting functions, which may be functions of time, allow specific setting of interferer levels. In theory, these functions may emulate the power control algorithm used in CDMA-PCS, but a more practical approach is to develop stationary scenarios for the distribution. In addition to being much simpler to implement, a stationary distribution facilitates easier "what if" analyses related to power control. Example specification of the weighting functions are given in the example in Section 5.7.1.

5.5 Timing and Synchronization

Another important consideration for the N/I model is understanding timing and synchronization for the CDMA-PCS system. Resulting effects that are implemented in the N/I model are 1) phase synchronization of logical channels on the forward link, 2) noncoherent reception of logical channels on the reverse link, and 3) implementation of spreading code offsets.

CDMA-PCS uses a universal time reference based on global positioning system (GPS) transmissions to achieve system synchronization. Long, I, and Q codes are synchronized at the transmitter and receiver via the GPS transmissions. Mobile stations acquire synchronization and system time via the following steps:

1. Mobile stations, upon entering the CDMA-PCS environment, scan for the base station pilot channel. The pilot channel is a continuous transmission of Walsh code 0.

2. Once the pilot channel has been located, the mobile station acquires timing and phase references for coherent demodulation. Phase synchronization is maintained between all channels on the forward link, making coherent demodulation possible.

3. After acquisition of the pilot channel, the mobile station uses the base station sync channel to obtain system configuration and timing information. Included are the tracking and timing offset information needed for proper decorrelation of the long, I, and Q spreading codes.

For the ITS N/I model, all logical channels on a single RF channel for any base station on the forward link are assumed to be synchronized. RF channels from nearby interfering base stations are not synchronized with respect to each other, and each uses a different I and Q spreading code offset.

On the reverse link, all mobile station transmissions are assumed to have a random $U[0,2\pi)$ phase offset and a random $U[0,T)$ delay, as received at the base station. However, all mobile stations assigned to a given base station use the same I and Q spreading code offset, not including propagation delay. Mobile stations in nearby interfering cells use the cell-assigned I and Q spreading code offset.

5.6 Interference Expressions

Section 3 presented the PCS cellular geometry of intrasystem interference in a generic, technology-independent form. Section 5, to this point, has described the waveform created by a single modulator on both the uplink and downlink. CDMA-PCS-specific N/I environments may be formulated using expressions derived in both sections. Single-modulator waveforms for the uplink and downlink can be substituted into the geometric expressions presented in Section 3 to characterize the CDMA-PCS system self-interference.

The methodology is similar to that used for the PCS 1900 self-interference characterization. Two cases are presented: 1) interference to the uplink and 2) interference to the downlink. For each case, numerous interferers are simulated by duplicating a single transmitter expression once for each represented interferer. Each interferer is then spatially distributed via the expressions derived in Section 3. Delay, multipath, propagation loss, and Doppler shift functions may also be incorporated in these expressions.

5.6.1 Uplink Interference Expressions

On the uplink, CDMA systems inherently experience intracell interference from other mobile stations within the cell, in addition to mobile stations transmitting on the same frequency in nearby cells. In general, each mobile station transmits a waveform into the waveform space shared by all other mobile stations assigned to the same RF channel, independent of cell assignment. Individual waveforms are discernable by code assignment.

Unlike TDMA-based systems, CDMA has a soft capacity that depends on several environmental parameters. Specifically, the intracell component of the self-generated CDMA-PCS uplink N/I waveform for a single RF channel will be a function of the:

1. number of mobile stations concurrently transmitting on the RF channel,
2. positions of the mobile stations with respect to the primary cell's base station receiver and each other,
3. channel conditions and propagation environment,
4. transmitted power distribution of the mobile stations and power control algorithm, and
5. design of spreading codes (correlative properties).

An appropriate N/I model for the CDMA-PCS uplink accounts for these factors, with facility for abstraction where possible. Note that these factors are not independent. For example, the positions of mobile stations within the primary cell determine their individual transmitted power. Assuming perfect power control, all mobile station waveforms incident at the base station receiver have equal power levels. Obviously, mobile stations near the border of the primary cell must transmit at a higher power level than those near the base station to accomplish this. Thus, the power distribution of mobile station waveforms measured at the mobile station transmitters is related to the position of the mobile stations.

Equations (3.1) give the technology-independent expressions for uplink intrasystem interference. The parameter b is set to zero in Equations (3.1), allowing superposition of multiple CDMA waveforms in the time domain. Equations (3.1) then become:

$$\begin{aligned} \overline{x_{FI\,(k,-)}}(t) &= \sum_{n=0}^{N_U-1} \overline{x_{FI\,(k,n)}}\left(t - \frac{r_{k,n}}{c}\right) a_{k,n}\left(r_{k,n}, \theta_{k,n}\right) \\ \overline{x_{FI}}(t) &= \sum_{k=0}^{N_I-1} \overline{x_{FI\,(k,-)}}(t). \end{aligned} \tag{5.10}$$

Because mobile stations sharing the same RF uplink channel mutually interfere within the primary cell, the number of interfering cells, N_I, must include the primary cell. The *k=0* index may arbitrarily represent the primary cell.

Frame boundaries and time slots are meaningless for the N/I model. Therefore, the interference component $\overline{x_{FI\,(k,n)}}(t)$ from the n^{th} interfering mobile station in the k^{th} cell, is defined over an arbitrary period of time. Although CDMA-PCS uses frame structures, the interference waveform need not include that level of detail. For convenience, $\overline{x_{FI\,(k,n)}}(t)$ may be defined in terms of an integer number of chips, or over an entire spreading code cycle. With the understanding that the time duration is arbitrary, $\overline{x_{FI\,(k,n)}}(t)$ is adapted from Equation (5.1), and expressed in terms of a single OQPSK modulator as:

$$\overline{x_{FI\,(k,n)}}(t,\boldsymbol{\alpha}) = A_{k,n}(t)\exp\left[j\varphi_{k,n}(t,\boldsymbol{\alpha}) + j\varphi_{0,(k,n)} \right], \tag{5.11}$$

where $\boldsymbol{\alpha} = \boldsymbol{\alpha}_{(k,n)}$ represents the symbol stream from the n^{th} mobile station in cell k, $\varphi_{(k,n)}(t,\boldsymbol{\alpha})$ is defined over one time slot as the continuously modulated phase based upon the transmitted symbol stream, $\boldsymbol{\alpha} = \boldsymbol{\alpha}_{(k,n)}$, $\varphi_{0,(k,n)}$ is a random phase term that is constant for the entire waveform, and $A_{k,n}(t)$ is the power-controlled output amplitude of the waveform.

Section 5.2 presented two methods for computing the output of a single reverse link OQPSK modulator. Note that Equation (5.11) also represents the waveform at the transmitter output of the n^{th} mobile station in the k^{th} cell, with two additional "features." Specifically, Equation (5.11) adds a power control function and a random constant phase term. Both are independent of the modulation scheme. Modulation-dependent components of $\overline{x_{FI\,(k,n)}}(t)$ are computed using Equations (5.1) or (5.6). Remember that modulation-dependent expressions include all processing before modulation, including spreading codes. These must be chosen appropriately for every $\overline{x_{FI\,(k,n)}}(t)$. Equation (5.10) results by taking the modulation-dependent components and incorporating the random constant phase term and power control function. Mathematically,

$$\overline{x_{FI\,(k,n)}}(t) = A_{k,n}(t)\bar{x}(t,\alpha)\exp(j\varphi_{0,(k,n)})$$

for Equation (5.1), and

$$\overline{x_{FI\,(k,n)}}(t) = A_{k,n}(t)\bar{x}(t)\exp(j\varphi_{0,(k,n)})$$

for Equation (5.6).

Aggregate interference caused by all mobile stations in the k^{th} cell, as received by the primary cell's base station, is expressed by combining Equations (5.10) and (5.11):

$$\overline{x_{FI\,(k,-)}}(t) = \sum_{n=0}^{N_U-1} A_{k,n}\left(t - \frac{r_{k,n}}{c}\right)\exp\left[j\varphi_{k,n}\left(t - \frac{r_{k,n}}{c}, \alpha\right) + j\varphi_{0,(k,n)}\right] a_{k,n}\left(r_{k,n}, \theta_{k,n}\right). \qquad (5.12)$$

Although $a_{k,n}\left(r_{k,n}, \theta_{k,n}\right)$ is not explicitly expressed as a time function, it may change value over time due to fluctuating channel conditions, or changing position of the mobile station. The product of the two amplitude functions is defined as:

$$W_{k,n}(t) = A_{k,n}(t) a_{k,n}\left(r_{k,n}, \theta_{k,n}, t\right). \qquad (5.13)$$

The new function $W_{k,n}(t)$ is directly related to the power control algorithm. By setting $W_{k,n}(t)$ constant for all *n* and setting *k=0*, perfect power control is represented within the primary cell. Explicit choice of the $W_{k,n}(t)$ allows different power control profiles to be represented in the N/I model. These can be either from a random distribution, or manually set according to a specific scenario.

To compute the total uplink interference waveform, Equation (5.12) is summed over all *k*, as given in the second part of Equation (5.10).

Rather than provide a table of values for the CDMA-PCS uplink interference waveform expressions as was done for the GSM uplink interference expressions in Section 4.6.1, an example is given in Section 5.7.2. This will most likely be more helpful, since the large number of possible parameter settings and techniques is difficult to cover in a succinct manner.

5.6.2 Downlink Interference Expressions

Forward link logical channels, unlike their reverse link counterparts, are combined before air transmission within each RF channel. At the base station, each logical channel is separated into in phase and quadrature components, which are converted to analog waveforms before filtering. Next, all logical channels are combined in the baseband analog domain, then modulated for air transmission. Forward link logical channels are thus synchronized, making coherent detection in the mobile station receiver possible.

Modeling the forward link involves proper synchronization of all logical channels within the RF channel. Equivalently, the logical channels may be modulated then summed, or summed then modulated. To illustrate this, Figure 5.10 reflects one possible logical channel-combining technique at the base station.

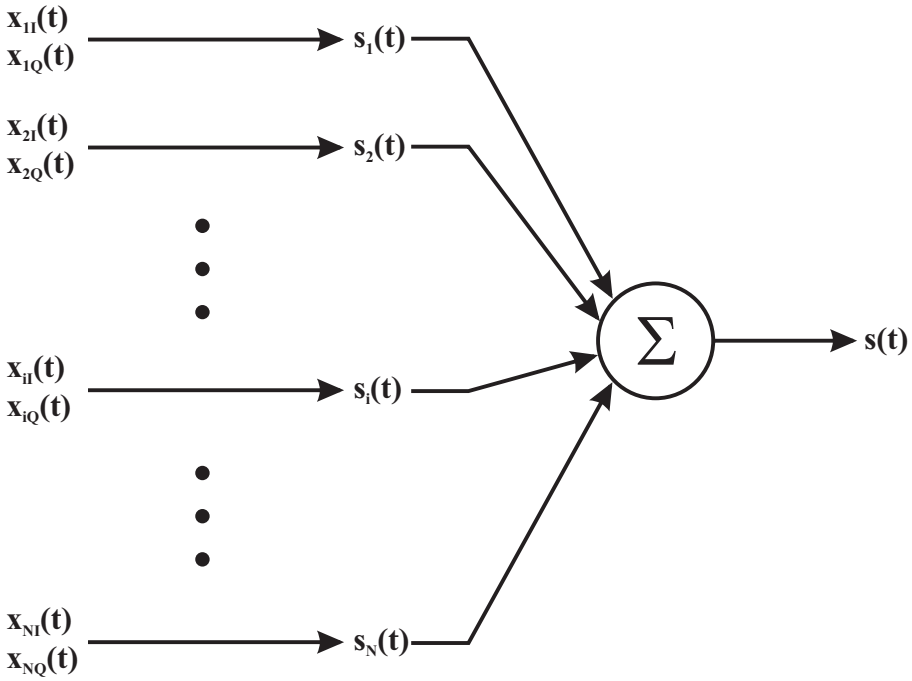

Figure 5.10. Technique 1 for CDMA-PCS forward channel combining.

In Figure 5.10, baseband analog versions of I and Q components, $x_{iI}(t)$ and $x_{iQ}(t)$, from each logical channel are QPSK-modulated to form N waveforms, $s_i(t)$, at carrier frequency f_c. The $s_i(t)$ are then summed and sent to the transmitter. This method employs N QPSK modulators. Another method for combining the logical channels on the forward link is shown in Figure 5.11. In this example, the I and Q baseband analog components, $x_{iI}(t)$ and $x_{iQ}(t)$, are summed separately to form aggregate I and Q components for the RF channel, $x_I(t)$ and $x_Q(t)$. These two components are then QPSK modulated and sent to the transmitter. Note that only one QPSK modulator is used.

Figure 5.10 yields:

$$\begin{aligned} s_i(t) &= x_{iI}(t)\cos(2\pi f_c t) + x_{iQ}(t)\sin(2\pi f_c t), \\ s(t) &= \sum_i x_{iI}(t)\cos(2\pi f_c t) + \sum_i x_{iQ}(t)\sin(2\pi f_c t) \end{aligned} \tag{5.14}$$

and from Figure 5.11:

$$\begin{aligned} x_I(t) &= \sum_i x_{iI}(t), \quad x_Q(t) = \sum_i x_{iQ}(t), \quad \text{and} \\ s(t) &= x_I(t)\cos(2\pi f_c t) + x_Q(t)\sin(2\pi f_c t). \end{aligned} \tag{5.15}$$

Clearly, using either method yields the same result for explicit modeling of the I and Q symbol streams from each logical channel. The second method is not appropriate if a Markov chain model is used to model each modulated symbol stream. For N/I modeling purposes, the I, Q, and long spreading codes may be applied in any order, since the xor function is communative. Note that the

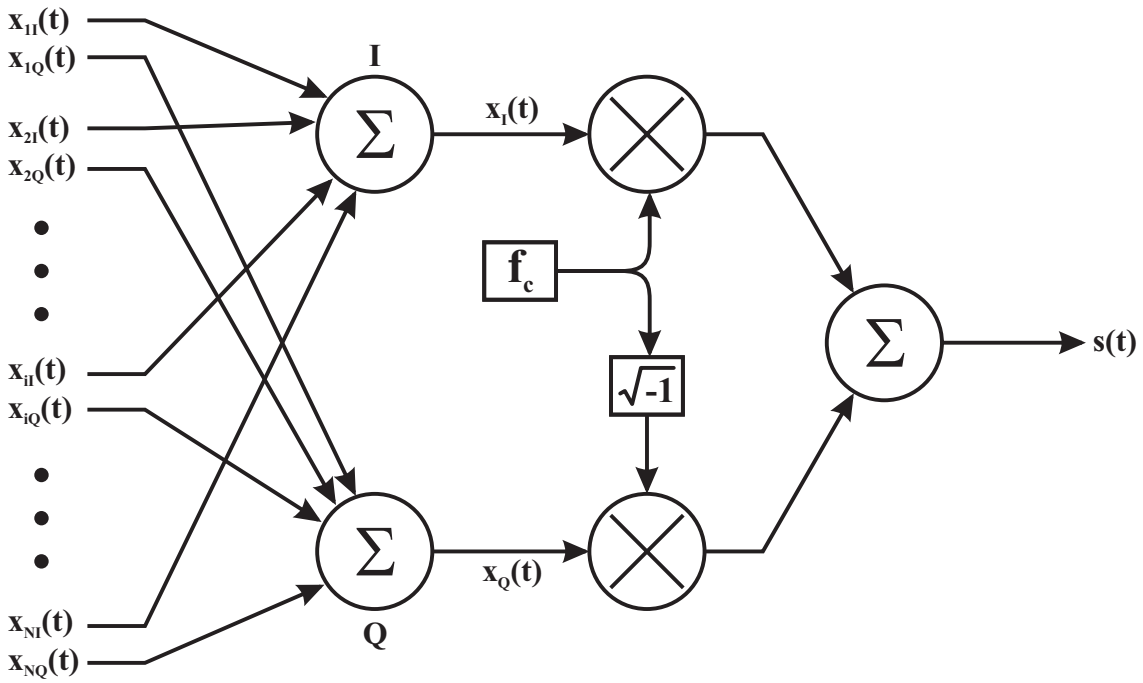

Figure 5.11. Technique 2 for CDMA-PCS forward channel combining.

real and imaginary parts of the complex baseband output of a single forward channel modulator, as given by Equation (5.9), correspond to $x_{iI}(t)$ and $x_{iQ}(t)$, respectively.

Equation (3.2) gives the technology-independent expression for downlink intrasystem interference. If the multiple QPSK modulator method of Figure 5.10 is used to generate a base station RF channel, then $s_i(t)$ is the bandpass version of $x(t,\alpha)$ as given by Equations (5.7) and (5.9). Using complex baseband notation, the interference waveform from the k^{th} interfering base station, as measured at the k^{th} base station's transmitter is:

$$\overline{x_{FI\,(k,n)}}(t,\alpha) = \sum_{i=1}^{N_u} A_{k,i}(t)\left[\bar{x}(t,\alpha)|_{k,i}\right], \tag{5.16}$$

where i indicates the i^{th} logical channel component of the waveform from base station k, and $\bar{x}(t,\alpha)|_{k,i}$ is the ith modulated component in complex baseband form. The index n indicates that the interference waveform $\overline{x_{FI\,(k,n)}}(t,\alpha)$ affects the n^{th} mobile station in the primary cell. Note that this expression is not dependent on n, since the waveform is assumed at the k^{th} base station's transmitter. The n is kept for notational consistency. The function $A_{k,i}(t)$ allows the relative amplitude of each logical channel to be adjusted. For example, the pilot channel is usually transmitted at a higher level than other logical channels within the RF channel to facilitate easier detection.

Substituting Equation (5.16) into Equation (3.2) gives the aggregate downlink interference expression from N_I nearby CDMA-PCS base stations, as seen by the n^{th} mobile station in the primary cell. Equation (3.2) is repeated below for convenience:

$$\overline{x_{FI\,(-,n)}}(t,\alpha) = \sum_{k=0}^{N_I-1} \overline{x_{FI\,(k,n)}}\left(t - \frac{r_{k,n}}{c}\right) a_{k,n}\left(r_{k,n}, \theta_{k,n}\right). \tag{5.17}$$

Downlink CDMA-PCS intrasystem interference at the primary cell's n^{th} mobile station is caused by nearby base stations radiating unwanted energy into the RF receive channel, and other downlink logical channels mutually interfering within the primary cell's base station channel. Because the primary cell's base station creates a waveform with interfering logical channels, the aggregate interference waveform must include all logical channels transmitted on the primary cell's base station downlink channel. Consequently, N_I must include the primary cell. The N/I waveform should ideally be synchronized with the "real" communication forward logical channel, as is the case for all logical channels in the forward link.

Alternatively, a test scenario may include a mobile station-to-base station link with a fully loaded forward channel. In this case, N_I does not include the primary cell's base station. However, the "real" base station must be able to transmit logical channels to mobile stations which may be required to physically exist in the test bed. If this is the case, registration and call setup procedures are needed for each mobile station; these are not incorporated into the N/I waveform models.

5.7 Computer Simulation of the CDMA-PCS Noise/Interference Environment

Part of the model validation and verification process for the CDMA-PCS was construction of computer simulations for the N/I waveforms derived in Section 5. These simulations provide valuable insight into the nuances of model implementation in a real-time hardware channel simulator. In addition, the computer simulation may be used as a tool to study N/I scenarios based on parametric inputs. This is particularly useful for CDMA-based systems, where power control impacts may be profiled by explicitly setting the transmitted power level of each individual interferer according to a prederived distribution, or via the CDMA-PCS power control algorithm.

The simulation code is readily adaptable to different CDMA systems. Unlike the PCS 1900 system, CDMA-PCS forward and reverse links differ in modulation scheme, spreading order, and synchronization. Fortunately, the parametric inputs to the code allow easy adaptation of the simulation to either uplink or downlink. To avoid repetition, only the uplink N/I simulation is detailed in this report.

The CDMA-PCS uplink N/I simulation is described below. Section 5.7.1 describes the methodology used for computer simulation of interference to the CDMA-PCS uplink, and Section 5.7.2 presents corresponding sample simulation results.

5.7.1 Uplink Noise/Interference Simulation

CDMA-PCS uplink interference simulation provides the aggregate interference waveform caused by mobile stations in the primary cell and nearby interfering cells, as seen at the primary cell's base station receiver. Assumptions simplify the computations in a similar manner to those made for the PCS 1900 uplink interference waveform simulation in Section 4.7.1. In fact, some assumptions are identical. These are:

1. All interfering cells within a given iteration of the program are equidistant from the primary cell's base station. This is a technology-independent assumption.
2. Each simulation iteration calculates the aggregate waveform due to a single radius within each layer of interfering cells. For example, the interference waveform from cells adjacent to the primary cell are computed in one iteration, since all cells are equidistant. Since two different distances are needed for the second layer of interfering cells, two iterations must be run. The total waveform is computed by adding several simulation iterations together. Obtaining the interference waveform due to interferers in both adjacent- and second-layer cells therefore requires three simulation iterations. Again, this assumption is technology-independent.
3. All interfering cells transmit on the same RF carrier frequency. Cells not contributing to the overall interference waveform (e.g., resulting from a cell reuse pattern) may be "zeroed out" during the computation.
4. Symbols are not aligned from interferer to interferer. There is a random uniform $(0, T]$ delay incorporated in each symbol stream.
5. Phase offset is random from interferer to interferer. There is a random uniform $(0, 2\pi]$ constant phase term added to each interferer's modulated phase. Effectively, this phase term results in a rotational offset of the OQPSK phase constellation.

A Matlab program was developed for simulation of the CDMA-PCS uplink interference waveform. Major steps, listed in order of execution, are given below.

1. Load all parameters for the simulation. These parameters, with corresponding descriptions and values, are given in Table 5.2.

Table 5.2. Parameters for CDMA-PCS Uplink Interference Simulation

Parameter/Function	Description	Value
f_c	RF channel carrier frequency; included as a parameter for frequency-dependent channel models	ranges from 1850 to 1990 MHz
P_{av}	Average (maximum) transmit power of each mobile station	2 W
T_{chip}	Chip duration for the I, Q, and long code pseudorandom sequences	0.813802×10^{6} s
N_{chips}	Total number of chips used in the simulation; determines the length of the interference waveform	2000
N_g	Number of samples/phase change	4
N_u	Number of active mobile stations per RF carrier in the primary cell	20
N_{uI}	Number of active mobile stations per RF carrier per interfering cell	20
c	Interference waveform propagation speed	3×10^{8} m/s
R	Cell radius	500 m
d_{x_k}	Linear X distance of each interfering cell's base station with respect to the primary cell's base station	1000 (depends on R and the geographical location of the interfering cell)
d_{y_k}	Linear Y distance of each interfering cell's base station with respect to the primary cell's base station	1000 (depends on R and the geographical location of the interfering cell)
N_{ic}	Number of interfering cells	Varies according to the iteration; equals 6 for adjacent cells, but may be set to any number
$a_{k,n}(r_{k,n}, \theta_{k,n})$	Propagation loss/Doppler shift function; may also be set explicitly to demonstrate a particular power distribution	Default is a simple $1/r^4$ propagation loss law

2. Design a baseband filter that is CDMA-PCS emissions-compliant. Baseband filtering tolerances are specified in terms of a minimum allowed mean squared error in document JTC(AIR)/94.11.21-022R8. Any filter that matches the specifications may be used. The ITS N/I model implements a Kaiser FIR filter design based on stopband level and frequency, passband frequency, and allowed passband ripple. Default parameters are summarized in Table 5.3.

Table 5.3. CDMA-PCS Filter Parameters

Parameter/Function	Description	Value
f_p	Passband cutoff frequency	590 kHz
f_{st}	Stopband cutoff frequency	740 kHz
A_p	Allowed passband ripple	3 dB
A_s	Stopband level, relative to the passband	40 dB

3. Calculate the positions of users in the primary cell. Mobile stations are randomly placed in the primary cell. The base station is assumed to be at the origin. Default distribution of mobile stations is random uniform. In polar coordinates, this means that the angular distribution is $U[0,2\pi)$, and the distance r from the base station has pdf $\frac{2r}{R^2}$, where R is the cell radius. The coordinates for each mobile station are stored in polar form.

4. Calculate the propagation loss/Doppler shift function for each mobile station in the primary cell. Any propagation loss/Doppler shift function may be implemented. The default is a simple $\frac{1}{r^4}$ propagation loss law.

5. Load all required spreading codes. Spreading codes are computed offline using a separate program. For this simulation, only the I and Q spreading codes were explicitly generated and loaded (long codes are too memory-intensive to simulate explicitly). Orthogonal modulation and long code spreading is simulated using a random number generator.

6. Set the power profile for primary cell mobile stations. The amplitude weighting function $W_{k,n}(t)$ given in Equation (5.13) may be explicitly set to match the power received from each interfering mobile station in the primary cell. This method was used in the ITS N/I model for different interferer amplitude distributions. Alternatively, the functions $A_{k,n}(t)$ and $a_{k,n}\left(r_{k,n},\theta_{k,n}\right)$ may be set to reflect the power control algorithm and propagation loss function, respectively.

Steps 7-9 are executed once for every mobile station in the primary cell.

7. Spread the data stream for the n^{th} mobile station in the primary cell. The data stream for the n^{th} mobile station in the primary cell is created using a random number generator, split into I and Q streams, and modulo-2 added to the preloaded I or Q codes. All mobile stations within the primary cell use identical I and Q code offset values. Zero offset is assumed for I and Q codes within the primary cell.

8. Filter and OQPSK modulate the n^{th} mobile station's symbol stream. After spreading, the I and Q symbol streams are baseband filtered (using the filter designed in step 2). The Q symbol stream is offset by one-half-symbol duration, then quadrature modulated. A random $U\left(0,2\pi\right]$ phase and random $U\left(0,T\right]$ delay is incorporated as part of the calculation.

9. Add the n^{th} mobile station's interference waveform to the aggregate waveform. This is performed iteratively for every mobile station in the primary cell.

Next, the interference waveform components from mobile stations in the k^{th} interfering cell are calculated. Steps 10-12 are executed for each interfering cell.

10. Calculate positions of users in the k^{th} interfering cell. Mobile stations are randomly placed in the k^{th} interfering cell. The k^{th} base station is assumed to be at the origin. Default distribution of mobile stations is random uniform. In polar coordinates, this means that the angular distribution is $U[0,2\pi)$, and the distance from the base station r has pdf $\frac{2r}{R^2}$. The coordinates for each mobile station are stored in polar form.

11. Calculate propagation loss/Doppler shift function for each mobile station in the k^{th} interfering cell. Any propagation loss/Doppler shift function may be implemented here. The default is a simple $\frac{1}{r^4}$ propagation loss law.

12. Set the power profile for k^{th} interfering cell mobile stations. The functions $A_{k,n}(t)$ and $a_{k,n}(r_{k,n},\theta_{k,n})$ are set to reflect the power control algorithm and propagation loss function, respectively, with respect to the n^{th} mobile station in the k^{th} interfering cell. The product function $W_{k,n}(t)$ is not set explicitly because power control does not exist between the k^{th} interfering cell and the primary cell.

Steps 13 -15 are computed for each mobile station in the k^{th} interfering cell.

13. Spread the data stream for the n^{th} mobile station. The data stream for the n^{th} mobile station in the k^{th} interfering cell is created using a random number generator, split into I and Q streams, and modulo-2 added to the preloaded I or Q codes. The I and Q codes are offset by at least 3*64 chip durations, relative to the I and Q codes of every other cell (including the primary cell) in the simulation. All mobile stations within the k^{th} interfering cell use identical I and Q code offset values.

14. Filter and OQPSK modulate the n^{th} mobile station's symbol stream. After spreading, the I and Q symbol streams are baseband filtered (using the filter designed in step 2). The Q symbol stream is offset by one-half symbol duration, then quadrature modulated. Random $U(0,2\pi]$ phase and random $U(0,T]$ delays are incorporated as part of the calculation.

15. Add the n^{th} mobile station's interference waveform to the aggregate waveform. This is completed iteratively for every mobile station in the n^{th} interfering cell.

16. Compute the interference waveform statistics. These include spectral plots, voltage envelope histograms, power envelope histograms, and phase distributions.

5.7.2 Example Results

As was the case for the PCS 1900 example, many possible scenarios may be investigated by choosing the parameters of the CDMA-PCS uplink interference simulation appropriately. For

demonstration purposes, three cases were developed and simulated using the parameters specified in Tables 5.2 and 5.3.

Case 1: Twenty mutually interfering mobile stations in the primary cell only, assuming perfect power control.

Case 2: Twenty mutually interfering mobile stations in the primary cell only, perfect power control for all but one mobile station, received 10 dB above the others.

Case 3: Aggregate interference waveform from 6 adjacent cells, with 20 interfering mobile stations in each adjacent cell.

All cases were simulated for 2000 chip durations. The results are summarized below.

Results for Case 1. Case 1 demonstrates the interference waveform generated by 20 mobile stations on an uplink RF channel, without any intercell interference. Perfect power control assumes all mobile station transmissions are received at the base station at equal power levels. As a result, the default propagation loss law is not implemented, since the receive level at the base station is set explicitly. All interferer levels were normalized before the statistical analysis was performed.

Figure 5.12 shows the voltage envelope histogram of the interference waveform incident at the primary base station's receiver. As was expected, the envelope appears to have a Rayleigh distribution. The corresponding power envelope histogram shown in Figure 5.13 is approximately exponentially distributed, and the phase envelope histogram plotted in Figure 5.14 appears to have a uniform distribution. Hence, the aggregate waveform due to uplink interferers within the primary cell appears as a Gaussian process. However, reception of a logical channel also depends on the correlative properties of the individual spreading codes, which are included in the interference waveform simulation, but not discernible in the histogram plots.

Results for Case 2. In case 2, the same parameters were used as in case 1, except one mobile station waveform is received at a power level 10 dB above the others. This is performed to illustrate a severe case of power control imbalance. An actual scenario may demonstrate a more variable distribution of mobile station power levels received at the base station.

Figure 5.15 shows the voltage envelope histogram of the interference waveform incident at the primary base station's receiver. This time, the envelope appears shifted to the right. The corresponding power envelope histogram shown in Figure 5.16 no longer appears exponentially distributed, and the phase envelope histogram plotted in Figure 5.17 now contains four clearly defined states. These states correspond to four randomly shifted phase states from the dominant

mobile station's OQPSK modulated waveform (the fourth state is "wrapped" around the $\pm\pi$ phase value). As a result, the aggregate waveform due to uplink interferers within the primary cell is not a Gaussian process. Although a 10-dB fluctuation may be unrealistic in an actual deployment, more subtle variations in the power control algorithm may also have a drastic impact on system capacity. For this reason, the N/I model presented here allows any distribution of interferers to be included in the aggregate waveform.

Results for Case 3. This case demonstrates the statistical properties of the aggregate interference waveform from nearby cells. Six interfering cells containing 20 mobile stations each were simulated. The aggregate interference waveform does not include transmissions from mobile stations in the primary cell. Since power control is not coordinated between the primary base station and mobile stations in nearby cells, the default propagation loss law was assumed, with all mobile stations transmitting at equal power. This assumption may not be realistic, since mobile stations at the border of their assigned cells will typically transmit at a higher level. In addition, a number of these mobile stations will tend to be much closer to the primary cell than others.

Figures 5.18, 5.19, and 5.20 show the voltage envelope, power envelope, and phase histograms, respectively. Scales in this case are not normalized, but individual power levels are accurate with respect to each other. Statistically, the aggregate waveform appears to have a Gaussian distribution. Correlative codes incorporated into the aggregate waveform may have additional impacts on the actual performance. For demonstration purposes, 100 mobile stations in the primary cell were simulated. The resulting interference spectrum is shown in Figure 5.21. The simulation program is capable of simulating an arbitrary number of mobile stations in a given cell.

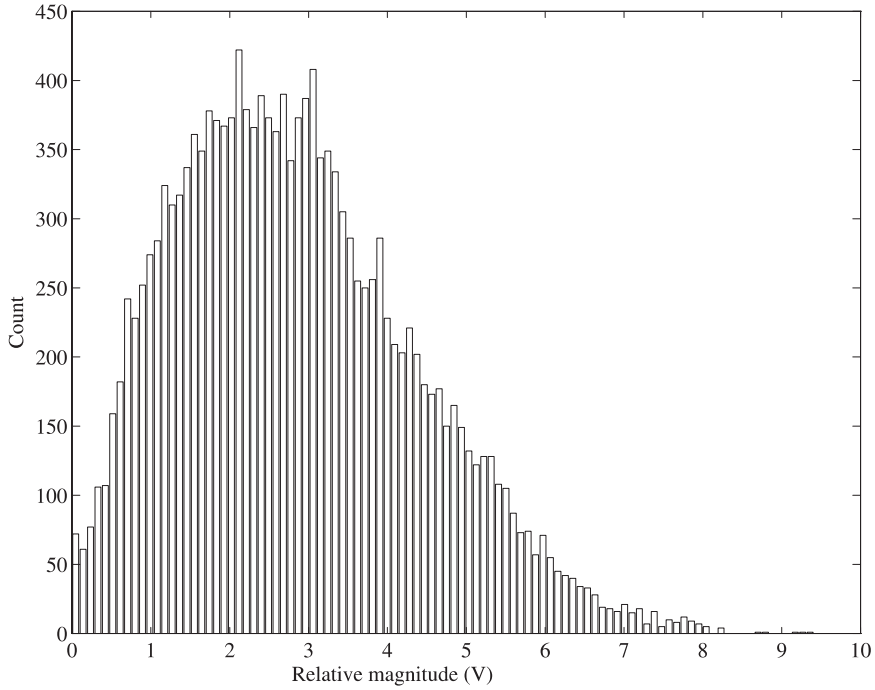

Figure 5.12. Voltage envelope histogram for case 1.

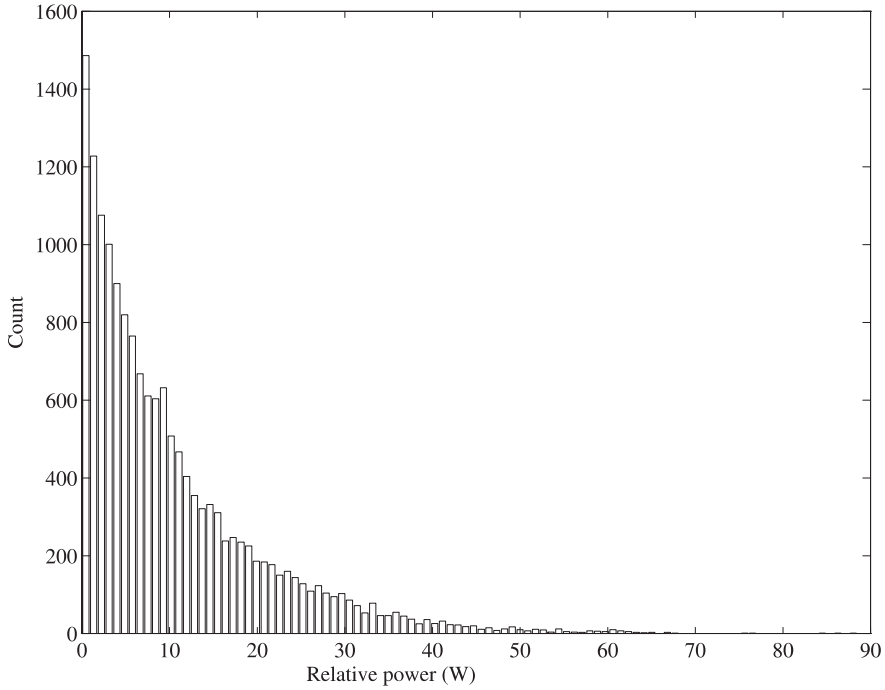

Figure 5.13. Power envelope histogram for case 1.

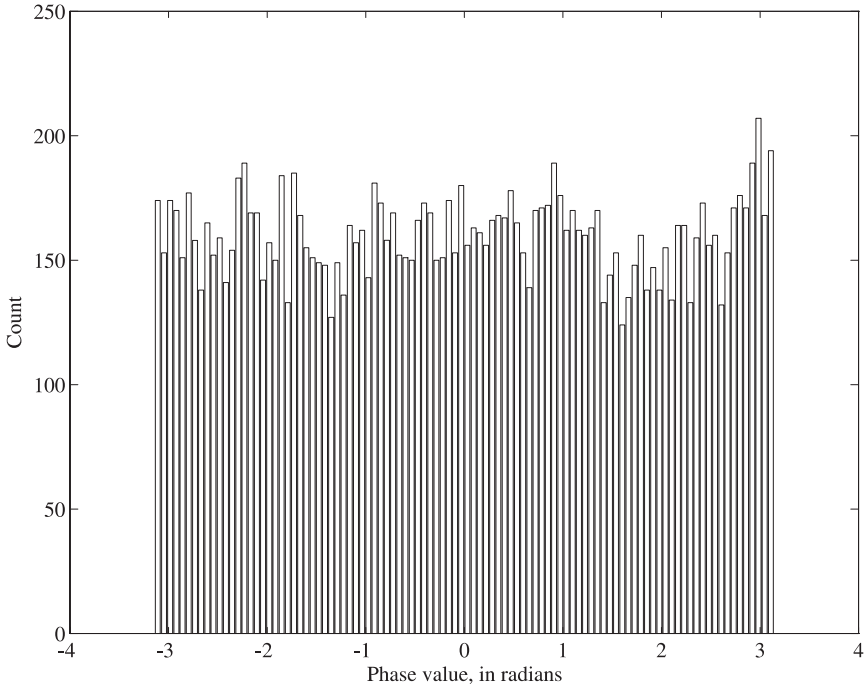

Figure 5.14. Phase envelope histogram for case 1.

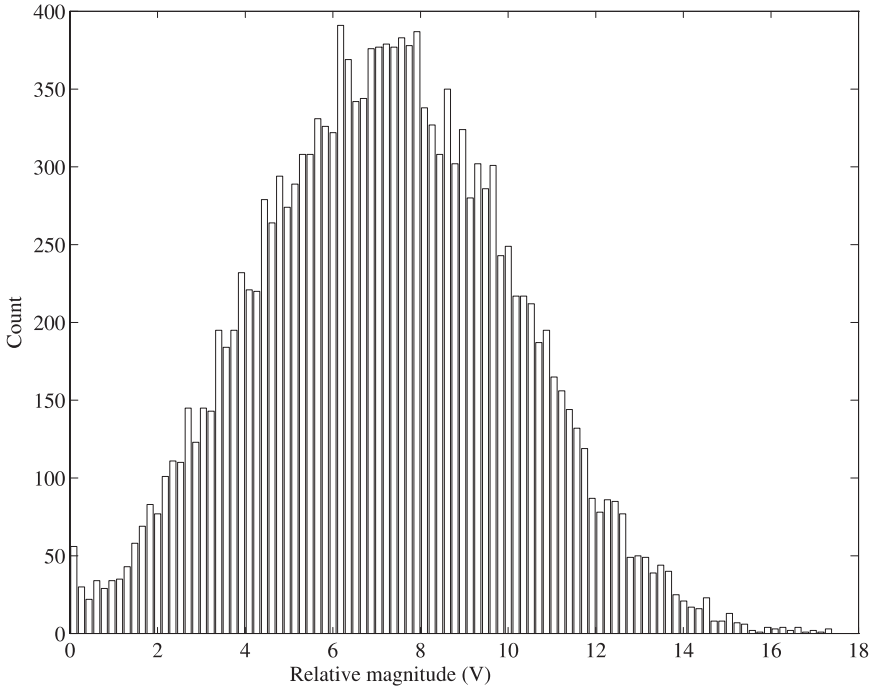

Figure 5.15. Voltage envelope histogram for case 2.

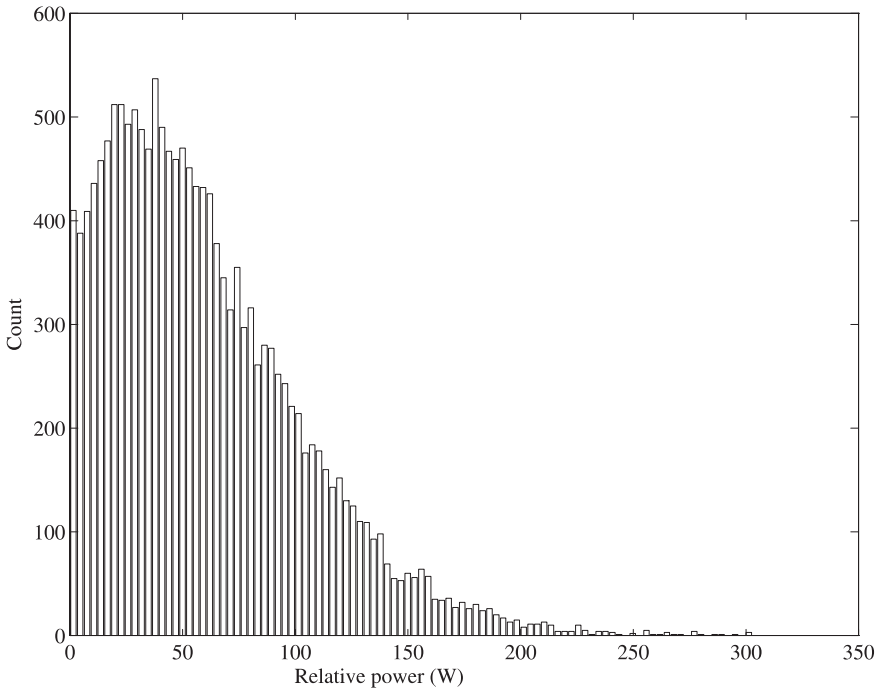

Figure 5.16. Power envelope histogram for case 2.

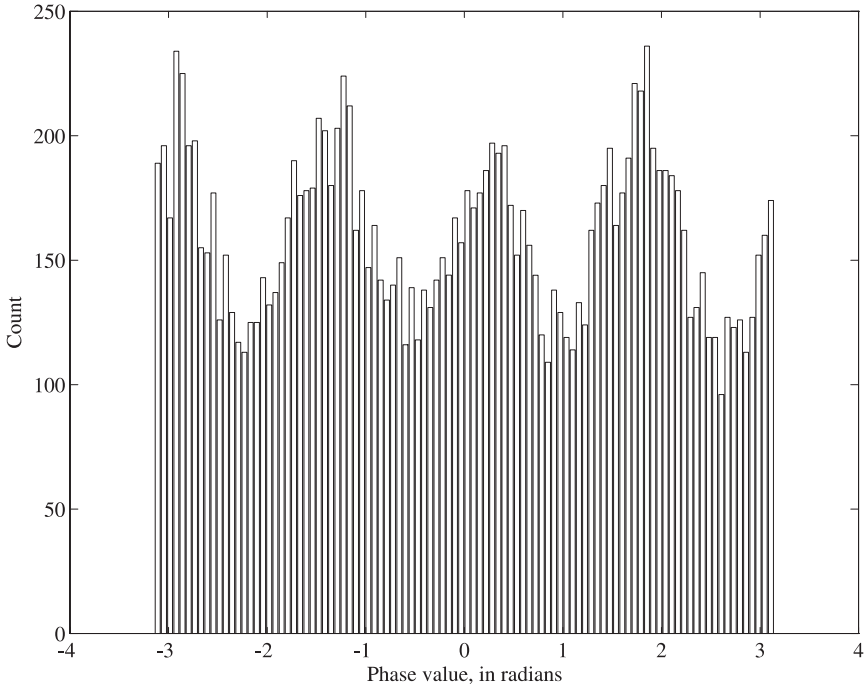

Figure 5.17. Phase envelope histogram for case 2.

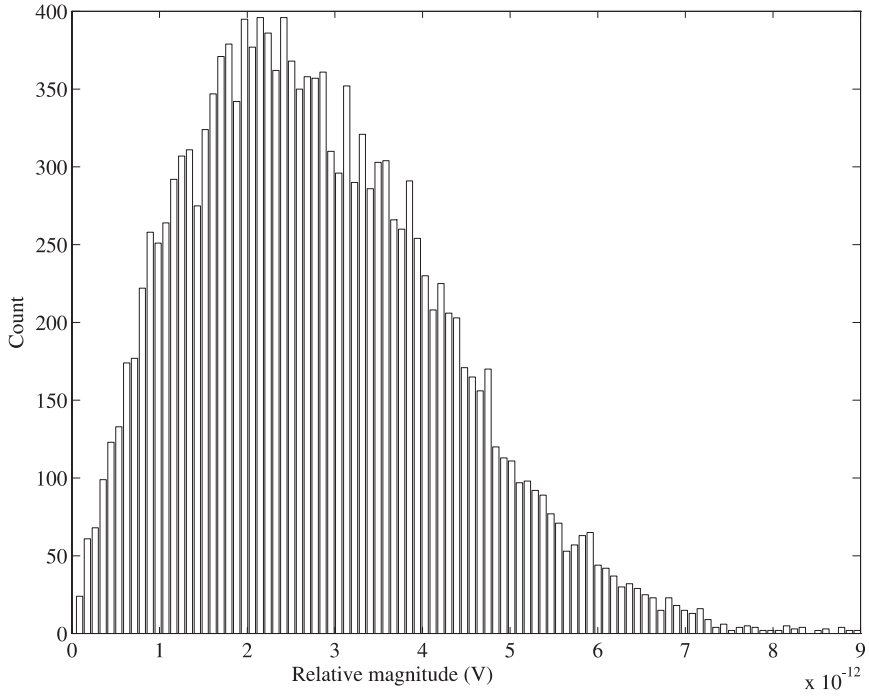

Figure 5.18. Voltage envelope histogram for case 3.

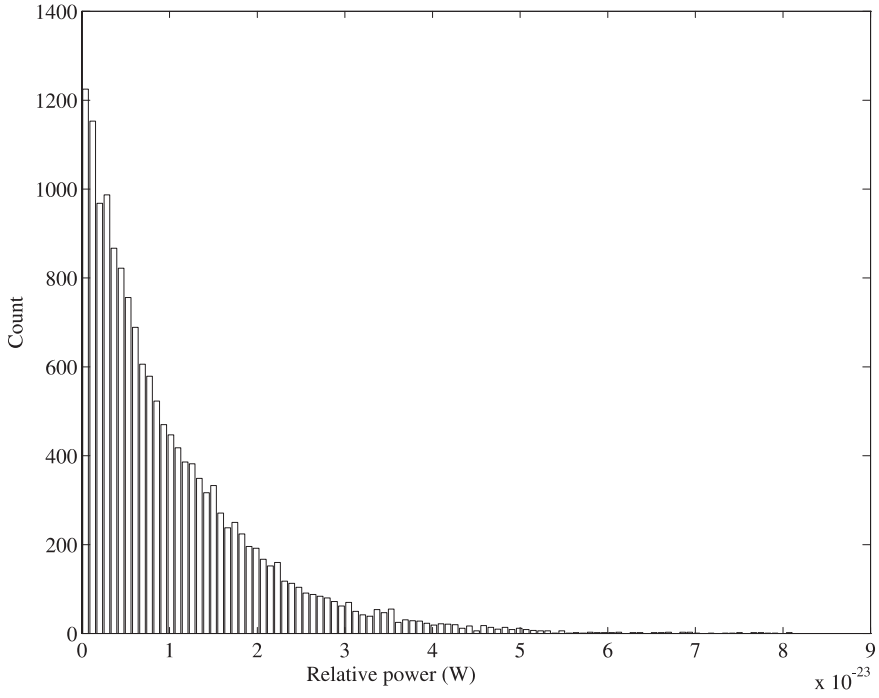

Figure 5.19. Power envelope histogram for case 3.

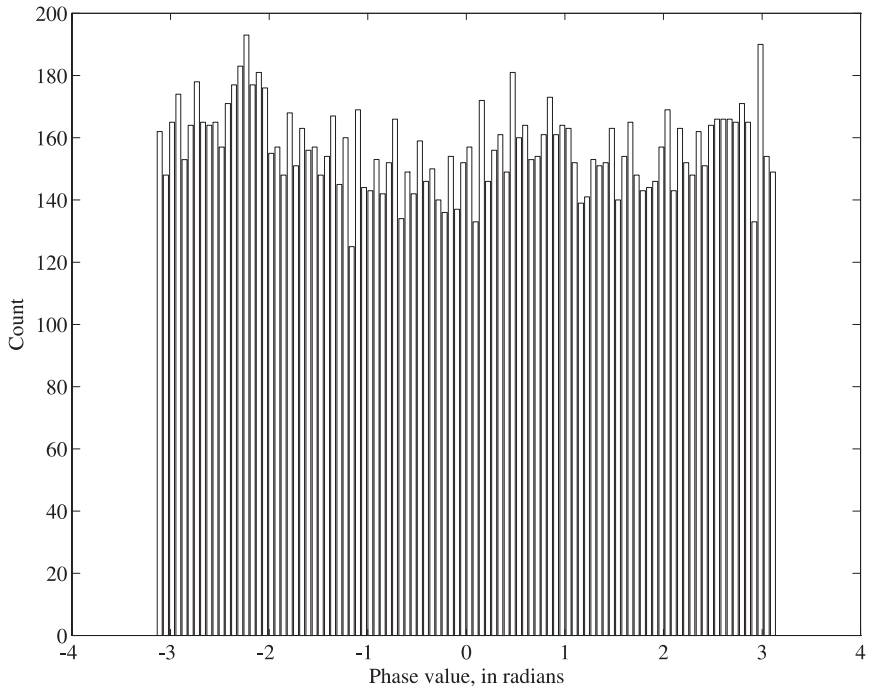

Figure 5.20. Phase envelope histogram for case 3.

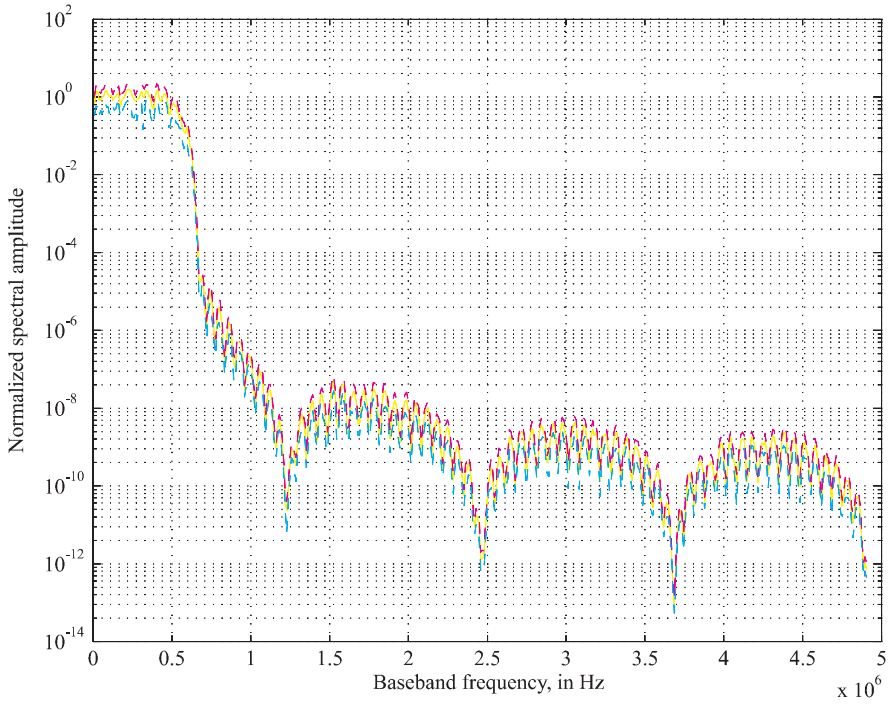

Figure 5.21. Aggregate interference waveform spectrum caused by 100 mobile stations in the primary cell.

6. SUMMARY AND CONCLUSIONS

A generic methodology for modeling noise and interference for cellular wireless technologies was presented in this report. Specifically, the Institute for Telecommunication Sciences has developed models of the self-interference created by a PCS network of individual communication links. This generic methodology was then applied to two proposed PCS systems: GSM-based PCS 1900 and IS-95-based CDMA.

Accurate noise and interference models are critical for meaningful PCS network testing, modeling, and evaluation. Advanced wireless systems can be tested via 1) channel simulation in real time or 2) large-scale software simulation for performance and interoperability evaluation. Noise and interference models described in this report are suitable for both applications. These capabilities directly benefit other Federal agencies with special performance requirements for PCS services; they also benefit small equipment and service providers without the resources to evaluate PCS technologies and equipment.

Using a geometric framework, generic expressions were developed for both uplink and downlink interference. The generic expressions then were modified for application to specific PCS systems. Models for PCS 1900 and CDMA-PCS were developed by extracting elements of each system that affect the noise and interference characteristics, and applying them to the modified generic expressions. Resulting expressions were specific to the PCS technology. Working examples of models for PCS 1900 and CDMA-PCS were then presented. In addition, computer simulation of PCS 1900 and CDMA-PCS was used to produce and analyze sample noise and interference waveforms.

Models of the noise and interference are essential for realistic characterization of the operating environment for proposed PCS technologies. Examples for both PCS 1900 and CDMA-PCS demonstrated that many enviromental and systematic influences affect the statistics of the aggregate interference waveform, and that a Gaussian distribution assumption is too simplistic in many cases.

In a future report, efficient real-time implementation of the PCS system-specific noise and interference waveforms will be described. Network-level simulations for interoperability and performance evaluation of proposed wireless technologies, which make use of the noise and interference models, will be presented in another future report.

7. REFERENCES

[1] A.D. Spaulding, "The natural and man-made noise environment in personal communication services bands," NTIA Report 96-330 (revised), May 1997.

[2] K.L. Blackard, T.S. Rappaport, and C.W. Bostian, "Measurements and models of radio frequency impulsive noise for indoor wireless communications," *IEEE Journal on Selected Areas in Communications*, Vol. 11, No. 7, pp. 991-1001, Sep. 1993.

[3] R. Prasad, A. Kegel, and A. de Vos, "Performance of microcellular mobile radio in a cochannel interference, natural, and man-made noise environment," *IEEE Trans. Vehic. Tech.*, Vol. 42, No. 1, pp. 33-40, Feb. 1993.

[4] Y.D. Yao and A.U.H. Sheikh, "Investigations into cochannel interference in microcellular mobile radio systems," *IEEE Trans. Vehic. Tech.*, Vol. 41, No. 2, pp. 114-123, May 1992.

[5] M. Laflin, "Technical report on RF channel characterization and system deployment modeling," JTC(AIR)/94/09/23-065-R6.

[6] J.J. Lemmon and J.A. Hoffmeyer, "Noise and interference aspects of the PCS operating environment," JTC(AIR)/93.03.08-064, Mar. 8, 1993.

[7] L.B. Milstein, D.L. Schilling, R.L. Pickholtz, V. Erceg, M. Kullback, E. Kanterakis, D. Fishman, W.H. Biederman, and D. Salerno, "On the feasibility of a CDMA overlay for personal communications networks," (submitted for publication in the *IEEE Journal on Selected Areas in Communications*)

[8] V. Kumar, "Applying 065 for air interface performance evaluation," JTC(AIR)/94/09/19-481-R2.

[9] P.W. Baier, "CDMA or TDMA? CDMA for GSM?," in *Proc. IEEE International Symposium on Personal, Indoor, and Mobile Radio*, P 3.2, pp. 1280-1284, 1994.

[10] R. Prasad and A. Kegel, "Improved assessment of interference limits in cellular radio performance," *IEEE Trans. Vehic. Tech.*, Vol. 40, No. 2, pp. 412-419, May 1991.

[11] J. Zou, V.K. Bhargava, and Q. Wang, "Reverse link analysis and performance evaluation for DS-CDMA cellular systems," in *Proc. IEEE International Symposium on Personal, Indoor, and Mobile Radio*, BC 1.2, pp. 50-54, 1994.

[12] R.F. Diesta and J.P. Linnartz, "Using Laplace transforms to compute performance of mobile radio links," in *Proc. IEEE International Symposium on Personal, Indoor, and Mobile Radio*, B 3.3, pp. 301-305, 1994.

[13] B.D. Woerner, J.H. Reed, and T.S. Rappaport, "Simulation issues for future wireless modems," *IEEE Communications Magazine*, Vol. 32, No. 7, pp. 42-53, Jul. 1994.

[14] A.G. Burr, T.C. Tozer, and S.J. Baines, "Capacity of an adaptive TDMA cellular system: comparison with conventional access schemes,"in *Proc. IEEE International Symposium on Personal, Indoor, and Mobile Radio*, E 2.2, pp. 242-246, 1994.

[15] Z.J. Haas, J.H. Winters, and D.S. Johnson, "Simulation study of the capacity bounds in cellular systems," in *Proc. IEEE International Symposium on Personal, Indoor, and Mobile Radio*, B 7.2, pp. 1114-1120, 1994.

[16] M.A. Couture and J.P. Linnartz, "Improved channel modeling for performance analysis of a DS-CDMA link," in *Proc. IEEE International Symposium on Personal, Indoor, and Mobile Radio*, C 8.3, pp. 705-710, 1994.

[17] Y. Li, B.D. Woerner, W Tanis II, and M. Hughes, "Simulation of CDMA using measured channel impulse response data," in *Proc. IEEE Vehic. Tech. Conf.*, pp. 428-431, 1993.

[18] J.G. Ferranto and J.J. Lemmon, "Simulation model of interference in PCS frequency bands," JTC(AIR)/93.08.23, Aug. 23, 1993.

[19] Personal Communications Services Air Interface Specification (ANSI J-STD-007-1996) (T1/TIA Joint Standard), American National Standards Institute, 11 West 42nd Street, New York, NY 10036, 1996.

[20] J.J. Tuma, *Handbook of Numerical Calculations in Engineering*, New York: McGraw-Hill, Inc., 1989, p. 196.

[21] "Draft Proposed American National Standard - Personal Station - Base Station Compatibility Requirements for 1.8- to 2.0-GHz Code Division Multiple Access (CDMA) Personal Communications Systems" T1 J-STD-008, Dec. 12, 1994.

APPENDIX A: MODULATED WAVEFORM NOTATION

This appendix describes the notation used for continuous modulated waveforms throughout this document, and contains a brief introduction to the theory of phase modulation.

A generalized modulated waveform can be expressed in the form:

$$s(t,\boldsymbol{\alpha}) = A(t,\boldsymbol{\alpha})\cos\left[2\pi f_c t + \varphi(t,\boldsymbol{\alpha})\right] \tag{A.1}$$

where $\boldsymbol{\alpha}$ represents values of a digital information alphabet sequence. Information can be included in the waveform by modulating the phase, rate of change of the phase (frequency), amplitude, or a combination of all the above. For a constant amplitude phase-modulated waveform, only $\varphi(t,\boldsymbol{\alpha})$ is a function of the digital information alphabet sequence. Letting

$$A(t,\boldsymbol{\alpha}) = \sqrt{\frac{2E_s}{T}} \tag{A.2}$$

yields the phase-modulated waveform:

$$s(t,\boldsymbol{\alpha}) = \sqrt{\frac{2E_s}{T}}\cos\left[2\pi f_c t + \varphi(t,\boldsymbol{\alpha})\right] \tag{A.3}$$

where E_s is defined as the energy per symbol, and T is the symbol duration. The phase expression $\varphi(t,\boldsymbol{\alpha})$ can be expressed in terms of the modulation index h, individual values of the digital information alphabet sequence α_i, and an arbitrary pulse $q(t)$:

$$\varphi(t,\boldsymbol{\alpha}) = 2\pi h\sum_{i=-\infty}^{\infty}\alpha_i q(t-iT). \tag{A.4}$$

For a general waveform $x(t) = \cos\left[\theta(t)\right]$, the instantaneous frequency is defined as:

$$f_I(t) = \frac{1}{2\pi}\frac{d\theta(t)}{dt} \tag{A.5}$$

Then, for the total angle expression $\theta(t) = 2\pi f_c t + \varphi(t,\boldsymbol{\alpha})$ in Equation (A.3), the instantaneous frequency expression becomes, using Equations (A.4) and (A.5):

$$\begin{aligned} f_I(t) &= \frac{1}{2\pi}\left[2\pi f_c + 2\pi h\sum_{i=-\infty}^{\infty}\alpha_i q'(t-iT)\right] \\ &= f_c + h\sum_{i=-\infty}^{\infty}\alpha_i g(t-iT), \quad \text{where} \\ q(t) &= \int_{\tau=-\infty}^{\infty} g(\tau)d\tau. \end{aligned} \tag{A.6}$$

Therefore, the pulse $q(t)$ modulates the phase of the waveform $s(t, \alpha)$, and its derivative $g(t)$ defines the instantaneous frequency. The function $g(t)$ may be chosen from numerous pulse shapes, and its shape determines the smoothness of the phase. Proper selection of $g(t)$ results in a PCS RF waveform that utilizes bandwidth efficiently.

APPENDIX B: COMPLEX BASEBAND NOTATION

This appendix is adapted from [1], and describes the theory and notation used for handling bandpass waveforms in complex baseband form. This is necessary because actual carrier frequencies used in proposed PCS systems are much greater than the waveform bandwidth, resulting in a prohibitively large Nyquist sampling rate.

The pre-envelope of a real bandpass waveform $g(t)$ is defined as:

$$g_+(t) = g(t) + j\hat{g}(t), \tag{B.1}$$

where $\hat{g}(t)$ is the Hilbert transform of $g(t)$. The Hilbert transform of the waveform $g(t)$ is expressed as:

$$\begin{aligned} \hat{g}(t) &= g(t) \otimes \frac{1}{\pi t}, \quad \text{or} \\ \hat{G}(f) &= G(f)(-j\,\mathrm{sgn}(f)). \end{aligned} \tag{B.2}$$

Note that $G_+(f)$ is equal to $G(f)$ for frequencies greater than zero (except for a scalar multiplier), and equals zero for all frequencies less than zero.

The pre-envelope $g_+(t)$ can also be expressed in terms of a complex envelope $\bar{g}(t)$, which forms a complex baseband representation of the real-valued bandpass waveform $g(t)$. $\bar{g}(t)$ is used for practical considerations; the sampling rate required at the RF carrier frequency for PCS systems is prohibitively large compared to the bandwidth of the waveform. Using complex envelope notation allows complete representation of the waveform within the complex baseband bandwidth, which is equal to the bandpass bandwidth of the actual (real) waveform.

The pre-envelope may be expressed in complex exponential form as follows:

$$g_+(t) = \bar{g}(t)\exp(j2\pi f_c t). \tag{B.3}$$

In Equation (B.3), $g(t)$ is a real-valued bandpass waveform at carrier frequency f_c and $\bar{g}(t)$ is the complex baseband representation of the waveform $g(t)$. Then

$$\begin{aligned} g(t) + j\hat{g}(t) &= \bar{g}(t)\exp(j2\pi f_c t) \\ &= \bar{g}(t)\left[\cos(2\pi f_c t) + j\sin(2\pi f_c t)\right]. \end{aligned} \tag{B.4}$$

Because $\bar{g}(t)$ is generally complex,

$$\bar{g}(t) = g_c(t) + jg_s(t) \tag{B.5}$$

where $g_c(t)$ and $g_s(t)$ are both real-valued functions. Using Equations (B.1), (B.3), and (B.5), $g(t)$ is expressed in canonical form as:

$$g(t) = \mathrm{Re}\left[g_+(t)\right] = g_c(t)\cos(2\pi f_c t) - g_s(t)\sin(2\pi f_c t). \tag{B.6}$$

$g_c(t)$ and $g_s(t)$ are known as the in phase and quadrature components of the waveform $g(t)$. Both are lowpass waveforms.

Filter implementations and transfer functions also may be formulated in complex baseband form. Below it is demonstrated that the real filter equation $y(t) = x(t) \otimes h(t)$ may be replaced by the equivalent complex baseband equation $\bar{y}(t) = \bar{x}(t) \otimes \bar{h}(t)$. To begin, a bandpass waveform $x(t)$ and a transfer function $h(t)$ are defined in canonical form:

$$x(t) = x_c(t)\cos(2\pi f_c t) - x_s(t)\sin(2\pi f_c t) \tag{B.7}$$

$$h(t) = 2h_c(t)\cos(2\pi f_c t) - 2h_s(t)\sin(2\pi f_c t). \tag{B.8}$$

The constant "2" in Equation (B.8) is arbitrary. The waveform $x(t)$ is input to a filter with transfer function $h(t)$. Using the complex baseband representation for $h(t)$:

$$h(t) = \mathrm{Re}\left[2\bar{h}(t)\exp(j2\pi f_c t)\right]. \tag{B.9}$$

Next, the waveform at the output port of the filter *h(t)* is defined as:

$$y(t) = \mathrm{Re}\left[\bar{y}(t)\exp(j2\pi f_c t)\right] = \int_{-\infty}^{\infty} h(\tau)x(t-\tau)d\tau. \tag{B.10}$$

Therefore,

$$y(t) = \int_{\tau=-\infty}^{\infty} 2\,\mathrm{Re}\left[h_+(\tau)\right]\mathrm{Re}\left[x_+(t-\tau)\right]d\tau. \tag{B.11}$$

To show that $\bar{y}(t) = \bar{x}(t) \otimes \bar{h}(t)$, an integral identity is needed. Given an expression

$$m(t) = \frac{1}{2}\mathrm{Re}\left[\int_{t=-\infty}^{\infty} g_{1+}(t)g_{2+}^*(t)dt\right] \tag{B.12}$$

where

$$\begin{aligned} g_{1+}(t) &\stackrel{\Delta}{=} g_1(t) + j\hat{g}_1(t) \\ g_{2+}(t) &\stackrel{\Delta}{=} g_2(t) + j\hat{g}_2(t), \end{aligned} \tag{B.13}$$

$g_1(t)$ and $g_2(t)$ are real functions, $\hat{g}_1(t)$ and $\hat{g}_2(t)$ are their respective Hilbert transforms, and "*" denotes complex conjugation. Equation (B.12) then becomes:

$$m(t) = \frac{1}{2}\mathrm{Re}\left[\int_{t=-\infty}^{\infty}(g_1(t)g_2(t) - jg_1(t)\hat{g}_2(t) + j\hat{g}_1(t)g_2(t) + \hat{g}_1(t)\hat{g}_2(t))dt\right] \tag{B.14}$$

Because $g_1(t)$ and $g_2(t)$ are real functions, Equation (B.14) can be reduced to

$$m(t) = \frac{1}{2}\int_{t=-\infty}^{\infty} g_1(t)g_2(t)dt + \frac{1}{2}\int_{t=-\infty}^{\infty}\hat{g}_1(t)\hat{g}_2(t)dt. \tag{B.15}$$

The cross-correlation of two Fourier-transformable functions has cross-power spectral density equal to the Fourier transform of the first function multiplied by the complex conjugate of the Fourier transform of the second function. This is given by the correlation theorem as:

$$\boldsymbol{FT}\left[R_{12}(\tau)\right] = G_1(f)G_2^*(f) = -j^2\,\mathrm{sgn}^2(f)G_1(f)G_2^*(f) = \hat{G}_1(f)\hat{G}_2^*(f) \tag{B.16}$$

Taking the inverse Fourier transform of the expression to the right of the last equality yields the cross-correlation of the Hilbert transforms of $g_1(t)$ and $g_2(t)$, respectively. Thus, from Equation (B.15):

$$\frac{1}{2}\int_{t=-\infty}^{\infty} g_1(t)g_2(t)dt = \frac{1}{2}\int_{t=-\infty}^{\infty}\hat{g}_1(t)\hat{g}_2(t)dt \tag{B.17}$$

and Equation (B.15) becomes:

$$m(t) = \frac{1}{2}\int_{t=-\infty}^{\infty} g_1(t)g_2(t)dt = \frac{1}{2}\int_{t=-\infty}^{\infty}\mathrm{Re}\left[g_{1+}(t)\right]\mathrm{Re}\left[g_{2+}^*(t)\right]dt. \tag{B.18}$$

Returning to Equation (B.12), and using Equation (B.17), the identity becomes

$$m(t) = \frac{1}{2}\mathrm{Re}\left[\int_{t=-\infty}^{\infty} g_{1+}(t)g_{2+}^*(t)dt\right] = \int_{t=-\infty}^{\infty}\mathrm{Re}\left[g_{1+}(t)\right]\mathrm{Re}\left[g_{2+}^*(t)\right]dt. \tag{B.19}$$

Now, if $g_2(t)$ is replaced with $g_3(t) = g_2(s-t)$, the identity becomes:

$$m(t) = \frac{1}{2}\mathrm{Re}\left[\int_{t=-\infty}^{\infty} g_{1+}(t)g_{2+}^*(s-t)dt\right] = \int_{t=-\infty}^{\infty}\mathrm{Re}\left[g_{1+}(t)\right]\mathrm{Re}\left[g_{2+}^*(s-t)\right]dt \tag{B.20}$$

which is the desired identity. Using Equation (B.20), Equation (B.11) becomes:

$$
\begin{aligned}
y(t) &= \int_{\tau=-\infty}^{\infty} 2\,\mathrm{Re}\left[h_+(\tau)\right]\mathrm{Re}\left[x_+(t-\tau)\right]d\tau \\
&= \mathrm{Re}\left[\int_{\tau=-\infty}^{\infty} h_+(\tau)x_+(t-\tau)d\tau\right] \\
&= \mathrm{Re}\left[\int_{\tau=-\infty}^{\infty} \overline{h}(\tau)\exp(j2\pi f_c t)\overline{x}(t-\tau)\exp(j2\pi f_c(t-\tau))d\tau\right] \\
&= \mathrm{Re}\left[\int_{\tau=-\infty}^{\infty} \overline{h}(\tau)\overline{x}(t-\tau)d\tau\exp(j2\pi f_c t)\right] \\
&= \mathrm{Re}\left[\overline{h}(t)\otimes\overline{x}(t)\exp(j2\pi f_c t)\right].
\end{aligned}
\tag{B.21}
$$

Therefore, the complex system output $\overline{y}(t)$ can be obtained by convolving the complex envelopes of $x(t)$ and $h(t)$, and all bandpass calculations may use an equivalent complex baseband representation of the real waveforms and transfer functions.

REFERENCE

[1] S. Haykin, Communication Systems, Second Edition, New York: John Wiley and Sons, Inc., 1983.

APPENDIX C: ACRONYMS

C/I	carrier-to-interference ratio
C/(N +I)	carrier-to-noise plus interference ratio
CDMA	code-division multiple access
CDMA-PCS	an IS-95-based standard for 1900 MHz PCS
FDD	frequency-division duplexing
FWPC	Federal Wireless Policy Committee
GMSK	Gaussian minimum-shift keying
GSM	Global System for Mobile
I	inphase waveform component
IS-95	CDMA cellular standard
ITS	Institute for Telecommunication Sciences
JTC	Joint Technical Committee
LPF	lowpass filter
N/I	noise/interference
NTIA	National Telecommunications and Information Administration
OQPSK	offset quadrature phase-shift keying
PACA	priority access and channel assignment
PCS	personal communications services
PCS 1900	a GSM-based standard for 1900 MHz PCS
PDF	probability density function
Q	quadrature waveform component
QPSK	quadrature phase-shift keying
RF	radio frequency
SNR	signal-to-noise ratio
STU-III	secure telephone unit - III
TDMA	time-division multiple access